AD NUMBER
AD803462
NEW LIMITATION CHANGE
TO **Approved for public release, distribution unlimited**
FROM **Distribution authorized to U.S. Gov't. agencies and their contractors; Critical Technology; MAY 1966. Other requests shall be referred to Army Engineer Waterways Experiment Station, Vicksburg, MS 39280.**
AUTHORITY
AEWES ltr dtd 24 Jan 1972

AD-803 462

Contract Report No. 3-101

THE FRICTION OF QUARTZ IN HIGH VACUUM

Research in Earth Physics

Phase Report No. 7

by

Leslie G. Bromwell

May 1966

Sponsored by

U.S. Army Materiel Command
Project No. 1-V-0-14501-B-52A-01

under

Contract No. DA-22-079-eng-457

with

U.S. Army Engineer Waterways Experiment Station
CORPS OF ENGINEERS
Vicksburg, Mississippi

Soil Mechanics Division
Department of Civil Engineering
Massachusetts Institute of Technology

Research Report R66-18

ABSTRACT

Resistance to shear deformation in a granular mass is mobilized at the points of contact between particles. A major part of this resistance arises from inter-particle friction. Therefore, any fundamental study into the mechanics of deformation of granular systems requires an understanding of the nature of solid-to-solid friction. Despite this there are few reports in the literature of friction measurements on minerals.

The purpose of this investigation was to determine the fundamental factors controlling the frictional properties of quartz surfaces, with emphasis on the effects of surface cleanliness. Ultra-high vacuums (to 10^{-10} torr) and high temperatures (to 350°C) were combined with chemical cleaning and careful handling techniques to produce the maximum surface cleanliness.

The coefficient of static friction under varying environmental conditions was measured for quartz, 304 stainless steel, and granite. Direct shear tests were run on a quartz sand (40-60 mesh Ottawa sand) and on 30-40 mesh glass balls.

The coefficient of friction of smooth quartz was found to vary from 0.1 to 1.0 depending on the surface cleanliness. The friction of rough surfaces showed a much smaller variation, which has important implications for granular soils.

Ultra-high vacuum, combined with a high temperature bake-out, produced significant increases in both the angle of friction, ϕ_μ, of quartz (about 8°) and the peak friction angle, ϕ_m, of quartz sand (about 5°). The cohesion intercept for the quartz sand also increased by about 0.02 kg/cm^2. A good correlation, using theoretical curves, was obtained between changes in ϕ_m and ϕ_μ for quartz.

The high vacuum-high temperature test conditions simulate aspects of the lunar environment. Therefore, the test results may yield useful information regarding the properties of postulated lunar soil models involving significant thicknesses of granular particles.

FOREWORD

The work described in this report was performed under Contract No. DA-22-079-eng-330 entitled "Research Studies in the Field of Earth Physics" between the U.S. Army Engineer Waterways Experiment Station and the Massachusetts Institute of Technology. The research is sponsored by the U.S. Army Materiel Command under DA Project 1-V-0-14501-B-52A-01, Earth Physics (Terrain Analysis). The above contract was replaced by Contract No. DA-22-079-eng-457 with the same title on August 1, 1965.

The general objective of the Research in Earth Physics is the development of a fundamental understanding of the behavior of particulate systems, especially cohesive soils, under varying conditions of stress and environment. Work on the project, initiated in May 1962, has been carried out in the Soil Mechanics Division (headed by Dr. T. William Lambe, Professor of Civil Engineering) of the Department of Civil Engineering under the supervision of Dr. Charles C. Ladd, Associate Professor of Civil Engineering.

This report presents only one portion of the overall research being conducted under the contract. Phases currently under investigation are:

1. In Situ Strength and Compression Properties of Natural Clays
   - (a) Effects of sample disturbance (i.e. excessive shear strains) on the undrained strength, stress-strain modulus, and one-dimensional compression behavior of natural clays.
   - (b) Effects of stress-system variables (anisotropic consolidation, intermediate principal stress, rotation of principal planes) on stress-strain behavior of clays during undrained shear.
   - (c) Correlation of laboratory data and field measurements.
2. Influence of Environment on Strength and Compression Properties of Soils
   - (a) Effect of high vacuum and temperature on the properties of granular systems.

(b) Effects of natural cementation and type of pore fluid on the strength and compression properties of saturated clays.

(c) The strength of clays at very low effective stresses and especially the nature and magnitude of "true cohesion".

3. The Structure of Clay

(a) Nature and magnitude of interparticle forces in clay-water systems.

(b) Fabric of kaolinite.

Many of the above topics complement and/or draw information from other research projects in the Soil Mechanics Division. This particular phase included support via a grant from the M. I. T. Center for Space Research.

This report was prepared by Mr. Leslie G. Bromwell under the supervision of Professor Ladd. Mr. Bromwell held a NASA Fellowship for two of the four years that he devoted to this study. He was a Research Assistant for the other two years. This report has also served as Mr. Bromwell's doctoral thesis.

The report constitutes work on Item c-(1), Article 1 of the forementioned Contract No. DA-22-079-eng-457.

Pertinent reports under Research in Earth Physics are:

1. "Research in Earth Physics, Progress Report for the Period June 1962-December 1962," Department of Civil Engineering Publication R63-9, M.I.T., Feb. 1963.
2. Ladd, C.C., "Stress-Strain Behavior of Saturated Clay and Basic Strength Principles," Phase Report No. 1, Part 1, Department of Civil Engineering Publication R64-17, M.I.T., April, 1964.
3. Bromwell, L.G., "Adsorption and Friction Behavior of Minerals in Vacuum," Phase Report No. 2, Department of Civil Engineering Publication R64-42, M.I.T., March, 1965.
4. Bailey, W.A., "The Effects of Salt on the Consolidation Behavior of Saturated Remolded Clays." Phase Report No. 3, Department of Civil Engineering Publication R65-19, M.I.T., May, 1965.

5. Ladd, C.C. and Varallyay, J., "The Influence of Stress System on the Behavior of Saturated Clays during Undrained Shear," Phase Report No. 1, Part II, Department of Civil Engineering Publication R65-11, M.I.T., July 1965.

6. Martin, R.T., "Quantitative Fabric of Consolidated Kaolinite," Phase Report No. 4, Department of Civil Engineering Publication R65-47, M.I.T., September, 1965 (in press).

7. Ladd, R.S. "Use of Electrical Pressure Transducers to Measure Soil Pressure," Phase Report No. 5, Department of Civil Engineering Publication R65-48, M.I.T., September, 1965 (in press).

8. Ladd, C.C. and Preston, W.B., "On the Secondary Compression of Saturated Clays," Phase Report No. 6, Department of Civil Engineering Publication R65-54, M.I.T., December, 1965 (in press).

TABLE OF CONTENTS

Page

LIST OF TABLES

LIST OF FIGURES

NOTATION

Symbols are generally defined where they are first used. The following is a compilation of symbols frequently used in this report:

A = total area

A_c = area of contact

c = Mohr-Coulomb cohesion intercept

N = normal load

q_u = normal stress required to cause plastic flow in a solid material; indentation hardness

T = tangential force; Temperature

V = volume

V_o = volume at the start of a shear test

α = angle of interlocking relative to the major principal plane

β = direction of sliding relative to the minor principal plane

μ = coefficient of friction; static coefficient of friction

μ_s = static coefficient of friction

μ_k = kinetic (sliding) coefficient of friction

$\bar{\sigma}_1, \bar{\sigma}_3$ = principal effective stresses

$\bar{\sigma}_v$ = vertical effective stress

σ_y = yield strength of a solid material

τ = shear strength or shear stress

τ_m = shear strength of a solid material

ϕ_{cv} = Mohr-Coulomb friction angle at critical void ratio

ϕ_m = Mohr-Coulomb peak friction angle

ϕ_μ = angle whose tangent is μ

I. INTRODUCTION

Resistance to shear deformation in a granular mass is mobilized at the points of contact between particles. A major part of this resistance arises from friction forces. Therefore, the usefulness and application of shear strength theories for granular assemblies depends upon the correct selection of the angle of inter-particle friction (generally designated ϕ_μ). Despite this, there are few reports in the literature of friction measurements on minerals. In addition, interpretation of previous data has been hampered for two reasons:

1. Lack of information regarding cleanliness of the surfaces
2. Lack of knowledge regarding the mechanism of friction in massive silicate minerals

1.1 Purpose of the Investigation

The purpose of this investigation was to measure the coefficient of friction of quartz under varying conditions of surface cleanliness, surface roughness, and normal load. Ultra-high vacuum (to 10^{-10} torr) [1] and high temperatures (to 350°C) were combined with chemical cleaning and careful handling techniques to produce the maximum surface cleanliness. The use of different surface roughnesses and normal loads provided information on the mechanism of friction in quartz; i.e., the relative importance of surface cleanliness (asperity bonding) vs. surface roughness (asperity interlocking).

The coefficient of friction measurements were correlated with the results of direct shear tests on a quartz sand (40-60 mesh Ottawa sand). Changes were produced in both ϕ_μ and ϕ_m (Mohr-Coulomb peak friction angle), which provided a means of correlating the results with theoretical equations relating ϕ_μ and ϕ_m.

---

[1] The torr is the standard pressure unit in vacuum technology. It is 1/760 of a standard atmosphere and is essentially equivalent to 1 mm. Hg.

From a practical point of view, the environmental conditions in these tests simulate the high vacuum-high temperature environment of the moon and may, therefore, provide useful information regarding the properties of a lunar model that assumes a granular surface layer.

It is fully realized that the high vacuum-high temperature environment simulates only one aspect of the lunar environment, and perhaps not even the most important one. Other effects, such as micrometeoroid impact, high radiation, etc., may have a much larger influence on the lunar surface layer. Nevertheless, it is of some value to know the effect of vacuum and temperature on soils, if only to help place limits on the permissible range of surface properties.

1.2 Scope of Test Program

1.2.1 Friction Tests

Atmospheric friction tests were run on sliding blocks of quartz, granite, and stainless steel. The effects of surface treatment and submergence in water were studied in these tests. The friction of quartz was also investigated at 10^{-8} torr and 350°C for surfaces with varying surface roughness and amount of pre-cleaning.

1.2.2 Direct Shear Tests

Direct shear tests were run under both atmospheric and high vacuum-high temperature conditions for two materials: 1) 30-40 mesh glass balls and 2) 40-60 mesh Ottawa sand. Vertical effective stresses ($\bar{\sigma}_v$) between 0.045 and 1.0 kg/cm^2 were used in these tests. All samples of a given material were prepared at the same void ratio, so that changes in shear strength (at the same $\bar{\sigma}_v$) could be related to changes in inter-particle friction.

II. BACKGROUND

2.1 Definintions

2.1.1 Coefficient of Static Friction

The coefficient of static friction[1] μ is defined as the tangential force T required to initiate sliding between two contacting solids under a normal load N as shown in Fig. 2.1. Experimentally, it is frequently found that a plot of T vs. N gives a straight line through the origin with a slope ϕ_μ. Thus,

$$\mu \equiv \frac{T}{N} = \tan \phi_\mu \tag{2.1}$$

As will be shown in Section 2.2, the frictional resistance is mainly due to formation of bonds between the two surfaces at the points of contact. The force T is that required to shear these bonds.

2.1.2 Coefficient of Kinetic Friction

The coefficient of sliding (or kinetic) friction μ_k is defined as the tangential force required to maintain the motion once sliding commences between two surfaces under a normal load N.

The kinetic coefficient is frequently smaller than the static coefficient. This has been attributed to a time-dependence for bond formation at the contacts (Bowden and Tabor, 1964, pg. 79).

2.1.3 Stick-Slip

The difference between the static and kinetic coefficients leads to the phenomenon known as stick-slip. Once sliding begins, a smaller force is required to maintain sliding than was required to initiate it.

---

[1] μ_s will be used to designate the static coefficient when it is being compared with other parameters, such as the kinetic coefficient.

Hence, part of the stored elastic energy in the loading mechanism is released, accelerating the slider and causing the measured force T to drop below that required for μ_k. The slider then stops and the force must be increased to that associated with μ_s to induce sliding again. Once sliding begins, the whole procedure of intermittent motion is repeated.

Bowden and Tabor (1950, pg. 105 ff) have analysed the stick-slip process and conclude that μ_k may be taken as one-half the distance between the peak force and the minimum at the end of the slip. However, the amount of slip should depend on the stiffness of the loading mechanism, hence the minimum force is probably a function of the equipment and not of the material being tested. Therefore, the suggested procedure probably gives only a rough estimate of μ_k.

2.1.4 Rolling Friction

The resistance to rolling between two bodies arises not from interfacial adhesion but from deformation losses (hysteresis and/or plastic flow) in the solids themselves (Bowden and Tabor, 1964, Ch. XV). Thus there is almost no "friction" as it was defined in the preceding sections.

The rolling coefficient of friction is generally quite low (as low as 10^{-3}) and is essentially independent of surface cleanliness or lubricants.

2.2 Historical Review

Bowden and Tabor (1964, Ch. 24) give an excellent review of the development of theories of friction since antiquity. They attribute the first quantitative study of friction to Leonardo da Vinci around 1500. da Vinci postulated the two basic laws of friction; namely,

1. The friction force is directly proportional to the normal force applied to surfaces.
2. The friction force is independent of the total area of the surfaces.

These observations were re stated by Amontons in 1699, and are generally known as Amontons' Laws.

Initial attempts to explain these laws employed the interlocking of projections on the surfaces. The coefficient of friction would then be given by the tangent of the angle of the surface irregularities. Various investigators, beginning with Desgauliers in 1724, questioned the validity of this explanation. Its most obvious shortcoming is that it predicts decreasing values of μ for progressively smoother surfaces, whereas it is generally found that μ is constant (or nearly so) over a wide range of surface roughness.

Sir W. B. Hardy (1919) examined the wear track produced by sliding of both clean and lubricated glass surfaces. From the tearing observed for the clean surfaces, Hardy concluded that sliding friction is due to cohesive forces between the surfaces. Hardy also realized that the actual area of contact was only a small fraction of the total area, and that the cohesive forces on a unit area basis were therefore quite large.

K. Terzaghi (1925), in his classic <u>Erdbaumechanik</u>, gave the first quantitative description of the friction process. Terzaghi reasoned that the normal load, N, acting on the very small area of actual contact would cause yielding of the contacting asperities, as shown in Figure 2.2. The contact area, A_c, would thus be given by

$$N = A_c q_u \tag{2.2}$$

where q_u is the normal stress required to cause plastic flow.[1] Terzaghi also assumed that adhesion would occur over the region of actual contact and that the junctions thus formed must be sheared before sliding could

[1] Early theoretical work used σ_y, the yield stress, instead of q_u, the indentation hardness. q_u is essentially a bearing capacity. Tabor (1951) has shown that for most metals, $q_u = 3\sigma_y$.

occur. If the material has a shear strength τ_m, then the tangential force T_{max} that will cause sliding is given by

$$T_{max} = A_c \tau_m \tag{2.3}$$

The static coefficient of friction μ is therefore

$$\mu = \frac{T_{max}}{N} = \frac{\tau_m}{q_u} \tag{2.4}$$

Terzaghi's analysis was proposed independently by Bowden and Tabor (1942) and shown by them to explain the frictional behavior of a wide variety of materials. The Terzaghi-Bowden-Tabor analysis is commonly called the Adhesion Theory of Friction. Its essential feature, that friction is due to cohesive bonds at points of contact, now serves as the starting point for essentially all frictional studies.

2.3 Factors Affecting the Coefficient of Friction

The analysis of the friction process given in the preceding section must be modified and extended in order to interpret experimental data from friction experiments. Rarely does an actual system exhibit the simple behavior suggested by the Terzaghi-Bowden-Tabor analysis.

2.3.1 Effect of Normal Load

Amontons' first law, that the friction force is proportional to the normal force, leads to a constant coefficient of friction, independent of normal load. Terzaghi's analysis explains this by assuming plastic behavior at the contacts, which gives a contact area proportional to the normal load. For most materials this appears to be the case over a wide range of loads. However, this analysis is not correct for a perfectly elastic solid that does not exhibit plastic deformation. Diamond approximates such a material.

2.3.1.1 The Friction of a Perfectly Elastic Solid

The contact area of a perfectly elastic material will not be given by a plastic yield equation. If the asperities are assumed to have spherical tips, the classical Hertz analysis may be applied, which predicts a plane circular contact of diameter d given by:

$$d = (\delta \, NR)^{1/3} \tag{2.5}$$

where N is the normal load, R is the radius of the tip, and δ is determined by the contact conditions and the elastic constants of the material (Timoshenko and Goodier, 1951, p. 372). For a spherical indenter on a plane surface δ is given by:

$$\delta = \frac{12\,(1 - \nu^2)}{E} \tag{2.6}$$

From equation 2.5, the contact area will be given by

$$A_c = KN^{2/3} \tag{2.7}$$

where

$$K = \frac{\pi}{4}\,(\delta R)^{2/3}$$

The friction force will be

$$T = \tau A_c = \tau K N^{2/3} \tag{2.8}$$

and the coefficient of friction:

$$\mu = \frac{T}{N} = \tau \, K N^{-1/3} \tag{2.9}$$

The coefficient of friction will vary as the minus one third power of the normal load.

The preceding analysis, which is for a single asperity on a flat plate, may not accurately describe the complex contact conditions between two surfaces that have a very large number of asperities. In this situation elastic deformation can occur by two mechanisms (Archard, 1957):

1. As the load increases the number of contacting asperities remains constant and the elastic deformation of each asperity increases. In this case the contact area is proportional to $N^{2/3}$.

2. As the load increases the number of contacting asperities increases proportionally and the deformation of each asperity remains essentially constant. The area of contact is proportional to N.

In an actual situation, the area of contact may be expected to vary as N^n, where n is between 2/3 and 1. By choosing a model where the main asperities have still smaller asperities on their surfaces, Archard calculates $n = \frac{44}{45}$, thus demonstrating that even elastic materials may have an approximately constant μ.

The problem of whether quartz behaves elastically (like diamond) or plastically (like most metals) is discussed in Section 2.4.1.

2.3.2 Effect of Surface Roughness

The Terzaghi-Bowden-Tabor analysis implies that friction is independent of surface roughness. For metals this is found to be the case over a wide range of surface finish (Bowden and Tabor, 1950, pg. 175).

As the surfaces become very rough, the possibility of asperity interlocking may increase the value of μ. If the asperities are assumed to have an average slope angle θ, then a force balance leads to the following equation for the coefficient of friction:

$$\mu_t = \tan(\phi_\mu + \theta) \qquad (2.10)$$

where ϕ_μ is the friction angle for a smooth surface.

Equation 2.10 predicts a higher coefficient of friction for rougher surfaces, which seems intuitively reasonable. However, to the author's knowledge a definitive set of experiments to verify this have not been run.

Because the contact situation between two real surfaces is so complex, it is probably not possible to determine the value of θ to use in Equation 2.10. Hence, the relationship between friction and surface roughness must be determined experimentally.

2.3.3 Effect of Surface Cleanliness

Surfaces that are exposed to the atmosphere can quickly become contaminated by adsorbed gases, dust, and organic compounds. When two such surfaces are put together, the amount of actual solid-to-solid contact, and hence the shear strength of the contact, will be influenced by the type and amount of material adsorbed onto the surfaces. Therefore, the value of μ that is measured may vary widely depending on the cleaning treatment and environmental conditions.

The friction measured under atmospheric conditions is seldom, if ever, between surfaces free of adsorbed material, i.e., clean surfaces. At atmospheric pressure, about 10^8 molecules per second impinge on each surface atom of an exposed solid. This generally results in rapid contamination.

2.3.3.1 Effect of Vacuum and Elevated Temperatures

To produce and maintain a surface free of any adsorbed contaminants requires a clean ultra-high vacuum.[1] In addition, elevated temperatures must generally be used to effect desorption, particularly

[1] Clean and ultra-high are not synonumous terms in this context. An inadequately trapped diffusion pump may produce a vacuum of 10^{-10} torr and still cover everything in the system with pump oil. This problem is discussed in detail in Appendix A.

of chemisorbed molecules.[1]

As surfaces become cleaner, more solid-to-solid contact occurs, and the shear strength of the contacts increases. Bowden and Tabor (1964, p. 74) give a theoretical analysis of the relationship between μ and τ/τ_m, where τ_m is the shear strength of the solid. Figure 2.3 presents the results of this analysis. As τ/τ_m increases (increasing surface cleanliness), μ increases. The analysis predicts an infinite μ for $\tau/\tau_m = 1.0$. This is the phenomenon known as "cold welding", which involves gross seizure of the surfaces.

Ductile metals that have been cleaned in a high vacuum can exhibit cold welding. Bowden and Tabor (1964, p. 75) attribute cold welding to an increase in the area of contact under the applied friction force. If the material behaves plastically,[2] it will deform under combined compressive stresses (σ) and shear stresses (τ) according to a plastic yield criterion such as that of von Mises (Nadai, 1950, p. 248), which in two dimensions is given by

$$\sigma^2 + 3\tau^2 = \sigma_y^2 \tag{2.11}$$

where σ_y is the uniaxial compressive strength.

If the asperities are initially loaded to $\sigma = \sigma_y$, as shown in Figure 2.4, then application of a small τ will require that σ become less than σ_y. Since the total normal force is a constant, this requires an increase in the contact area. As τ increases, the contact area must continue to increase to maintain plastic equilibrium. If the junction does not shear until $\tau = \tau_m$, the shear strength of the bulk solid, then σ must

[1] An analysis of the temperature and pressure conditions required to desorb molecules with a known adsorption energy is given in Appendix C.

[2] The ability to deform plastically under shear stresses is an essential feature of this analysis.

decrease to zero, which requires an infinite area of contact, or gross seizure over the entire area. It is this process of junction growth that produces cold welding and extremely large coefficients of friction in a high vacuum.

2.4 The Friction of Brittle Materials

The discussion of friction in the preceding sections has pertained mainly to ductile materials because the Adhesion Theory was developed for these materials. This section will discuss the applicability of the theory to brittle materials such as quartz. There are two main elements of the theory that must be considered--the mode of deformation at the regions of contact and the magnitude of adhesion at the contacts.

2.4.1 Plastic Flow of Brittle Materials

Brittle materials are characterized by catastropic fracture at small strains. However, if tensile stresses are prevented, as for example in an indentation hardness test,[1] permanent deformation can be induced without large-scale fracture. The geometric similarity of the hardness test to the contacting asperities between solid surfaces is obvious. For stress levels less than the hardness, the asperities will deform elastically. When the stress exceeds the hardness, the contacts will deform plastically.

[1] The hardness test, which involves pushing a suitably shaped indenter into a flat test surface is a direct measure of q_u, the resistance to plastic flow. The high confining stresses that develop around the tip of the indenter inhibit brittle fracture. Indentation hardness is expressed as the normal force divided by the residual area of deformation after the indenter is removed.

For quartz, with a hardness of about 1100 $kg/mm.^2$ (Brace, 1963), the stress on an asperity must exceed 1,500,000 psi to produce plastic deformation.[1] Whether or not this stress is reached for a significant number of asperities in a granular soil mass is still a matter for speculation.

3.4.2 Adhesion of Brittle Materials

There is good evidence that the frictional resistance of brittle materials, just as for metals, is due to cohesive forces acting at the contact points. Cleaning the surfaces (for example, by outgassing in a vacuum) has been shown to produce increases in the coefficient of friction of rock salt,[2] diamond,[3] and sapphire.[3]

Material	μ air	μ vacuum
rock salt	0.7	1.3
diamond	0.05	0.5
sapphire	0.10	1.0

Very high temperatures were used in these experiments (up to 1100°C for sapphire), which may have produced some surface flow or sintering. However, the significant point is that no large-scale seizure or "cold-welding" was observed. The coefficient of friction increased due to the increased strength of the cleaner contacts, but no appreciable junction growth occurred.

---

[1] There is some doubt whether the observed permanent deformation in quartz is truly plastic or whether it is a result of micro-fracturing on a scale too small to be seen (Brace, 1963).

[2] King and Tabor (1954).

[3] Bowden, Young, and Rowe (1952).

In summary, the friction of brittle solids generally involves both elastic and plastic deformation at the regions of contact. Strong interfacial adhesion can occur, leading to coefficients of friction of the order of unity. However, these materials behave in a ductile manner only when they are under high confining pressures. As junction growth begins, the decrease in confining pressure shifts deformation back to the brittle range, causing shear at a coefficient of friction of about unity.

2.5 The Friction of Quartz

2.5.1 Theoretical Considerations

2.5.1.1 The Surface of Quartz

A freshly broken quartz crystal would produce surfaces such as shown schematically in Figure 2.5a. The surface consists of one anionic site and one cationic site every 24.3 $\mathring{A}^2$. Under atmospheric conditions, the surface charges are rapidly satisfied by adsorption of a gas such as H_2O, as shown in Figure 2.5b.

2.5.1.2 Adhesion of Quartz

If a quartz crystal were broken in an ultra-high vacuum, the two charged surfaces might retain their initial structure (Fig. 2.5a) for a considerable time. If the broken surfaces were put back into contact, they would probably readhere with considerable strength.

The bonding between two hydrated surfaces (Fig. 2.5b) would be considerably less. Exposure to other contaminants (atmospheric and otherwise) would decrease the bonding still further.

If an ultra-high vacuum and high temperatures were used to desorb the silanol surface shown in Fig. 2.5b, it is not likely that the charged surface shown in Fig. 2.5a would result. The hydrated silanol surface, when heated, may decompose to form a siloxane surface, as shown in Fig. 2.5c. The siloxane surface is not charged.

Even if the quartz surfaces could be cleaned so that the interfacial bonds were as strong as bulk quartz, the friction would not be extremely high. As was shown in Section 2.4.2, brittle materials such as quartz will not exhibit "cold-welding". However, the friction of quartz, as for other materials, should reflect changes in the type and amount of adsorbed material on the surfaces.

2.5.2 Previous Work on the Friction of Quartz

The most comprehensive investigation of mineral friction to date is that by Horn (1961, Horn and Deere, 1962). Horn summarizes earlier work by Terzaghi (1925), Tschebotarioff and Welch (1948), and Penman (1953) among others.

All of these investigators, including Horn, found that the friction of polished quartz surfaces in the dry condition was very low (0.10 to 0.16). When the surfaces were submerged in water the friction increased by about a factor of three to four. Horn also studied the effects of surface roughness on the friction of quartz. His results are summarized in Figure 2.6. Rougher surfaces gave higher values of μ. The air-dry friction for a rough surface was about 0.53 ($\phi_\mu = 28°$). The highest friction for quartz that Horn measured was 0.71 ($\phi_\mu = 35°$). This was for a 240 grit ground surface submerged in water.

Horn concluded that the low μ for the smooth surfaces in the dry condition was the result of adsorbed molecules of a highly effective boundary lubricant. Water presumably disrupts the orientation of this boundary layer, thus reducing its effectiveness and leading to higher values of μ. These conclusions appear to be based on the work of Sir W. B. Hardy (1936, pg. 618 ff) who found that water did not change the value of μ for a carefully cleaned glass surface (here clean refers to a surface free from dust and organic contamination). However, water increased the friction for glass surfaces that had been coated with thin films of lubricant.

Sjaastad (1963) measured the effect of vacuum (to 10^{-6} torr) and temperature (200°C) on the friction of glass and quartz. These conditions appeared to remove some of the adsorbed contamination as shown below:

Material	μ air	μ vacuum
glass	0.12	0.49
quartz	0.33	0.60

The value of μ for dry quartz (0.33) probably indicates a higher degree of surface cleanliness than is normally obtained. Sjaastad used chemical solvents (benzene and acetone), whereas the other investigators relied mainly on detergent washes to clean the surfaces (Horn wiped his surfaces with an acetone-soaked piece of cotton, but it is not certain whether the net effect of this would be to remove or to add contamination).

After the tests reported herein were completed, the author found that Sir W. B. Hardy had measured values of μ for dry quartz as high as 0.77 (Hardy and Doubleday, 1922). These results appear to have been largely ignored by previous investigators, but they offer substantiation to the values found in this investigation.

Hardy found that quartz surfaces cleaned by heating in a strong solution of chromic acid gave $\mu = 0.73$, but that the friction dropped with increasing temperature to a value of 0.09 at 110°C. This suggested that a temperature-sensitive film might still be adhering to the quartz. When the quartz faces were vigorously rubbed with clean fingers under a stream of water after the chromic acid treatment, the friction was constant at 0.77 from 17°C to 110°C. This suggested that traction was necessary to remove the film.

2.6 Relationships Between Friction and the Shear Strength of Granular Soils

2.6.1 Components of Shear Strength

The relationship between the coefficient of friction μ (or tan ϕ_μ) of the solid surface and the Mohr-Coulomb angle of friction ϕ_m has been studied by many investigators, including Caquot (1934), Bishop (1954), Newland and Allely (1957), Rowe (1962), Sjaastad (1963), and Scott (1964).

Rowe (1962) shows that the strength of an assembly of particles arises from three sources:

1. Frictional resistance at points of contact (ϕ_μ term)
2. Particle rearrangements
3. Dilation or work done by volume expansion against the confining pressure

Figure 2.7 illustrates the contribution of these three terms to the shear strength of a granular soil. At low porosities, the peak strength (ϕ_m) is reached before appreciable movements between particles can occur. Thus the shear strength is due to the friction and dilation terms. At the highest stable porosity (the critical void ratio) there is no net volume change, hence the dilation term is zero. The friction angle is higher than ϕ_μ by the amount of the rearrangement term. This term reflects the fact that the planes of sliding between the particles are inclined at various angles to the direction of the maximum shear stress. Thus, on a microscopic scale, volume changes are occurring as particles shear past each other. These microscopic volume changes are both positive and negative, and for the mass as a whole they cancel out. However, an additional energy input is required for the positive volume changes over that required to overcome interparticle friction.

At intermediate porosities, all three terms contribute to ϕ_m. For a given geometrical arrangement of the particles the strength resulting from rearrangement and dilation should be constant. Thus, by preparing all of the samples of a given soil

at the same initial void ratio and then varying ϕ_μ (by high vacuum treatment for example) it should be possible to determine the effect of changes in inter-particle friction (ϕ_μ) on peak friction angle (ϕ_m).

2.6.2 Equations Relating ϕ_μ and ϕ_m

By considering equilibrium of externally applied forces and internal forces at contacts between particles, it is possible to derive theoretical relationships between ϕ_μ and ϕ_m for regular packings of uniform spheres. Two limiting conditions have been investigated; namely, dense packing (n = 26%) and the critical void state (n = 42%). Figure 2.8 shows the relationships that have been developed by various investigators.

Dantu (1961), Rowe (1962), and Scott (1964) have studied the force equilibrium for dense packings. Dantu (1961) develops the following equation:

$$\sin \phi_m = 3 \; \frac{\sqrt{2} + 2 \tan \phi_\mu}{5\sqrt{2} + 2 \tan \phi_\mu} \qquad (2.12)$$

Rowe (1962) gives the following equation:

$$\left(\frac{\bar{\sigma}_1}{\bar{\sigma}_3}\right)_{max} = \tan^2 (45 + \frac{\phi_m}{2}) = \tan \alpha \tan (\phi_\mu + \beta) \qquad (2.13)$$

where $\bar{\sigma}_1$ and $\bar{\sigma}_3$ are the major and minor principal effective stresses at failure; α and β are functions of the geometrical packing of the assembly.

For hexagonal close packing (α = 71 6°, β = 54.7°), Rowe's equation gives the same results as the Dantu equation. For face-centered cubic (FCC) packing (α = 60°, β = 45°), Rowe's equation gives somewhat different results, as shown in Figure 2.8. Both face-centered cubic and hexagonal close packing have the same porosity (26%), but differ slightly in the manner in which the close-packed planes are stacked. Rowe (1962)

states that the hexagonal is the more stable packing under a general stress system.

The Dantu equation leads to $\phi_m = 90°$ (infinite shear strength) at $\mu = 0.71$ ($\phi_\mu = 35°$). The Rowe relationship for FCC packing leads to $\phi_m = 90°$ at $\mu = 1.0$ ($\phi_\mu = 45°$).

Scott (1964) has also developed an equation for dense packed arrays by relating the shear forces and normal forces on the potential sliding surface.[1] The resulting equation is as follows:

$$\tan \phi_m = \frac{\sqrt{3} + 4\sqrt{2} \tan \phi_\mu}{2(\sqrt{6} - \tan \phi_\mu)} \qquad (2.14)$$

The Scott equation and the Rowe FCC equation agree well up to $\mu = .75$ ($\phi_\mu = 37°$). At higher values of μ they diverge. The Scott equation does not go to infinity until $\mu = 2.44$ ($\phi_\mu = 68°$), while the Rowe equation goes to infinity at $\mu = 1.0$. This is apparently a result of different assumptions regarding the orientation of the external stresses relative to the packing geometry of the assembly.

Rowe's systems have the close-packed planes in a pre-determined orientation with respect to $\bar{\sigma}_1$ and $\bar{\sigma}_3$. Scott, on the other hand, analyzes the shear and normal forces at the contacts and allows the external stress system to orient itself relative to the packing geometry so as to minimize the work on the system. Both analyses are correct, but they will only relate to a real system if their relative assumptions are valid. Rowe's equation, for example, would apply to a triaxial test where the major principal stress was applied perpendicular to the close-packed planes. Scott's equation would probably apply to a plane strain situation, where rotation of principal stresses could occur.

---

[1] This analysis was originally given by Thurston and Deresiewicz (1959). It was extended by Scott, who resolved forces normal and tangential to the potential plane of sliding, thereby obtaining a relationship for $\tan \phi_m$.

Caquot (1934), Bishop (1954), and Horne [Lee (1966)], have studied the relationship between ϕ_μ and ϕ_m at the critical void state, which occurs at a porosity of 42% for uniform spheres.

The Caquot equation is given by

$$\tan \phi_m = \frac{\pi}{2} \tan \phi_\mu \tag{2.15}$$

Caquot obtained this equation by integrating normal and tangential forces over the surface of a semi-sphere. This involves the assumption that sliding occurs simultaneously at sphere-to-sphere contacts inclined in all the tangential directions of a spherical surface. This appears to be a reasonable approximation of the critical voids state.

Bishop does not give details of the analysis that led to the following equation:

$$\sin \phi_m = \frac{3}{2} \tan \phi_\mu \tag{2.16}$$

but he states that it is for a condition of plane strain.

Lee (1966) gives tabulated values of ϕ_m vs. ϕ_μ predicted by Horne, based on unpublished work at Manchester University. He states that Horne's equations cannot be simply expressed, but that they agree closely with experimental values, whereas Bishop's and Caquot's equations do not, particularly at higher values of ϕ_μ.

In Chapter V the Scott and Horne relations will be used to correlate experimentally determined values of ϕ_μ for quartz with values of ϕ_m measured on Ottawa sand.

2.7 Previous Work on the Shear Strength of Soils in High Vacuum

Since 1960 a large amount of work has been done on the behavior of soils in a high vacuum. Most of this work has been directed towards ascertaining the probable nature of the surface of the moon, where a vacuum of about 10^{-10} torr exists. Mitchell (1964) has

summarized the research in this area. He notes about thirty current research projects on the nature of the lunar surface layer.

2.7.1 Adhesion Measurements

Several investigators (Halajian, 1964; Salisbury and Glaser, 1964; Ryan, 1965) have noted high-vacuum induced adhesion between silicates. Ryan has measured the magnitude of adhesion between silicates, glass, and metals. He obtained adhesion values as high as several hundred milligrams for 0.5 cm diameter cylindrical specimens of orthoclase that had been outgassed at 100-200°C for several days and then tested at room temperature and 10^{-10} torr. Extensive surface damage was observed in these tests, indicating that the bonding forces across the interface were of the same order of magnitude as those in the crystal itself.

The adhesion in these experiments generally showed a dependence on the amount of compressive load that had been put on the samples before they were pulled apart. Compressive loads as high as 500 grams were used to produce an adhesion of 300 milligrams. This was probably due to some remaining surface contamination that had to be penetrated before strong bonds could form.

It would be very useful if these adhesion results could be translated into the corresponding cohesion intercept that an orthoclase soil would show under the same test conditions. However, this cannot be done without making questionable assumptions regarding contact areas and contact stresses.

2.7.2 Direct Shear Tests in Vacuum

Two test programs have been reported that measured changes in the direct shear strength of soils under high vacuum.

Vey and Nelson (1965) ran tests on powdered quartz and basalt at vacuum levels down to 8×10^{-10} torr and temperatures to 125°C. The small particle sizes that were used (25% to 35% less than 10 microns)

caused difficulty in outgassing the samples. It was estimated that the pressure in the soil was as much as two orders of magnitude higher than that measured in the chamber.

The changes in shear strength that were measured were of the same order of magnitude as the experimental error, i.e., reproducibility of results. The highest value of normal stress that was used was 2 psi. The quartz powder gave an increase in shear strength of 0.3 psi at this value of normal stress. The olivine powder gave essentially the same shear strength in high vacuum as in the atmosphere. Because of the low stress levels used and lack of information regarding the surface cleanliness of the materials,[1] it is not possible to make a meaningful interpretation of this data.

Sjaastad (1963) ran direct shear tests on glass spheres and nickel shot at 10^{-6} torr and up to 200°C. By using larger particles (2 mm. diameter) Sjaastad eliminated the outgassing problem that occurs with fine powders. All of the vacuum tests were run at a normal stress of 0.7 psi. Thus it was not possible to separate the vacuum test data into cohesion and friction components. The largest increase in shear strength that was measured for the glass balls was 0.3 psi. Coefficient of friction tests were run on plates of the same glass. These tests showed that μ increased from 0.12 in the atmosphere to 0.49 at 10^{-6} torr and 200°C. When the test specimens were cooled back to room temperature before testing, μ decreased to 0.36. Many measurements on glass have indicated that it has a μ of about unity when carefully cleaned (Holland, 1964). Therefore, it seems probable that Sjaastad's tests were run on only partially cleaned surfaces.

---

[1] Di sion pumping was used to produce the high vacuum. Inadequate trapping of such a vacuum system can contaminate test surfaces with pump oil in a very short time (see Appendix A).

DEFINITION OF COEFFICIENT OF FRICTION

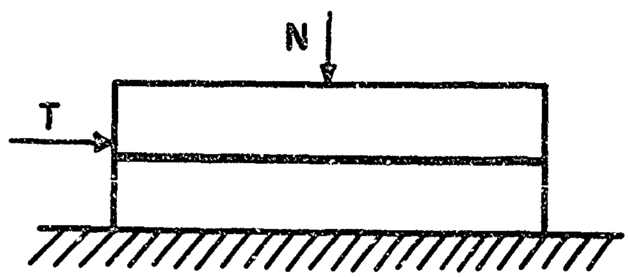

$$\mu = \frac{T}{N} = \tan \phi_{\mu}$$

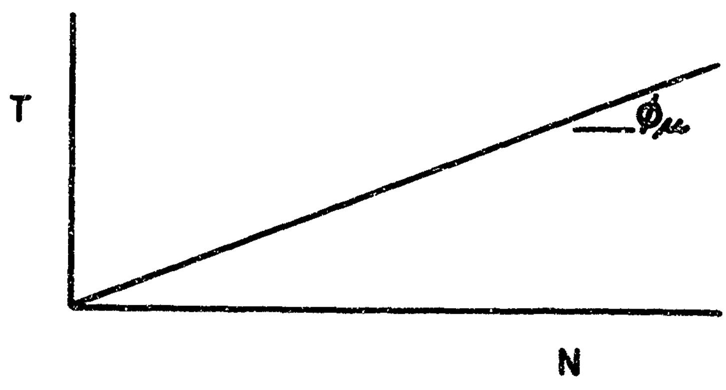

FIGURE 2.1

MICROSCOPIC VIEW OF FRICTIONAL RESISTANCE

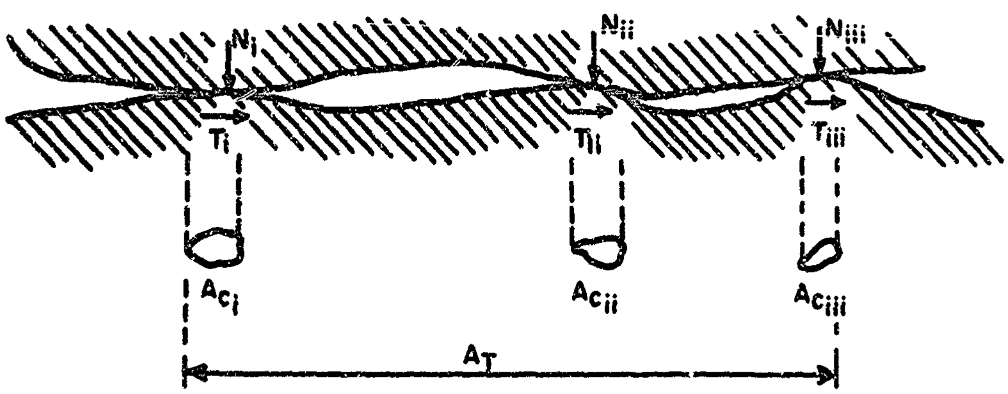

$$N = \sum N_i = \sum A_{c_i} q_u$$

$$T = \sum T_i = \sum A_{c_i} \tau_m$$

$$\mu = \frac{T}{N} = \frac{\tau_m}{q_u}$$

FIGURE 2.2

FRICTION AS A FUNCTION OF INTERFACIAL SHEAR STRENGTH

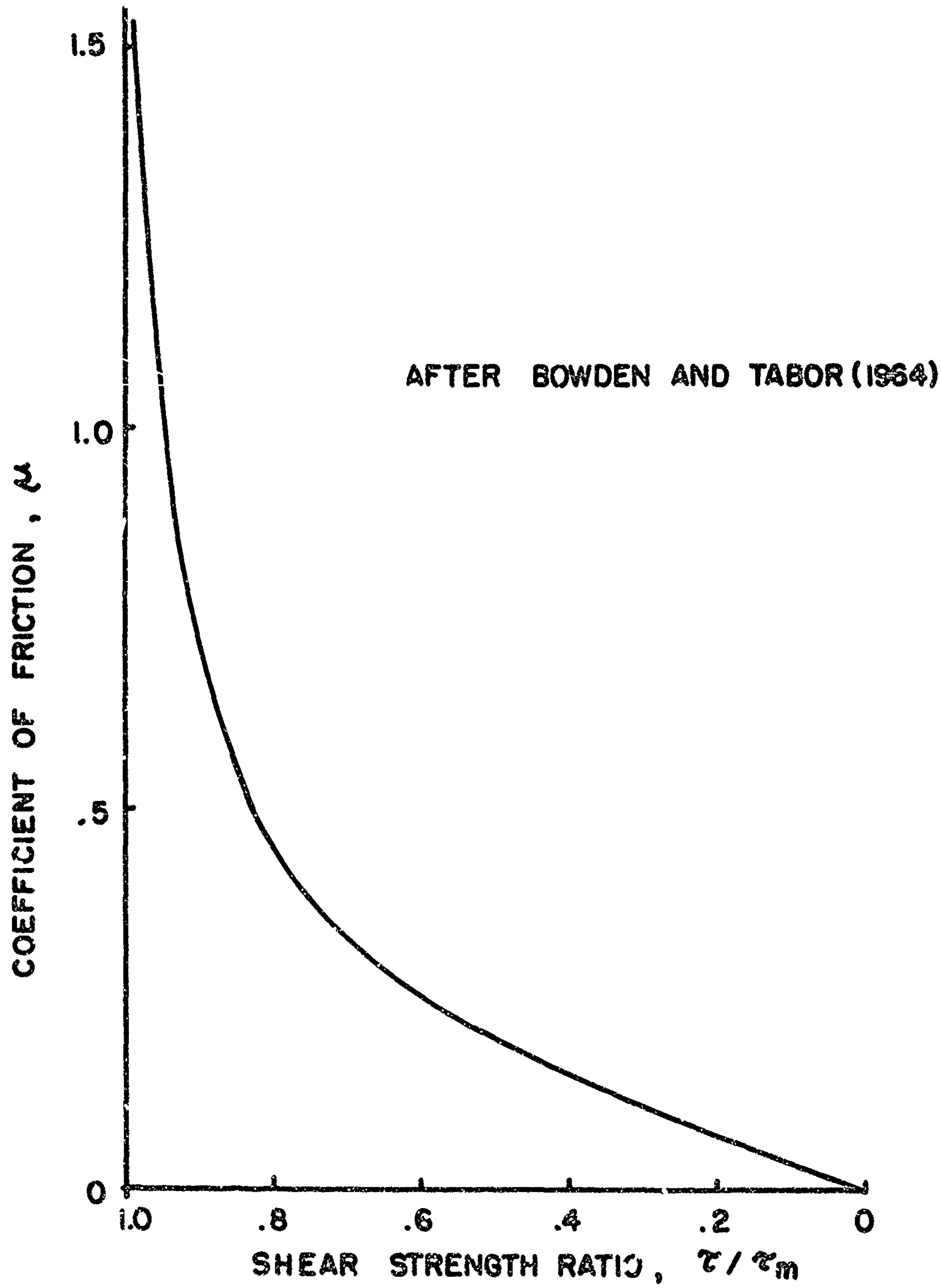

FIGURE 2.3

EXPLANATION OF COLD-WELDING

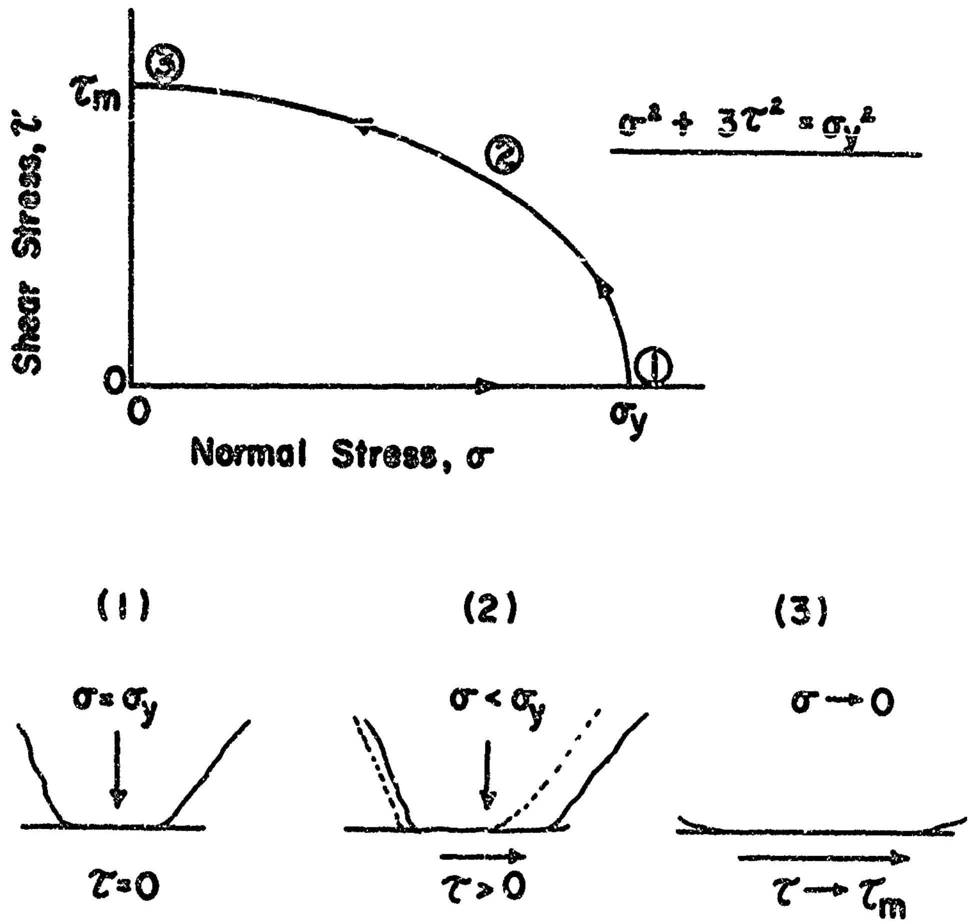

FIGURE 2.4

THE SURFACE OF QUARTZ

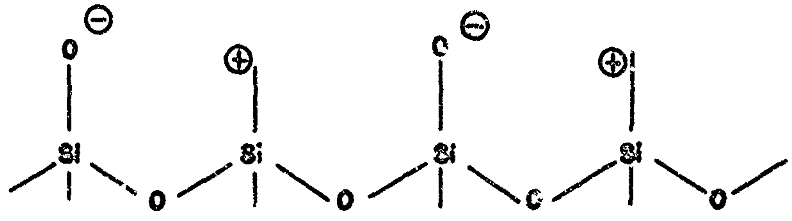

a) Freshly broken quartz surface

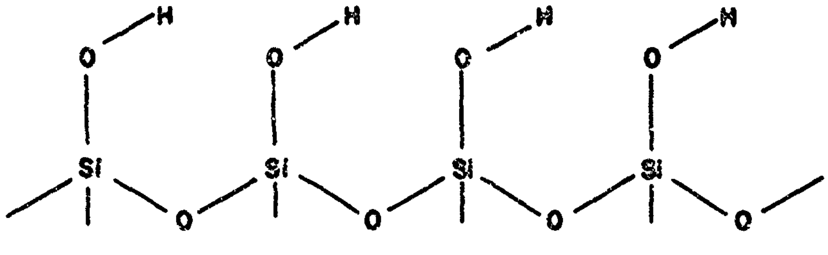

b) Hydrated quartz silanol surface

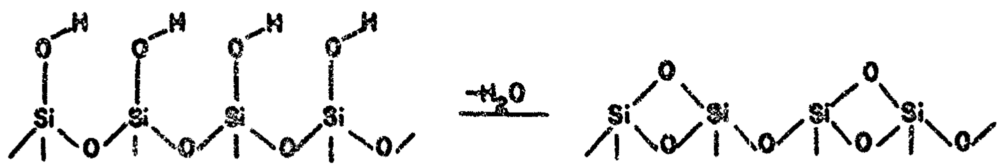

silanol surface | siloxane surface

c) Desorption of a quartz surface

FIGURE 2.5

PREVIOUS FRICTION RESULTS ON QUARTZ
(after Horn & Deere, 1962)

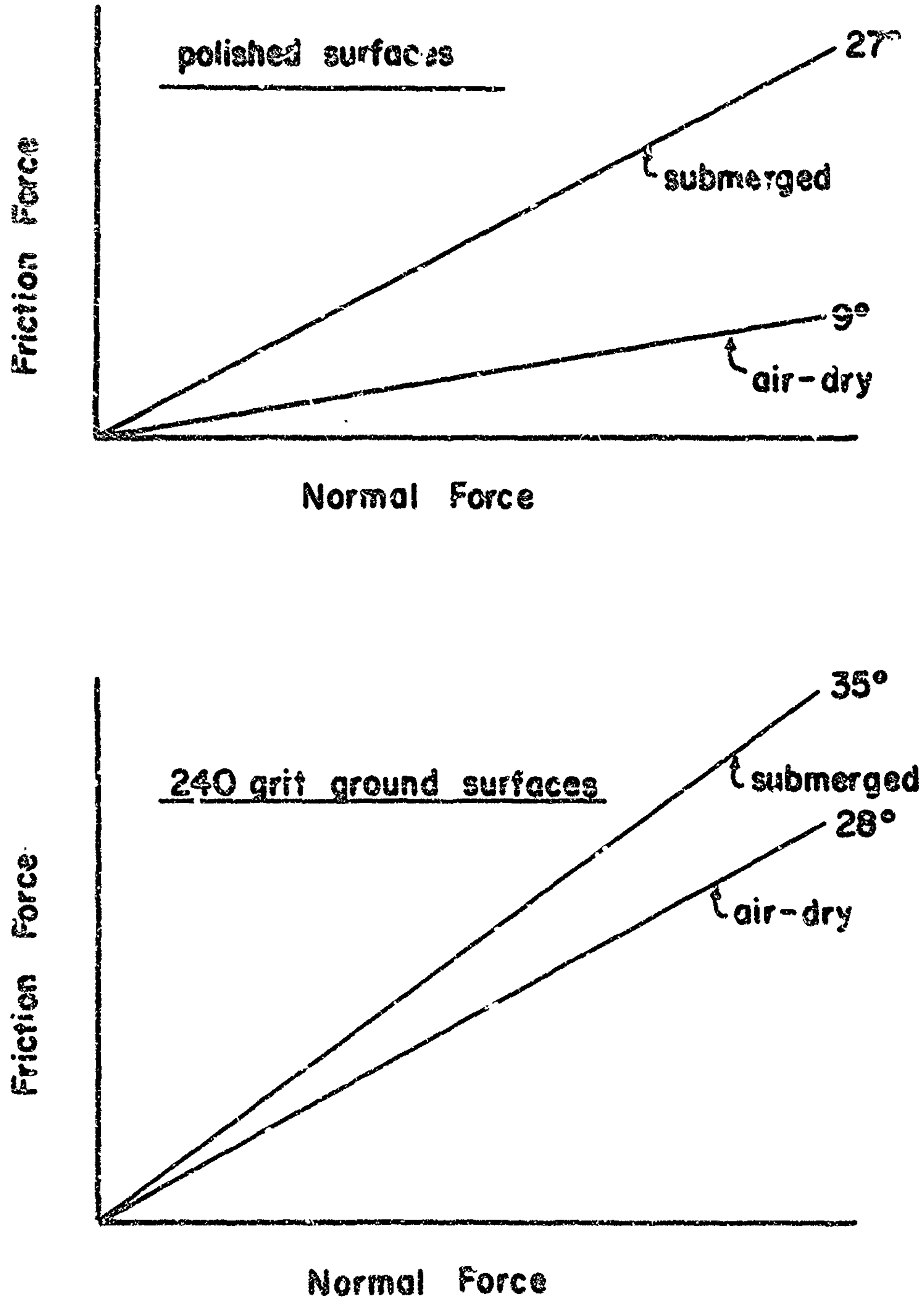

FIGURE 2.6

COMPONENTS OF SHEAR STRENGTH

'ter Rowe, 1962)

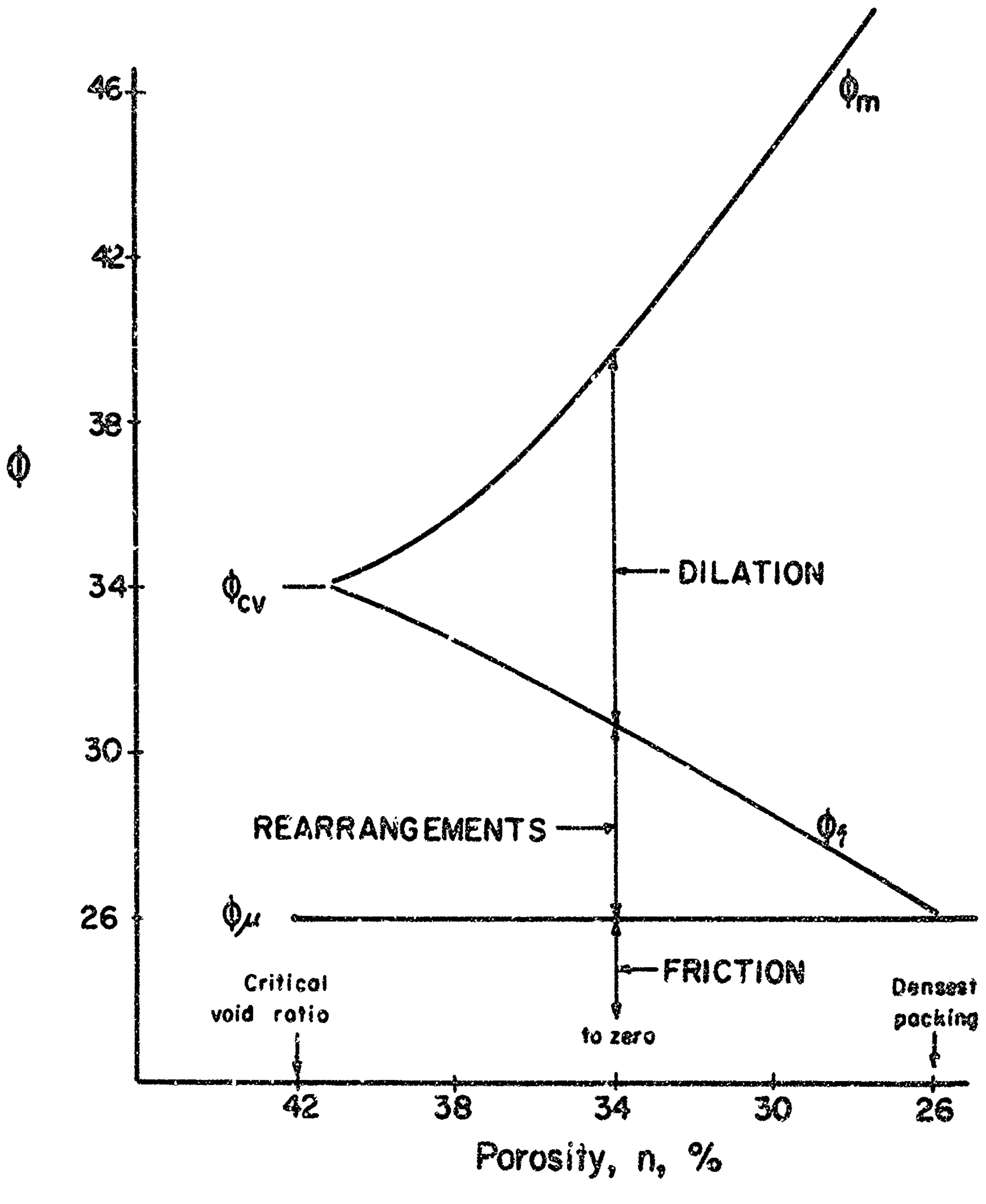

FIGURE 2.7

THEORETICAL CURVES RELATING ϕ_m AND ϕ_μ

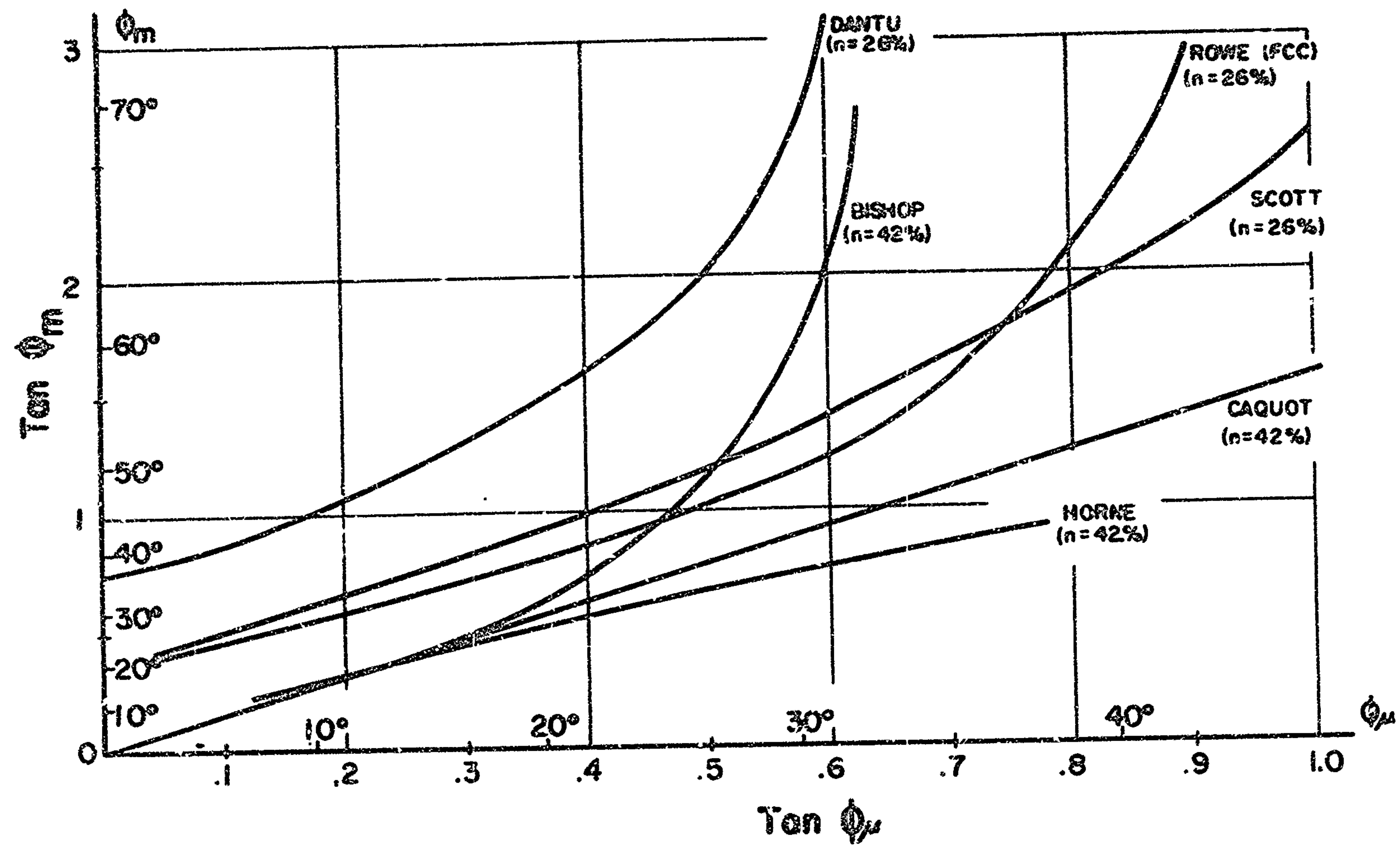

FIGURE 2.8

III. TEST APPARATUS AND PROCEDURES

Photographs of the test apparatus are shown in Figure 3.1. Figure 3.2 is a schematic drawing of the vacuum pump and shear device. Figure 3.3 shows the test chamber.

3.1 Vacuum Pumps

3.1.1 Ion Pump

A 20 liters/sec. Varian Associates ion pump was used to obtain high vacuums. The ion pump was assisted by a titanium sublimation pump with a speed of 400 liters/sec. for getterable gases (such as H_2O, O_2, N_2, CO_2).

The ion pump uses a high voltage discharge to ionize gas molecules and a magnetic field to aid in removing them from the system by immobilizing them at the pump cathodes. The pump uses no working fluid, thus minimizing contamination due to backstreaming. Any backstreaming that might occur would probably be low molecular weight gases. The continuous formation of an organic film, such as can occur with diffusion pumps,[1] is not possible.

The ultimate pressure of the ion pump is below 1×10^{-10} torr. The lowest gauge reading obtained in this investigation was 1×10^{-11} torr.[2]

3.1.2 Forepump

A Dresser mechanical vacuum pump was used to pump-down

---

[1] Holland (1964, p. 343) cites organic contamination growth rates of 5 Å/hr for diffusion-pumped systems.

[2] At these pressure levels the accuracy of any gauge can be seriously questioned. The problem of pressure instrumentation is discussed in Appendix B. Unless stated otherwise, pressure values are given as gauge readings throughout this report.

from atmospheric pressure to about 10^{-3} torr,[1] at which point the ion pump could be started. Three liquid nitrogen cooled glass traps were used in series to prevent contamination due to backstreaming of oil from the mechanical pump. Tests with wettable stainless steel strips showed that this system produced no measurable contamination after 24 hours of continuous pumping. Since a normal test involved only a 15 to 20 minute pumpdown period with the mechanical pump, it is felt that no significant contamination occurred in any of the reported tests..

3.2 Vacuum Chamber

The vacuum chamber was fabricated from a 6 inch O. D. stainless steel tee having 1/4 inch walls. The tee was supplied by Varian Associates with 6 side ports of 1 1/2 in. diameter. Varian also welded a 1/2 in. thick stainless steel plate to the interior of the chamber to serve as a support for mounting the shear box and friction sample holder. A schematic drawing of the chamber is shown in Figure 3.3.

3.3 Shear Box

The shear box is 3 in. I. D. x 0.75 in. high. It was constructed of 304 stainless steel. The bottom of the box was perforated with 1/4 in. dia. holes to facilitate outgassing of the sample. A porous stainless steel plate prevents soil from falling through the perforations.

To perform coefficient of friction measurements, a sample holder of the same size and with the same connections replaced the shear box. The friction tests were run on 1.5 in. square x 7/16 in. high blocks of material.

---

[1] Measured with an NRC thermocouple gauge.

3.4 Application and Measurement of Forces

Both the normal force and the shear force were fed into the vacuum using flexible stainless steel bellows, as shown in Figure 3.3. The normal force was applied by dead weight loading. For very light loads, stainless steel weights were placed directly on top of the shear box. Normal loads between 1 kg. and 50 kg. were used in these tests.

The shear force was applied by a variable speed transmission through a series of reducing gear boxes. The shear force in each test was measured both with a proving ring and a force transducer. The proving ring and force transducer could be read with an accuracy of about 50 gms. However, due to hysteresis (particularly in the stainless steel bellows) the shear force was only accurate to about ± 150 gms.

The shear force connection to the shear box was made with a length of flexible wire rope, which acted as an essentially moment-less connection.

The normal force and shear force were maintained vertical and horizontal, respectively, by using Thompson ball bushings, which have very little friction. Periodic calibrations were made both in air and vacuum to account for the friction in the device and for the bellows' spring constants.

3.5 Measurement of Displacements

Extensometers with 0.0001 in./division accuracy were used to measure shear displacement and height changes of direct shear samples. Only shear displacements were measured for the friction tests. All of these measurements were made outside of the vacuum chamber.

Due to elasticity in the connecting pieces and to seating effects, the recorded shear displacements do not reflect actual displacements of the shear box. In the direct shear tests, this was corrected by extrapolating the stress-strain curves back to the strain axis. In the friction

tests, it can be assumed that no displacement occurred except during slips (if stick-slip occurred) or until the load vs. time curve reached a maximum load (if no stick-slip occurred). Sliding would then commence and continue at this load.

At high temperatures, the apparent "seating effect" became more pronounced. The accuracy of measured displacements is therefore even poorer under these conditions.

Because the loading mechanism for the normal load was relatively rigid, the recorded height changes (hence calculated volume changes) are felt to be more accurate.

3.6 Heating

High temperatures were obtained by mounting 500 watt GE infrared lamps beneath the shear box (for direct shear tests) or at the height of the sample interface (for the friction tests). Variacs were used to adjust the voltage to the lamps in order to achieve desired temperatures. Temperatures in the direct shear tests were measured by means of a chromel-alumel thermocouple mounted approximately 1/2 inch inside the soil sample, parallel to the shear surface and about 1/8 inch below it.

For the friction tests, two lamps were used (one on either side of the test blocks) to achieve uniform heating. A calibration curve was obtained of heater voltage vs. temperature (measured 1/8 inch above the interface between the top and bottom blocks) in a dummy run. This calibration curve was used to reproduce the desired temperature in all of the high temperature friction tests.

As a check on the accuracy of this procedure, a skin-temperature thermometer was placed on the top flange of the vacuum chamber. During the calibration run, this thermometer was read to obtain a curve of T_{inside} vs. $T_{outside}$. In all of the high temperature tests, this thermometer read the same as had been obtained in the calibration run within $\pm 2°C$. For a sample temperature of 350°C, this thermometer read 67°C

in both the friction tests and in the direct shear tests, indicating good reproducibility of desired temperatures.

3.7 Pressure Measurement

The pressure level in the high vacuum tests was measured with a GE cold cathode gauge. The accuracy of this gauge is felt to be adequate for the pressure levels (10^{-8} to 10^{-10} torr) used in this investigation. Also, the cold cathode gauge can be read below 2×10^{-10} torr, the usual limit for Bayard-Alpert ionization gauges.

The GE gauge was calibrated against a Bayard-Alpert gauge in the 10^{-8} to 10^{-10} torr range. The results of this calibration, along with a further discussion of accuracy of pressure measurements, is given in Appendix B. In this report, the pressure levels given are gauge readings unless otherwise noted.

3.8 Cleaning and Handling Techniques

Carefully cleaning and handling techniques are an extremely important part of high vacuum technology. The most common contaminants are oil and grease from the hands. Therefore, nylon gloves or stainless steel tongs were used to handle anything that would be exposed to the vacuum.

The test surfaces for the friction tests were never allowed to touch anything after they had been cleaned until they were placed in contact in the test device.

The interior of the vacuum chamber and all pieces of equipment that would be exposed to the vacuum were cleaned periodically with detergents and chemical solvents and occasionally with an acid bath (40% HNO_3, 3% HF at 140°F for 20 minutes). Just before sealing the chamber prior to each vacuum test, it was wiped with acetone to remove any last traces of gross contamination.

The various cleaning techniques that were used for the direct shear and friction test samples will be described in the sections dealing with these tests.

ULTRA HIGH VACUUM CHAMBER
FOR FRICTION AND DIRECT SHEAR TESTS

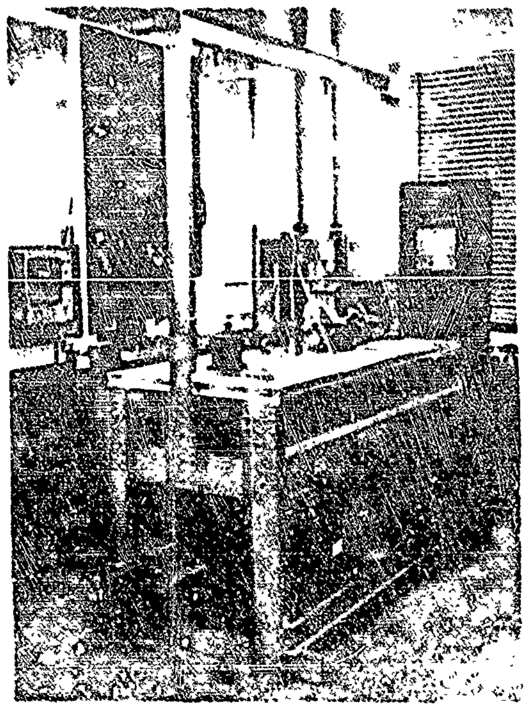

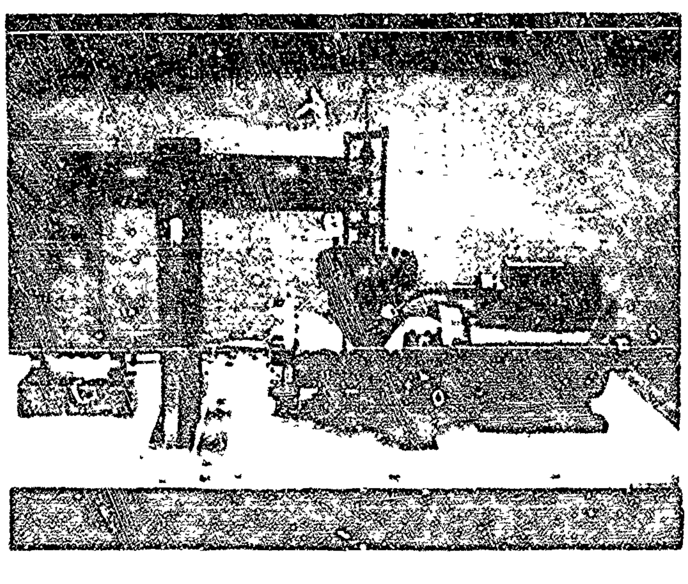

FIGURE 3.1

ULTRA-HIGH VACUUM DIRECT SHEAR DEVICE

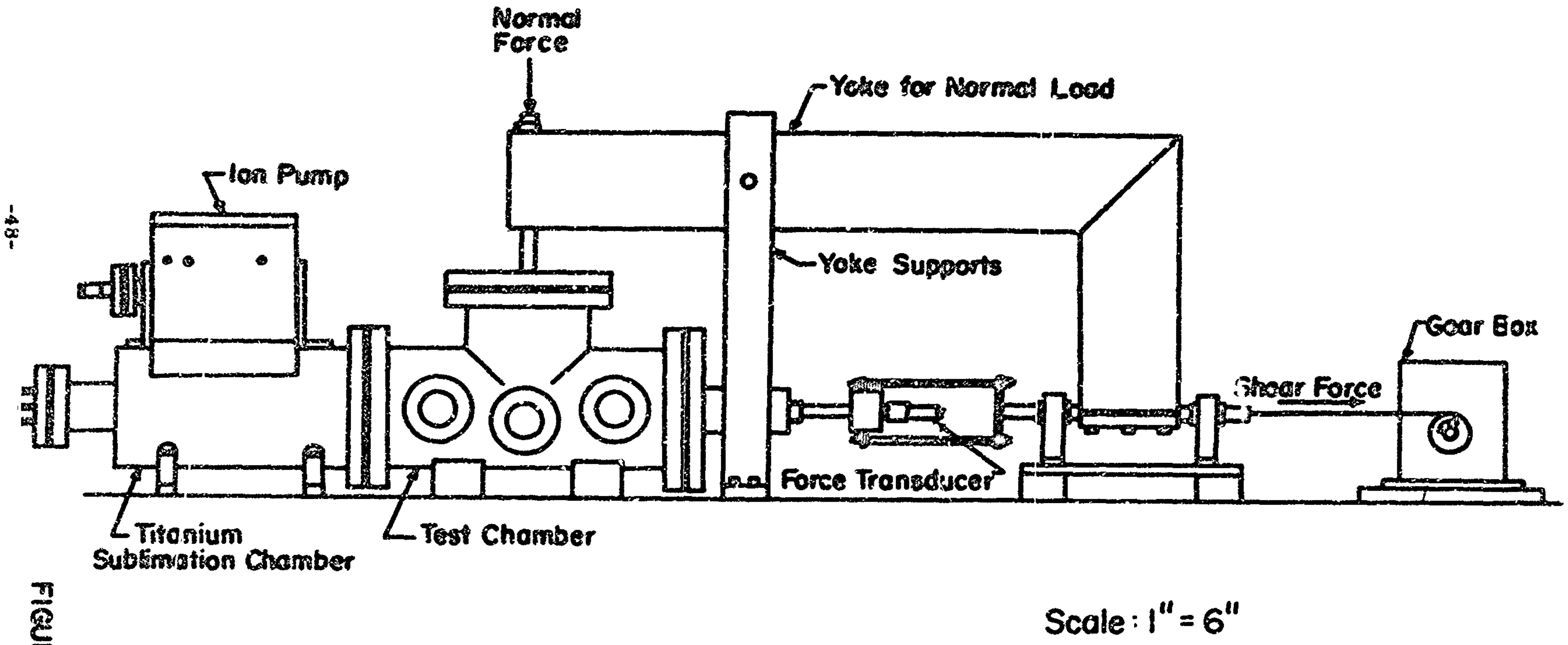

FIGURE 3.2

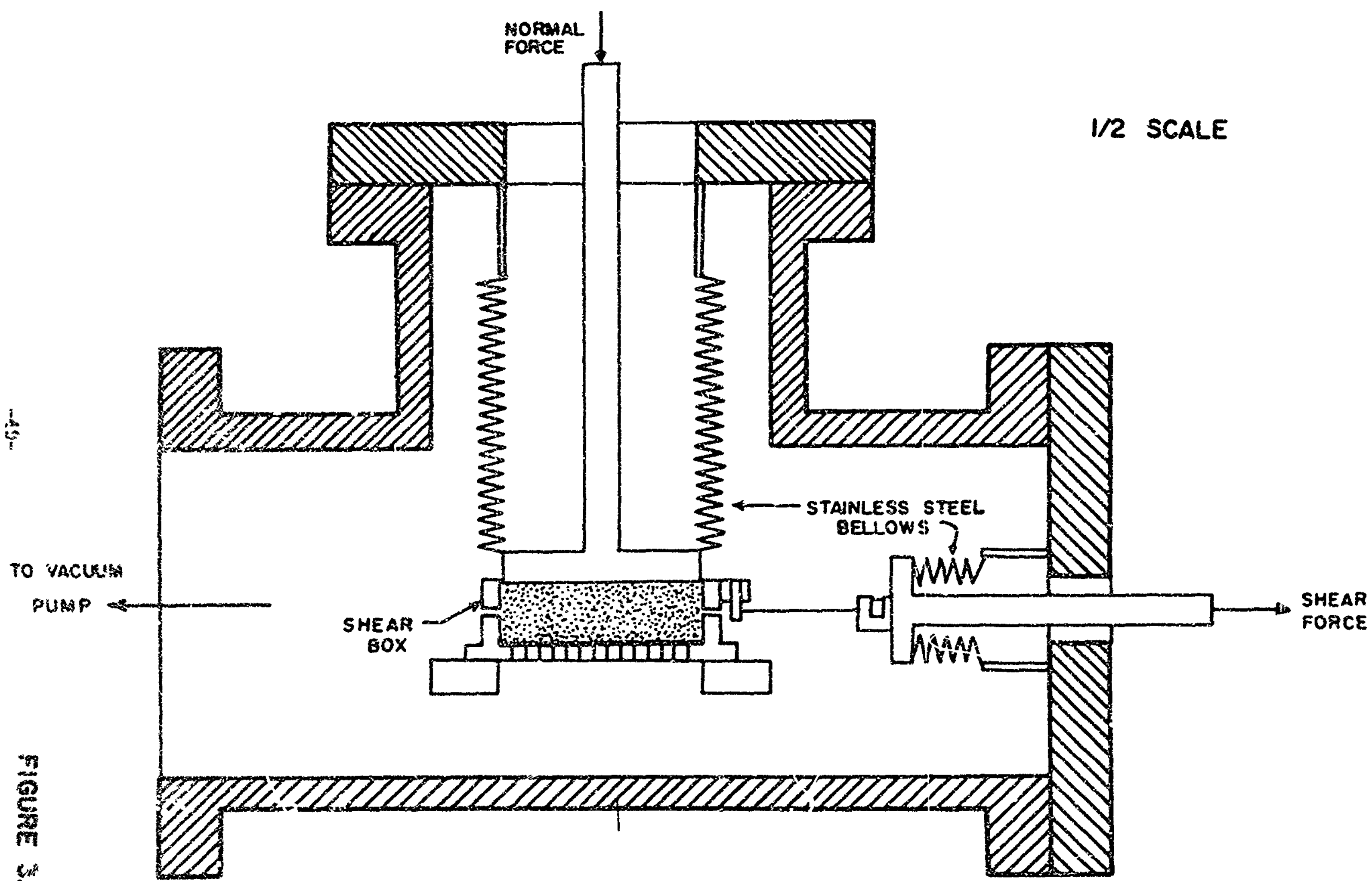

ULTRA-HIGH VACUUM TEST CHAMBER

FIGURE 3.3

IV. FRICTION TESTS ON SLIDING BLOCKS

4.1 Scope of Tests

Coefficient of friction measurements were made on blocks of material 1.5 in. x 1.5 in. square. Atmospheric tests were run on 304 stainless steel, Westerley granite, and quartz. The effects of cleaning procedure and submergence in distilled water were investigated in these tests.

High vacuum-high temperature tests were run on quartz samples with two surface roughnesses and varying amounts of pre-cleaning.

4.2 Test Specimens

4.2.1 Materials Used

High purity quartz crystals were supplied by Western Electric.[1] These crystals are carefully grown to meet the exacting requirements of piezoelectric applications. They have fewer impurities and imperfections than natural quartz crystals. Two sets of friction specimens could be prepared from each crystal, which was approximately 5 in. x 2 in. x 2 in. in size.

Tests were also run on Westerley granite specimens cut from a single rock piece[2] and on machined and polished specimens of 304 stainless steel.

4.2.2 Specimen Preparation

The quartz samples were cut from the crystals so that the test surface was parallel to the seed plane.[3] The finished specimen size was

---

[1] Merrimack Valley Works, North Andover, Massachusetts.

[2] Supplied by J. Byerley, M.I.T. Geology Department

[3] Cutting and finishing of the quartz and granite specimens was done by Ceramics Grinding Co., Inc., Waltham, Massachusetts.

1.498 in. square by 7/16 in. high. The top specimen was chamfered 1/16 in. around the edges of the test face so that an overhang would not occur when the top specimen began sliding over the bottom one.

Two finishes were used for the test faces. The first, designated smooth, was obtained by grinding with a No. 600 grit diamond wheel. The surfaces were essentially mirror smooth, giving specular reflection of light. Also, interference fringes could be seen when two such surfaces were put together. This indicates that the surface asperities were no larger than about 1/4 the wave length of light, or about 1000 Å (4 micro inches).

The second finish, designated rough, was obtained by grinding with a No. 220 grit diamond wheel. The surfaces appeared frosted and did not give specular light reflection.[1] It is felt that these surfaces gave a fairly good representation of the surface roughness of sand grains, which appear similarly frosted under low power microscopic examination.

4.2.3 Cleaning Techniques

Two cleaning techniques were generally used for the friction tests. These have been designated normal cleaning and chemical cleaning.

Normal Cleaning Normal cleaning consisted of a good washing with laboratory detergent,[2] followed by rinsing with distilled water and drying at 110°C. If there was any likelihood of prior organic contamination the specimens were cleaned with acetone before the detergent wash.

This is essentially the same cleaning procedure used by Horn (1961) and by many other investigators. In addition, polyethylene gloves were worn during the cleaning process. The clean specimens were

---

[1] The average roughness of these surfaces was probably about 40 micro inches (10,000 Å). This is the value obtained for granite surfaces ground with a No. 240 carborundum wheel [J. Byerley (private communication, 1965)].

[2] Lakeseal Laboratory Glassware Cleaner

handled with stainless steel tongs and care was taken to see that nothing contacted the test surfaces prior to putting them together.

Chemical Cleaning A more effective cleaning procedure, using chemical solvents and de-greasers, was developed during this investigation. This cleaning procedure was based, to a large extent, on the techniques used to maintain clean surfaces for ultra-high vacuum work.[1]

The following steps were used in the chemical cleaning procedure:

1. Trichlorethylene rinse
2. Acetone rinse
3. Detergent wash
4. Distilled water rinse
5. Methyl alcohol rinse
6. Acetone rinse

Polyethylene gloves were used to handle the specimens through step 4. Thereafter, only stainless steel tongs were allowed to touch them. Immediately after step 6 the specimens were mounted in the testing device to minimize atmospheric contamination. Since the acetone readily evaporates at room temperature no final drying step was required.

4.3 Application and Measurement of Forces

4.3.1 Normal Force

The normal force for the friction tests was applied by stacking nested dead weights on the top specimen. The specimen holder centered the weights and prevented any tilting or cocking.

The range of normal loads used generally varied from 3.65 to approximately 16 kg. (see footnote 2 below). For the vacuum tests,

---

[1] The cleaning techniques were to a large extent suggested by Varian Associates (Vacuum Products Catalog, 1964) and by Holland (1964, Ch. 5)

[2] A load of 44 kg. was used in two of the stainless steel tests.

stainless steel weights were used to minimize contamination.

4.3.2 Shear Force

The connections for the shear force and the method of application were described in Section 3.4. The shear force was measured with both a proving ring and a force transducer in each test. The force transducer was generally connected to an x-y recorder that gave a continuous trace of the shear force. Shear displacements were measured with an extensometer that had 0.0001 in. divisions.

4.3.3 Accuracy of Force Measurements

The normal load, which was applied by dead weights, was accurate to ± 50 grams. The accuracy of measuring the shear force--about ±150 grams--was limited by hysteresis in the bellows. At the lightest normal load (3.65 kg.) this sets a limiting accuracy on the friction measurements of $\Delta\mu = \pm 0.04$ or $\Delta\phi_{\mu} = \pm 2°$. Thus a great deal of significance should not be attached to small changes in μ for tests at low normal loads. At higher loads the accuracy is $\Delta\phi_{\mu} = \pm 1°$ or better.

4.4 Test Procedure

After cleaning, the specimens were mounted in the test chamber. They were then separated slightly and a stream of helium gas was blown between them to remove any dust that might have been on the surfaces. The top and bottom specimens were then re-aligned, the shear force connection was made, and the normal load applied. The test was then run if it was an atmospheric test. If a vacuum test was being run, the chamber was sealed and pumpdown began.

The shear displacement was generally applied at a rate of 0.01 in./minute. The friction did not appear to vary with rate of strain, as variations of a factor of 10 in several tests did not alter the shear force readings.

At the completion of a test, the normal load was removed and the test specimens were either removed or, in many cases, separated and returned to the initial position for running a new test. If a second test were to be run on the same surfaces, a stream of helium was again blown between the surfaces to remove any loose particles.

4.5 Results of Friction Tests on Quartz in the Atmosphere

4.5.1 Smooth Quartz

The results of the atmospheric friction tests on smooth quartz surfaces are shown in Figure 4.1 and Table 4.1. Table 4.1 also describes the surface treatment for each test. Tests within a group (such as F-13, F-14, and F-15) were successive runs without any cleaning between tests. Tests F-3 through F-8 were run on the same surfaces. After test F-8 a new top specimen was installed and tests F-10 through F-18 were run.

4.5.2 Rough Quartz

The results of the atmospheric friction tests on rough quartz surfaces are shown in Table 4.2, along with a brief description of the surface treatments, and in Figure 4.2. All of the tests (F-19 through F-41) were run on the same surfaces. However, prior to test F-27 the specimens were etched in an acid bath, which produced a visible increase in frostiness (hence roughness) of the surfaces. Tests F-27 through F-41 were run on these etched surfaces.

4.6 Results of Friction Tests on Quartz Under High Vacuum and High Temperature

Table 4.3 shows the results of the high vacuum-high temperature friction tests on quartz. Figure 4.3 presents a graphic comparison of atmospheric and vacuum tests.

A new set of specimens was used for each of the vacuum tests except test Q-6, which used the same specimens that had been used for

test Q-3. Except for tests Q-1 and Q-2, an atmospheric test was run prior to evacuation in order to provide a direct comparison of the effect of vacuum and temperature on friction. The atmospheric μ values for tests Q-4 and Q-6 do not agree, although both samples were prepared by the normal cleaning procedure. This procedure does not remove all of the surface contamination, hence the actual surface cleanliness varies from test to test depending on the prior contamination of the surfaces.

4.7 Results of Friction Tests on Stainless Steel

Table 4.4 shows the results of atmospheric friction tests run on polished specimens of 304 stainless steel. All of the tests (S-1 through S-13) were run on the same surfaces. However, prior to test S-8 the specimens were cleaned in an acid bath that also appeared to increase the surface roughness. Succeeding tests were run on these lightly etched surfaces.

4.8 Results of Friction Tests on Granite

The results of atmospheric friction tests on smooth granite specimens are shown in Table 4.5. All of the tests (G-1 through G-8) were run on the same surfaces. The reported μ values, except for the first test, were greatly affected by this multiple testing. Therefore, these results are only presented for comparison purposes with the quartz tests.

4.9 Recorder Traces

Figures 4.4 through 4.10 are typical traces from the x-y recorder during friction tests. The x-axis was set for a 50 sec./in. time sweep. Displacement readings from the extensometer were marked on the trace during the test.[1] Thus the figures show a load vs. displacement curve. Calculated values of μ are written on the trace at pertinent points. These values do not always agree exactly with those given in

[1] Due to seating effects and elasticity in the shear force mechanism, actual displacement of the two surfaces did not, in general, occur until about .0175 in. displacement had been recorded. For those tests showing marked stick-slip, the first slip can be taken as the point at which displacement began.

the tables, as the tabulated values are an average of the proving ring and x-y recorder readings.

4.10 Discussion of Results

4.10.1 Friction of Quartz in the Atmosphere

4.10.1.1 Effect of Surface Cleanliness

The friction tests on quartz clearly illustrate the dominant role that surface cleanliness plays in determining the friction values that are measured. Essentially all of the changes in friction that were measured can be most satisfactorily explained in terms of changes in surface cleanliness. The marked effect of surface cleanliness on the friction of smooth quartz surfaces is shown in Figure 4.1 and in Table 4.1. Chemically cleaned surfaces gave values of $\mu = 0.73$ and $\phi_{\mu} = 36°$, which are much higher than the values normally obtained for quartz. Surfaces that had been chemically cleaned and then dried at 110°C for 15 min. gave $\mu = 0.46$ ($\phi_{\mu} = 25°$). This indicates that contamination of a very clean surface occurs quite rapidly. Further tests need to be run to delineate the effects of time and oven temperature on μ. However, it appears that the low friction values measured by previous investigators may in part have been a result of the elevated drying temperatures and long drying times that were used.

Normally cleaned smooth surfaces gave $\mu = 0.31$ ($\phi_{\mu} = 16°$).[1] A low value of μ was also obtained for chemically cleaned surfaces that were allowed to air-equilibrate in a covered container for 12 days, as shown in Table 4.1 (Tests F-42, F-43). For these surfaces, μ was 0.36 ($\phi_{\mu} = 19°$), indicating progressive contamination due to contact with atmospheric gases.

---

[1] This is an average value. Since normal cleaning did not remove all surface contamination, the value of μ obtained by this cleaning technique varied with the amount of contamination on the surfaces before they were cleaned.

Throughout most of this investigation it was assumed that the value of $\mu = 0.73$ was the maximum that could be achieved for smooth quartz surfaces. However, after it was discovered that Hardy [Hardy and Doubleday (1922)] had obtained a similar value, part of his cleaning procedure (scrubbing the surfaces under running water),[1] was incorporated into the chemical cleaning procedure for test Q-3a (Table 4.3). A value of $\mu = 0.86$ was obtained. This test was repeated, with the same result, prior to closing the chamber and running the vacuum test. There is no assurance that even this value is the maximum obtainable. A more effective cleaning procedure may produce still higher friction.

The range of μ values for rough quartz surfaces is much less than for smooth surfaces. This may have important practical implications, since soil particles all have rough surfaces, not mirror-smooth surfaces. Table 4.2 shows that a chemically cleaned rough quartz surface gave $\mu = 0.46$. After additional cleaning, μ increased to 0.61 ($\phi_\mu = 31°$), which is the maximum value that was obtained. It is interesting to speculate why, with the same cleaning, the rough surfaces gave lower values of μ than the smooth surfaces, since the opposite behavior might be expected. However, the lower μ values for clean rough surfaces were consistently observed, even in the high vacuum-high temperature tests.

There are two reasonable explanations for this behavior. The first is that the rough surfaces were not as clean as the smooth surfaces, even though they had received the same treatment. Hardy (1919) found that smooth glass surfaces gave higher values of μ than ground glass and concluded that it was not possible to clean the ground glass as effectively as the smooth glass.

The second explanation is that the rough surfaces had a smaller contact area than the smooth surfaces. Since both types of surfaces (when clean) showed no marked dependence of μ on normal load (as discussed

---

[1] Hardy rubbed the surfaces with his fingertips. A nylon brush was used by the author.

in Section 4.10.1.4), the contact area must have been essentially proportional to the normal load for both rough and smooth surfaces. Thus there is no reason to expect the contact areas were very different. Therefore the best explanation for the higher friction of chemically cleaned smooth surfaces is that they were cleaner than the rough surfaces.

Attempts to produce higher μ values for rough quartz surfaces by acid etching produced an even lower μ. Although the etched surfaces were visibly rougher, μ was only about 0.50. The effect of etching on the surface structure of quartz is not known,[1] but it does not appear to increase the surface cleanliness above what is produced by chemical cleaning.

4.10.1.2 Effect of Surface Roughness

As discussed in the previous section, the effect of surface roughness cannot be separated from the effects due to cleanliness of the surface. If both a rough and a smooth surface could be prepared with the same cleanliness, the rougher surface generally should have a higher coefficient of friction (see Section 2.3.2).

Subjecting the two surfaces to a rigorous chemical cleaning treatment does not appear to produce the same cleanliness since the smooth surface has a higher μ. If both surfaces are exposed to atmospheric contamination, however, the rougher surface will show a much larger μ (Tests F-38 to 41 vs. F-42 and F-43). Atmospheric contamination is very effective in reducing the friction of a smooth surface. Because the contamination is a thin layer and acts as a boundary lubricant, it is rather ineffective on a rough surface. Thus the higher value of μ for the rough surface is primarily a result of its being poorly lubricated.

---

[1] Etching may produce a porous surface, similar to a glass surface that has been chemically attacked. Adsorption on and in such a surface may be the key to explain its unusual friction behavior. Support for this point of view appears to be provided by the large decrease in μ (to 0.39) when the surfaces were submerged in water.

Until an independent means can be found for measuring surface cleanliness, there does not appear to be any way to study the effect on μ of the surface roughness alone.

4.10.1.3 Effect of Water

Water does not change the friction of a chemically cleaned quartz surface, as shown in Figures 4.1 and 4.2. Water increases the value of μ for normally cleaned smooth surfaces. Both of these observations agree with Hardy's (Hardy and Hardy, 1919) results on glass. The second observation also agrees with Horn's (1961) results on polished quartz. The effect of water on a normally cleaned surface is to disrupt the adsorbed boundary lubricant, hence reducing its effectiveness. On a chemically cleaned surface, the amount of contamination is small, and water does not change the friction value.

The effects of water on the friction of quartz must involve its ability to change the surface cleanliness. Explanations involving viscosity or capillarity clearly cannot explain the fact that water can 1) increase, 2) decrease, or 3) not alter friction values depending on previous surface treatment. In this regard, it is interesting to compare the effects of water on the friction of quartz and stainless steel:

Condition	Effect of water on μ	
	Quartz	Steel
contaminated	μ increases	no change
chemically cleaned	no change	μ decreases

Water is intrinsically a lubricant for stainless steel. If the steel is already lubricated (contaminated), then water has no effect. For quartz, water is intrinsically neutral. However, if the surface is contaminated, an apparent anti-lubricating effect of water is observed.

4.10.1.4 Effect of Normal Load

In one series of tests (F-10, F-11, F-12) on smooth quartz (Table 4.1), ϕ_μ decreased from 15° to 8° with increasing load. These surfaces were contaminated with oil, which acted as a very effective boundary lubricant. Decreasing values of friction with increasing load have been previously observed for boundary lubricated surfaces under very light loading (Bowden and Tabor, 1950, p. 109). No significant variation of μ with normal load was found in any of the other tests.

The normal stresses, based on total area, were rather low in these tests.[1] Horn (1961) and other investigators have used hemispherically shaped sliders or chips, thereby producing high pressures. By using low values of $\frac{N}{A}$, elastic deformation of the contacts, rather than plastic deformation might be expected. Also, lower pressures might not cause penetration of contaminating surface films. Both of these effects probably would produce a load-dependent friction coefficient. Except for the aforementioned oil-contaminated tests, there is no evidence that either of these phenomena occurred in this investigation.

4.10.1.5 Effect of Multiple Testing of Same Surface

The surfaces used in these tests were prepared by a commercial grinding company, using diamond wheels. Because the grinding procedure was very time-consuming, several tests were run on a given surface before it was re-ground.

The first test program on smooth quartz surfaces (Tests F-3 through F-18) indicated that multiple testing of the same surface did not significantly influence the results. There are several indications that

[1] The total area of the sliding block was approximately 12.3 cm.^{2} The normal pressure ($\frac{N}{A}$) therefore varied from .3 kg/cm^2 to 1.3 kg/cm^2. However, since actual contact only occurred over a small fraction of the total area, the contact pressures were very high (probably 10^6 psi or so).

this was the case:

1. The μ values were reasonably reproducible within any given test series.

2. No visible wear of the surfaces was observed on any of the quartz surfaces involved in multiple tests.

The most convincing evidence of the validity of multiple tests on quartz is actually provided by the test series on smooth granite surfaces (Table 4.5). Clearly, multiple testing of the granite surfaces did not give reproducible results. The friction increased with each slip in a given test and also increased with each successive test. Figure 4.5, the recorder trace from granite Test G-4, shows how μ increased with each slip. This is probably due to progressive surface damage, such as gouging of the feldspar portions of the surfaces by the harder quartz portions of the opposing surface.

Figure 4.6 shows a typical recorder curve for a quartz surface. The friction is essentially constant for each slip. In many of the quartz tests, the friction actually decreased after the first slip, as shown in Figure 4.7. Some of the quartz tests, particularly those involving smooth surfaces under water, did show increasing friction with increasing shear displacement.[1] However, all of these tests eventually reached an equilibrium value of μ, beyond which μ did not increase. This behavior probably indicates that sliding produced further cleaning of the surfaces.

Figure 4.4, the recorder trace for stainless steel Test S-8, shows a very marked dependence of μ on the shear displacement. In

[1] For example, see Tests F-4, F-7, F-8, F-17 and F-18 in Table 4.1.

this test the surfaces were clearly seizing and then being gradually sheared until they seized again. It is hard to define a single coefficient of friction for the behavior shown in Figure 4.4. Fortunately, in the quartz tests an equilibrium value was reached and this equilibrium was taken as μ. In those tests where the first peak was higher than subsequent peaks, the first peak was taken as μ.

4.10.2 Friction of Quartz in High Vacuum

The curves in Figure 4.3 show that the coefficient of friction of quartz in vacuum depends greatly on 1) the cleanliness of the surfaces prior to evacuation and 2) whether or not a bake-out was used. This points out that there is not an unique value of μ for quartz in a high-vacuum environment.

4.10.2.1 Effect of Vacuum on Friction

Tests Q-1 and Q-6 show the effect of 10^{-8} to 10^{-9} torr vacuum[1] alone on the friction of quartz. Both of these tests were run at room temperature, with no elevated temperatures (bake-out) used at any time. The friction was essentially the same in vacuum as in air. That is, vacuum alone did not produce any increase in the coefficient of friction. This is interpreted to indicate that vacuum alone is not sufficient to remove contamination from quartz surfaces.

4.10.2.2 Effect of High Temperature Bake-out

The use of elevated temperatures, in conjunction with high vacuum, produced marked increases in the coefficient of friction. Test Q-2,

---

[1] The vacuum level in these tests was the ultimate that could be obtained without using a bake-out to reduce surface outgassing within the chamber. Since the intent was to study the effect of vacuum alone, bake-outs were not permissible.

run at 1×10^{-8} torr and 350°C, gave $\mu = 1.01$, the highest coefficient of friction for quartz that was recorded in this investigation. In Test Q-3 a modification of the chemical cleaning procedure was used, producing an atmospheric value of $\mu = 0.86$.[1] This was the highest atmospheric value of μ for quartz that was recorded. Subjecting this surface to 10^{-8} torr and 350°C did not significantly increase μ. The reason for this behavior is not known. All of the other vacuum tests at high temperatures gave increases in ϕ_μ of about 7° (Fig. 4.3).

4.10.2.3 Effect of Initial Cleanliness

The coefficient of friction in vacuum (and also in high temperatures) was very dependent on the cleanliness of the surfaces prior to evacuation. Chemically-cleaned smooth surfaces gave $\mu \cong 1.0$ at 10^{-8} torr and 350°C. However, normally cleaned surfaces under the same conditions only gave $\mu = 0.47$. This shows that the cleaning effect of the vacuum and elevated temperature is not sufficient to remove all of the contamination that remains after a normal cleaning procedure. It is not possible, therefore, to take an initially dirty specimen and produce a very clean one by baking it at 350°C in a high vacuum.

These conclusions must be tempered somewhat, since the test surfaces were not separated during evacuation and bake-out. There was no indication that the surfaces were not completely outgassed,[2] but neither is there any assurance that they were outgassed as completely as separated surfaces would be. Therefore, the increases in friction that were observed may not represent maximum obtainable values. Also, it

---

[1] The atmospheric test was repeated to verify this μ value. These tests are designated Q-3a and b in Table 4.3.

[2] For example, no pressure rise was ever noted at any time while shearing a friction test. If the surfaces were not completely outgassed, at least a small, momentary pressure rise would have been expected.

is felt that even higher values of friction might be produced by combinations of

1. increased initial cleanliness
2. better vacuum
3. higher temperature

4.10.2.4 Effect of Surface Roughness

Only one high vacuum-high temperature test was run on a rough quartz surface (Test Q-5). However, the results of this test confirm the general pattern of the other tests. μ increased from 0.58 in the atmosphere to 0.77 at 10^{-8} torr and 350°C for a chemically cleaned surface.

The high vacuum-high temperature friction for rough surface is less than for a smooth surface (Test Q-2 vs. Q-5). This is the same trend that was observed in the atmospheric tests. It points out again the impossibility of studying the effects of surface roughness independent of surface cleanliness.

4.10.2.5 Discussion of Recorder Traces

Figures 4.8, 4.9, and 4.10 are recorder traces from three of the vacuum tests (Q-3, Q-4, and Q-5 respectively). They illustrate the types of behavior that were observed after the first slip.

Test Q-3 is representative of the vacuum behavior of the chemically cleaned smooth surfaces (Test Q-1, Q-2, and Q-3). The friction in these tests showed a very large decrease after the first peak. Since similar drops in friction after the first peak were not observed in the atmospheric tests, this behavior is difficult to explain. It may be that the friction results in the high vacuum-high temperature test are not reliable after the first slip (due to surface damage resulting from rupture of the strong bonds). Since the surface conditions after the first slip are completely unknown, most friction investigations of this type report only the first peak, and do not try to interpret the subsequent behavior.

Figure 4.9 shows the recorder trace from a normally cleaned

smooth quartz surface. The friction did not decrease with increasing displacement, but was essentially constant. Figure 4.10 shows the recorder trace from a chemically cleaned rough surface. In this test the friction decreased somewhat with increasing shear, but not so markedly as with the clean smooth surfaces.

Figure 4.10 also shows that a small slip occurred at $\mu = 0.52$, after which the surfaces seized and, except for another minute slip, did not shear further until $\mu = 0.78$. A similar small slip at $\mu \cong 0.5$ was observed in all of the high vacuum-high temperature tests. This probably indicates that the initial contact points were not as clean as the rest of the surfaces. Thus a small slip from the initial position would cause contact with cleaner areas of the surface and lead to increased values of μ.

4.10.3 Summary of Friction Results on Quartz

The most obvious conclusion from the friction tests on quartz is that the frictional behavior is far from simple. No single value of μ can be assigned to quartz. The experimental conditions (environment, surface treatment, cleaning procedure, etc.) must be carefully defined. Even though a great deal of effort was devoted to defining the experimental conditions as carefully as possible, major unknowns regarding the actual state of the surfaces at the time of testing limits the interpretation of the results from a fundamental point of view.

Several general observations can be made, however:

1. The coefficient of friction of quartz depends greatly on the cleanliness of the surfaces. All of the results obtained in this investigation lead to this conclusion. There seems to be no other way to explain the fact that the friction could be made to increase or to decrease merely by altering the cleaning procedure. Figure 4.11 summarizes the available

friction results on smooth quartz surfaces. The friction varies from 8° to 43°, depending on the surface treatment and the test conditions.

2. The effects of surface roughness on friction cannot be studied independently of surface cleanliness. The same cleaning procedure does not appear to produce the same surface cleanliness on both smooth and rough surfaces. This leads to lower values of friction for a chemically cleaned rough surface than for a smooth surface.

3. The range of friction values for rough surfaces is much smaller than for smooth surfaces. If an indiscriminate average is taken of all of the ϕ_μ values for rough surfaces in Table 4.2, a value of 27.3° is obtained, with a standard deviation of 0.7°. This value agrees very well with Horn's value of 28° for rough surfaces, and also with Rowe (1962), who found $\phi_\mu = 26° \pm 4°$ depending on grain size. ϕ_μ for rough surfaces at 10^{-8} torr and 350°C increases to 38°.

4. Since the surfaces of cohesionless soils are invariably rough, the use of $\phi_\mu = 26°$ to 28° appears to be reasonable. It does not seem likely that ϕ_μ for quartz soil particles will exhibit the large fluctuations that can be produced on smooth quartz surfaces.

5. Elevated bake-out temperatures must be used in conjunction with high vacuum to increase the friction of quartz. Vacuum alone is not effective.

6. The value of μ that is obtained in high vacuum-high temperature tests depends greatly on the cleanliness of the surfaces prior to the high vacuum-high temperature treatment.

TABLE 4.1 RESULTS OF ATMOSPHERIC FRICTION TESTS ON SMOOTH QUARTZ SURFACES

TEST NO.	TREATMENT	N(kg)	μ	ϕ_μ	REMARKS
F-3	Chemically cleaned	3.65	0.73	36°	
F-4		6.65	.69	35°	1st peak
			.76	37°	5th peak
F-5	Rinse with Me OH and acetone--dry at 110°C for 15 min.	3.65	.44	24°	no stick slip
F-6		6.65	.48	26°	small slips
F-7	Rinse with Me OH and acetone--submerge in H_2O	3.65	.75	37°	equilibrium value after 2 slips
F-8		6.65	.77	38°	equilibrium value after [illegible] slips
F-10	New top block--Surfaces contaminated with oil, then wiped with clean cloth	3.65	.26	15°	stick slips (all tests)
F-11		6.65	.21	12°	
F-12		16.21	.14	8°	
F-13	Scrub with acetone-soaked cotton, wash with detergent, rinse with distilled H_2O, dry at 110°C for 1 hour.	3.65	.33	18°	no stick slip
F-14		6.65	.33	18°	no stick slip
F-15		16.21	.29	16°	stick slip
F-16	Let sit overnight	6.65	.30	17°	small slips
F-17	Submerge in H_2O	6.65	.31	17°	sliding began
			.44	24°	after sliding .07"
			.51	27°	stick slip began
			.55	29°	equilibrium value (.10")
F-18		16.21	.40	22°	1st peak
			.65	33°	equilibrium value (.05")
F-42	New surfaces--lab equilibrated for 12 days in covered container	7.48	.35	19°	one peak, then sliding w/o slips
F-43		13.71	.37	20°	small slips

TABLE 4.2 RESULTS OF ATMOSPHERIC FRICTION TESTS ON ROUGH QUARTZ SURFACES

TEST NO.	TREATMENT	N(kg)	μ	ϕ_μ	REMARKS
F-19	Chemically cleaned	3.65	.46	25°	no stick-slip
F-20	Re-rinsed with Me OH and acetone	3.65	.54	28°	small slips
F-21	Chemically cleaned again	3.65	.61	31°	stick-slip
F-22		6.65	.61	31°	stick-slip
F-23	Submerge in H_2O	6.65	.57	30°	stick-slip
F-24	Chemically cleaned again	3.65	.58	30°	stick-slip increases with increasing N
F-25		6.65	.62	32°	
F-26		15.65	.60	31°	
F-27	Chemically re-cleaned including 10 min. acid wash (40% HNO_3, 3% HF) at 50°C: Surfaces visibly rougher	3.65	.56	29°	very small slips
F-28		6.65	.51	27°	stick-slip
F-29		15.65	.50	27°	1st peak
			.47	25°	2nd and following peaks
F-30	Submerge in H_2O	3.65	.40	22°	one peak, then sliding w/o slips
F-31		15.65	.38	21°	small slips
F-32	Chemically re-cleaned	3.65	.54	28°	small slips
F-33		6.65	.56	29°	
F-34	Chemically re-cleaned	3.65	.49	26°	very small slips
F-35		6.65	.47	25°	
F-36	Submerge in H_2O	3.65	.46	25°	one peak, then sliding w/o slips
F-37		6.65	.47	25°	
F-38	Let sit for 2 days in covered container	3.65	.53	28°	
F-39		6.65	.52	27°	
F-40		15.65	.54	28°	1st peak
			.52	27°	2nd and following peaks
F-41		15.65	.52	27°	1st peak
			.49	26°	2nd and following peaks

TABLE 4.3 RESULTS OF HIGH VACUUM FRICTION TESTS ON QUARTZ BLOCKS

SMOOTH SURFACES

TEST NO.	TREATMENT	Pressure (torr)	Temp. (°C)	N(kg)	μ	ϕ_μ	REMARKS
Q-1	Chemically cleaned	4.7×10^{-9}	23° (no bake-out)	3.65	.72	36°	1st peak
					.58	30°	2nd peak
					.52	28°	sliding without slips
Q-2	Chemically cleaned	1.4×10^{-8}	350°	7.48	1.01	45°	1st peak
					.44	24°	Following peaks
Q-3a b	Chemically cleaned including scrubbing under running water	atmosphere	23°	3.65	.86	41°	test repeated with same result
Q-3		1×10^{-8}	350°	3.65	.88	41°	1st peak
					.55	29°	2nd peak
					.36	20°	following peaks
Q-4a	Normal cleaning, including 110°C oven for 16 hrs.	atmosphere	23°	3.65	.35	19°	no stick-slip
Q-4		1.3×10^{-8}	350°	7.48	.47	25°	1st peak
					.49	26°	2nd peak
					.50	27°	Equilibrium value
Q-6a	Normal cleaning, including 110°C oven for 2.5 hrs.	atmosphere	23°	3.65	.45	24°	no stick-slip
Q-6		6.1×10^{-10}	23° (no bake-out)	7.48	.42	23°	no stick-slip

ROUGH SURFACES

TEST NO.	TREATMENT	Pressure (torr)	Temp. (°C)	N(kg)	μ	ϕ_μ	REMARKS
Q-5a	Chemically cleaned, including scrubbing under H_2O	atmosphere	23°	3.65	.58	30°	small slips
Q-5		6.4×10^{-9}	350°	7.48	.77	38°	1st peak
					.74	36°	2nd, 3rd, 4th peaks
					.66	33°	5th peak

TABLE 4.4 RESULTS OF FRICTION TESTS ON POLISHED STAINLESS STEEL

TEST NO.	TREATMENT	N(kg)	μ	ϕ_μ	REMARKS
S-1	As-received condition	3.65	.14	8°	no stick-slip
S-2		6.65	.15	9°	
S-3		16.21	.14	8°	
S-4	Submerged in H_2O	3.65	.13	7°	no stick-slip
S-5		6.65	.15	9°	
S-6		44.20	.12	7°	
S-7	Chemically cleaned	3.65	.46	25°	small stick-slips
S-8	Chemically re-cleaned, including acid wash (40% HNO_3, 3% HF) for 10 min. at 140°F	3.65	1.26	52°	
S-9		6.65	1.23	51°	
S-10		44.20	1.16	49°	large wear track noted
S-11		3.65	1.04	46°	1st peak
			1.79	61°	3rd peak
S-12	Submerged in H_2O	3.65	.84	40°	stick-slip
S-13		6.65	.86	41°	

TABLE 4.5 RESULTS OF FRICTION TESTS ON SMOOTH GRANITE BLOCKS

TEST NO.	TREATMENT	N(kg)	μ	ϕ_μ	REMARKS
G-1	chemically cleaned	3.65	.53	28°	1st peak
			.60	31°	10th peak
G-2	chemically re-cleaned	3.65	.47	25°	1st peak
			.53	28°	20th peak
G-3		6.65	.64	33°	1st peak
			.76	37°	5th peak
G-4		15.65	.70	35°	1st peak
			.77	38°	2nd peak
			.80	39°	3rd peak
G-5	Let sit overnight	3.65	.53	28°	1st peak
			.69	35°	3rd peak
G-6		3.65	.70	35°	1st peak
			.76	37°	3rd peak
G-7		6.65	.75	37°	1st peak
			.79	38°	4th peak
G-8		15.65	.65	33°	1st peak
			.73	36°	4th peak

RESULTS OF ATMOSPHERIC FRICTION TESTS ON SMOOTH QUARTZ SURFACE

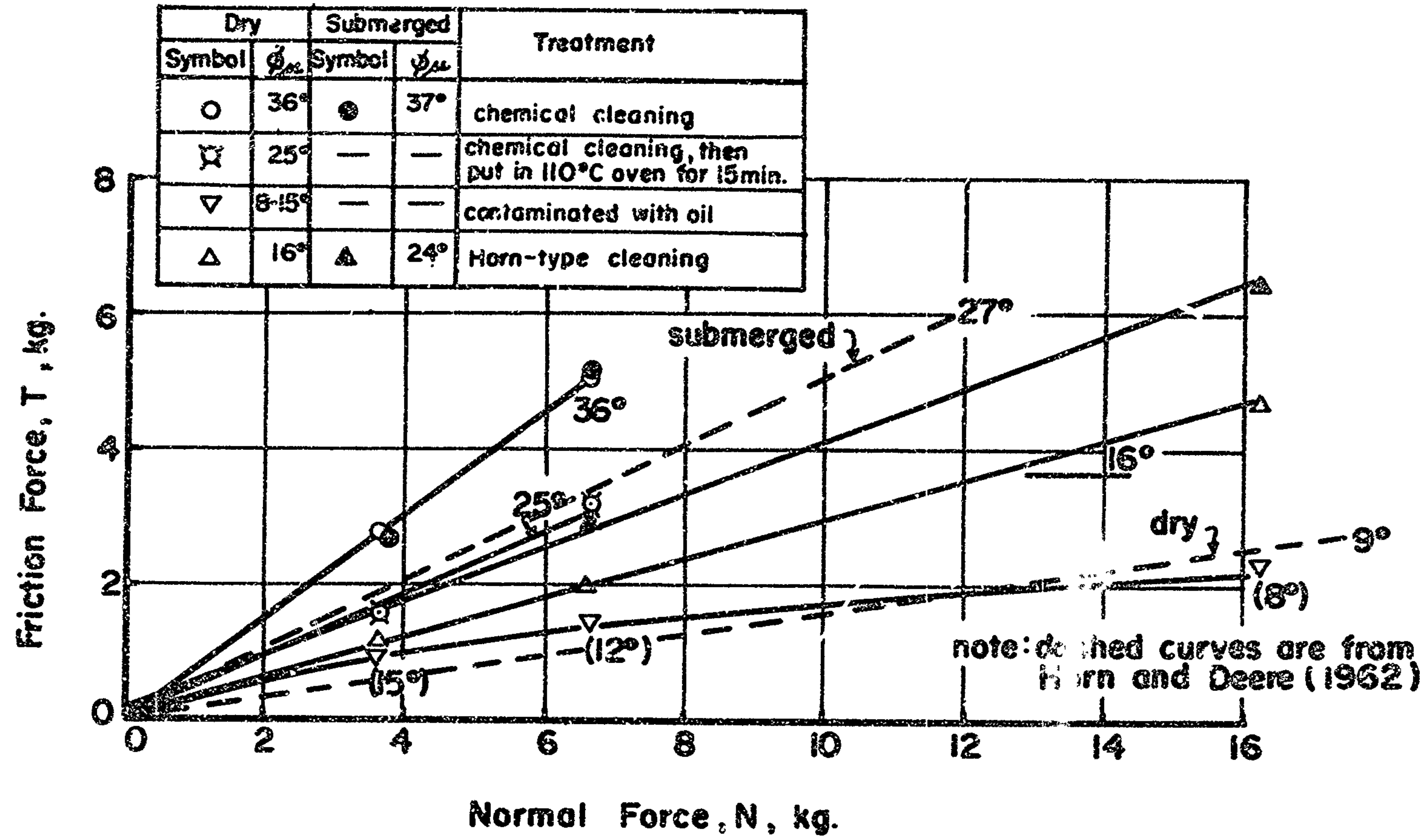

FIGURE 4.1

RESULTS OF ATMOSPHERIC FRICTION TESTS ON ROUGH QUARTZ SURFACES

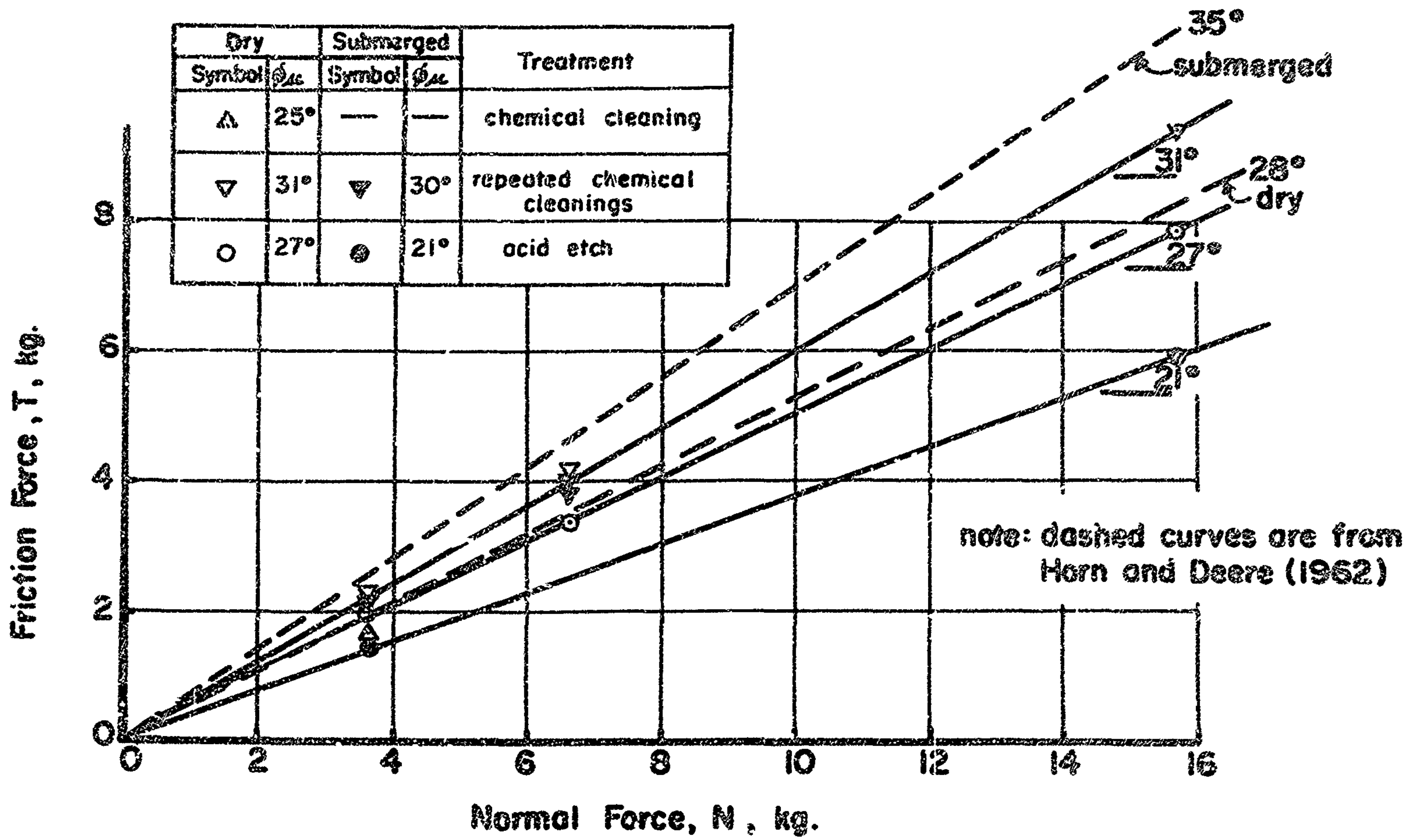

FIGURE 4.2

EFFECT OF VACUUM AND TEMPERATURE ON FRICTION OF QUARTZ

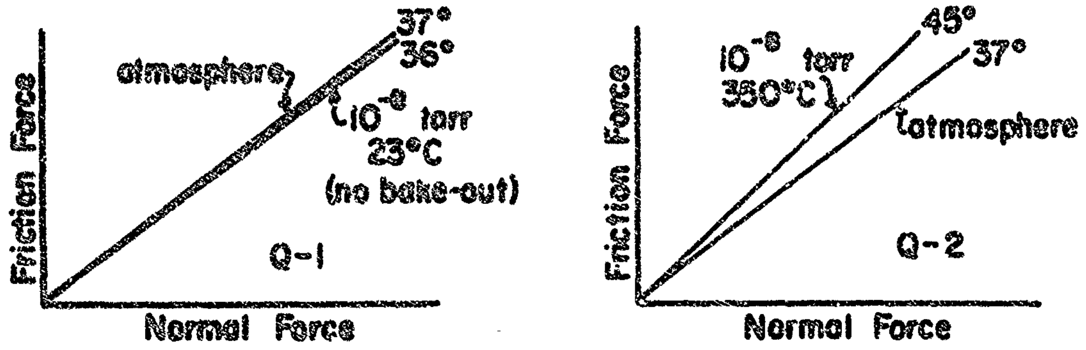

Smooth Surfaces - Careful Cleaning

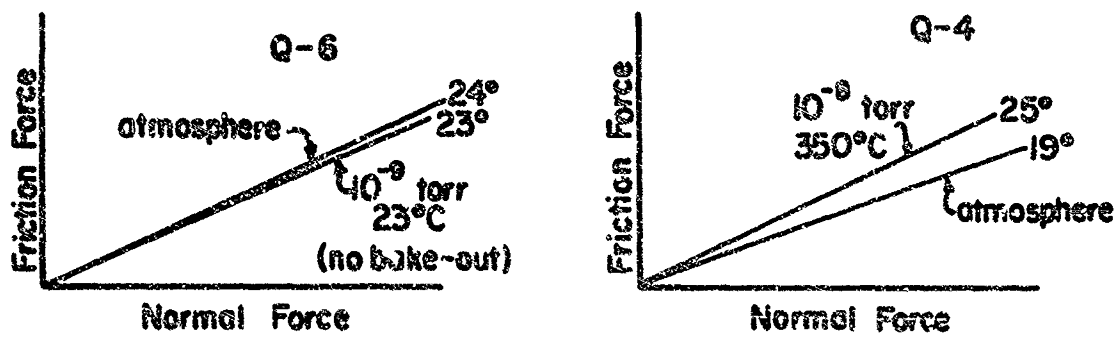

Smooth Surfaces - Normal Cleaning

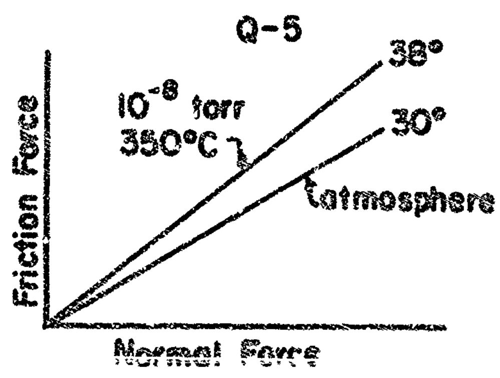

Rough Surfaces - Careful Cleaning

FIGURE 4.3

Recorder Trace
Test S-8
N = 3.65 kg.

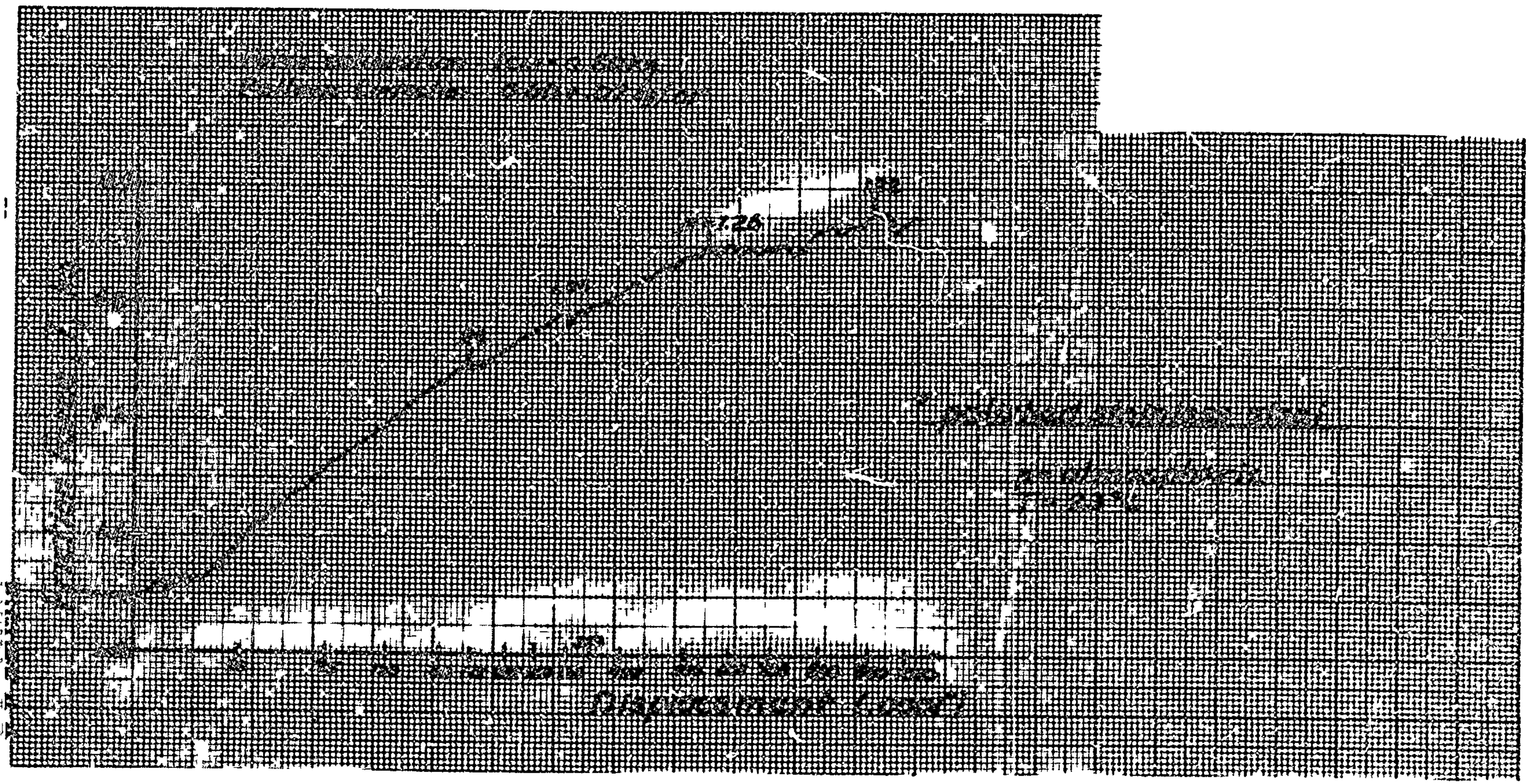

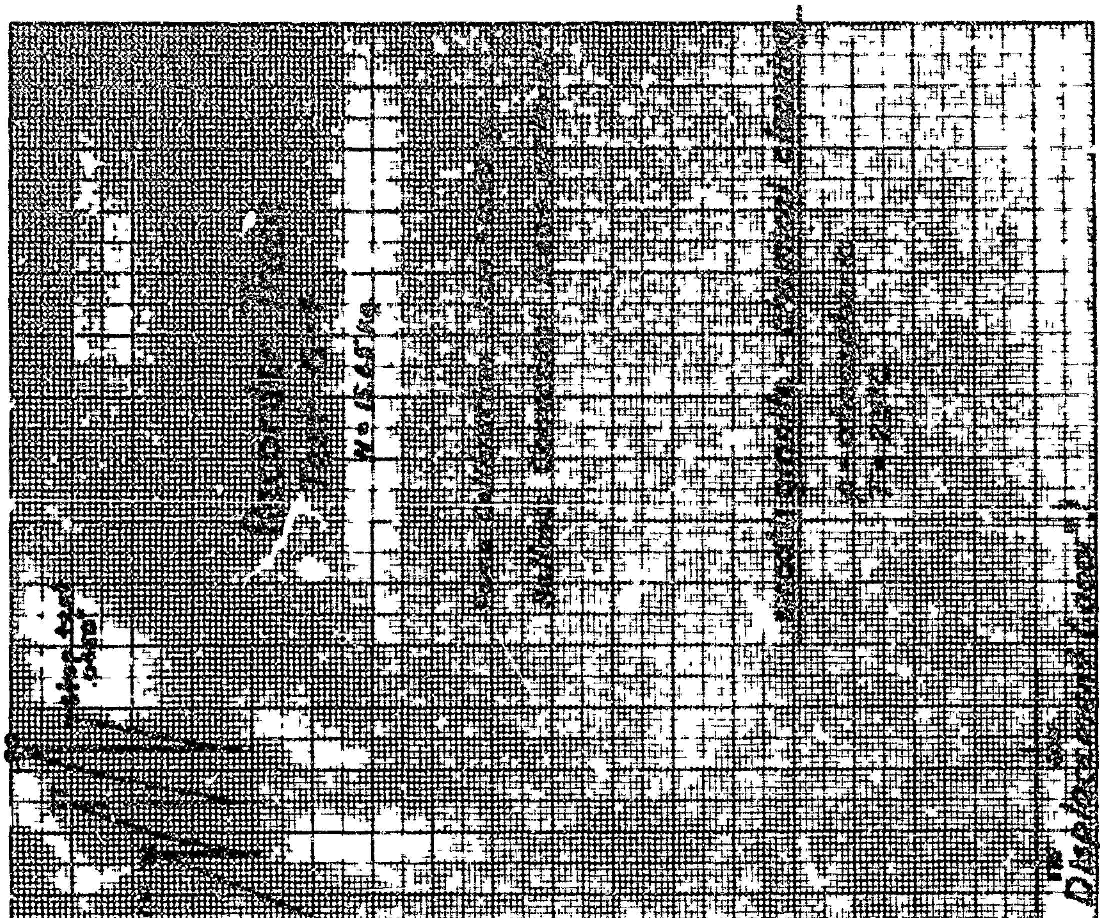

FIGURE 4.5

FIGURE 4 6

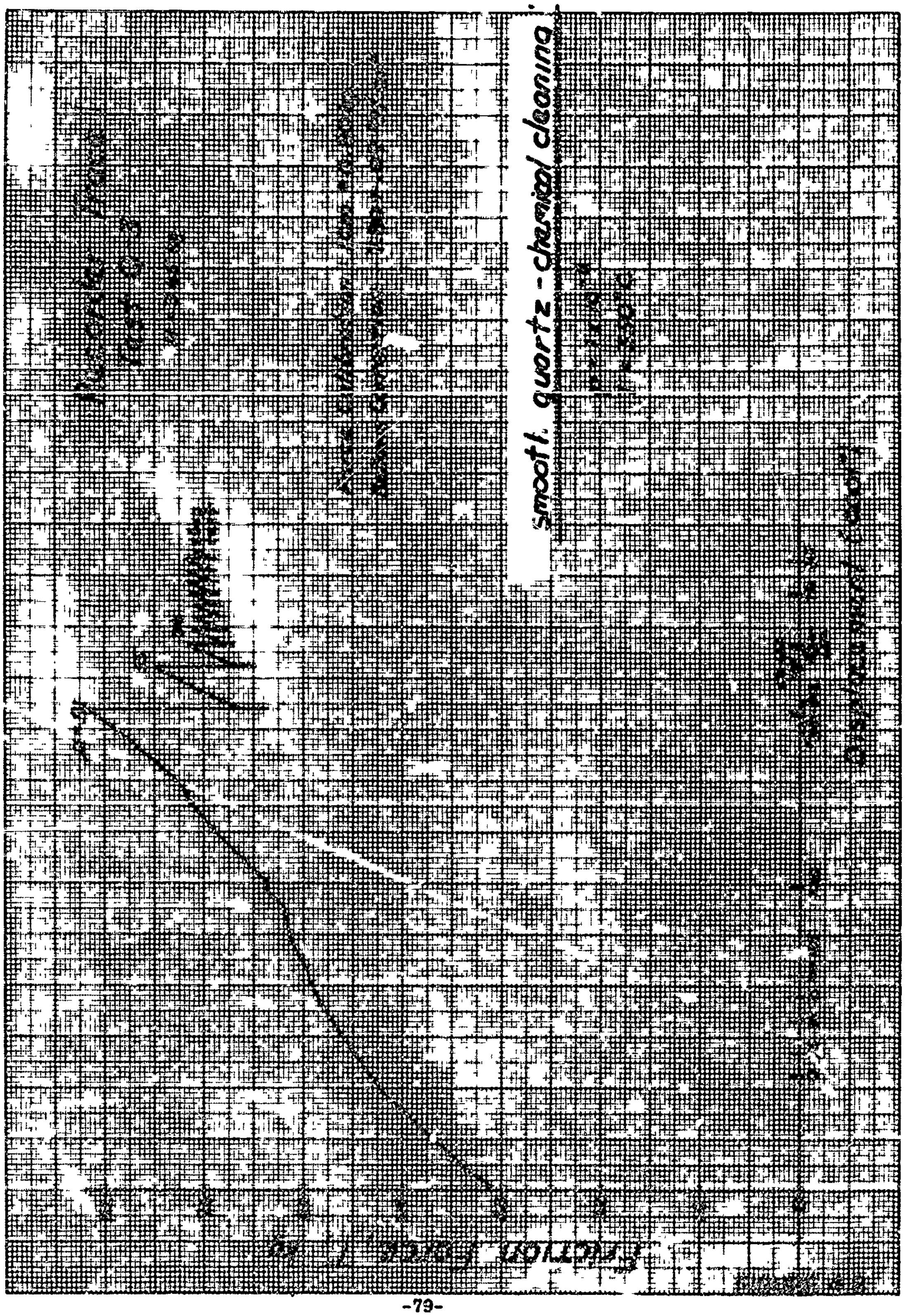
smooth quartz - chemical cleaning
Friction Force, F, kg

Recorder Trace
Test Q-4
N = 7.48 kg

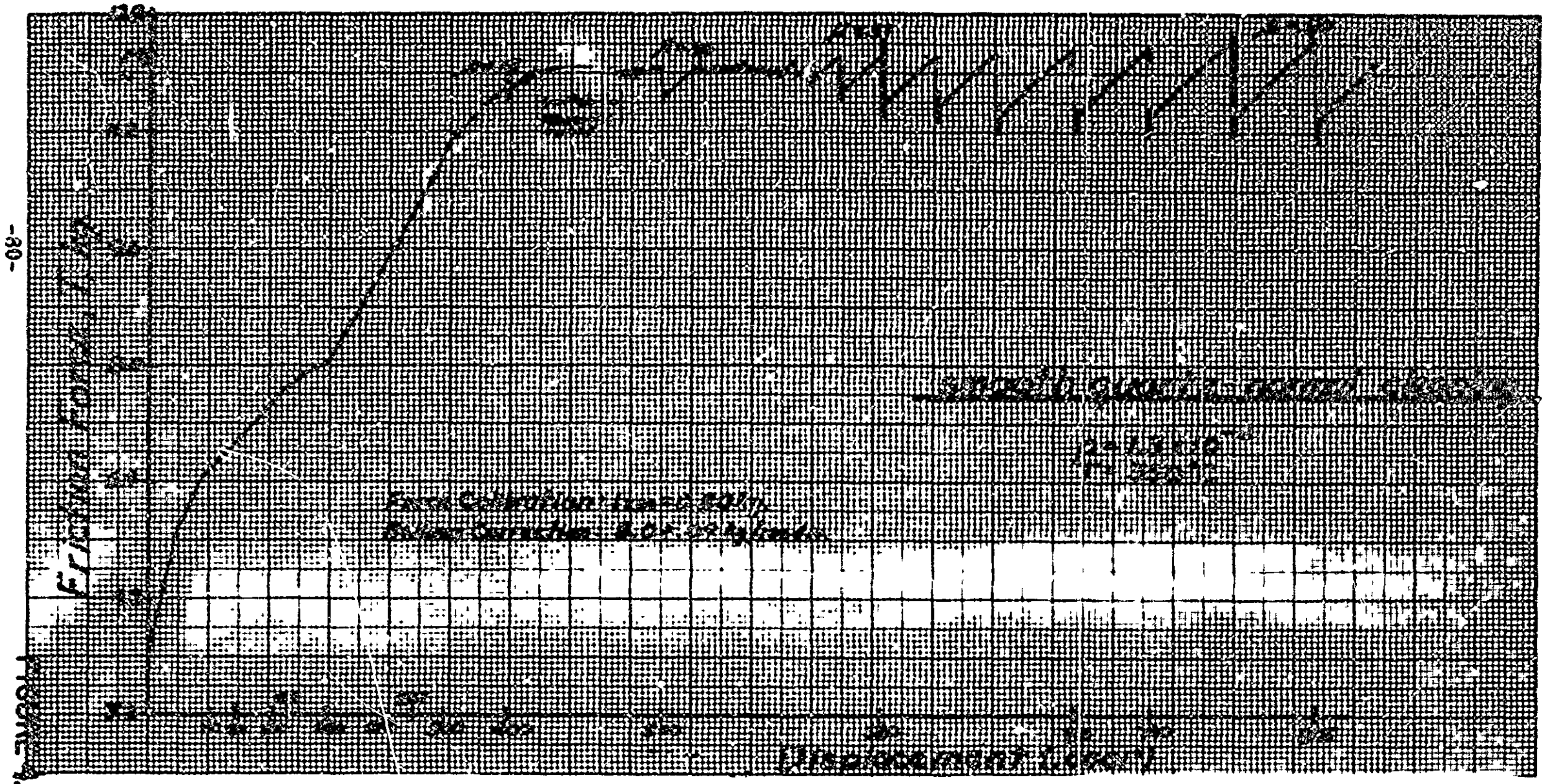

FIGURE 4.9

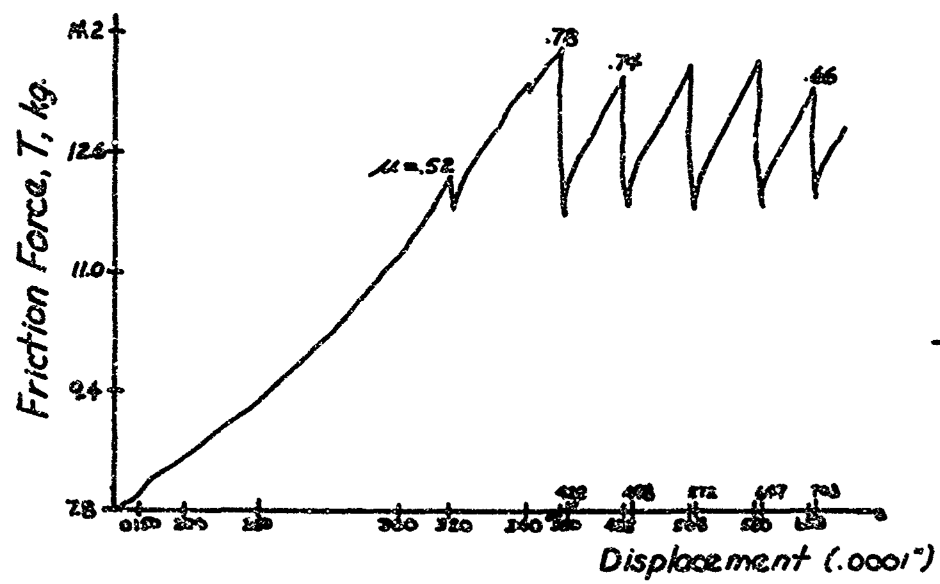

Recorder Trace
Test Q-5
N = 7.48 kg.

Force calibration : 1cm = 0.80 kg.
Bellows Correction : 780 + .09 kg/.01"

rough quartz - chemical cleaning

p = 6.4 x 10^-9 torr
T = 350°C

FIGURE 4.10

EFFECT OF SURFACE CLEANLINESS ON FRICTION OF SMOOTH QUARTZ

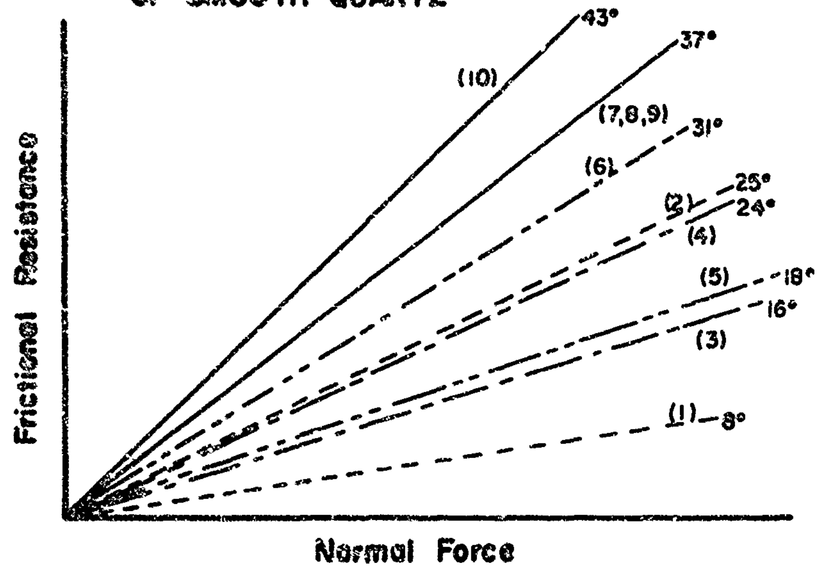

LINE NO.	INVESTIGATOR	ϕ_μ	μ_s	TREATMENT
(1)	Horn (1961)	8°	.14	Acetone wash, detergent wash, 110°C for 24 hrs., air-equilibrate
(2)	Horn (1961)	25°	.46	same as (1), then submerge in H_2O
(3)	Bromwell (1966)	16°	.30	Acetone wash, detergent wash, 110°C for 12 hrs., air-equilibrate
(4)	Bromwell (1966)	24°	.45	same as (3), then submerge in H_2O
(5)	Sjaastad (1963)	18°	.33	Benzene wash, acetone wash, dry at 70°C
(6)	Sjaastad (1963)	31°	.60	same as (5), then 10^{-5} torr, 200°C
(7)	Hardy (1922)	37°	.76	Hot chromic acid, scrub under running water
(8)	Bromwell (1966)	37°	.75	Trichloroethylene rinse, acetone rinse, detergent wash, distilled H_2O rinse, methyl alcohol rinse, acetone rinse, very careful handling
(9)	Bromwell (1966)	37°	.75	same as (8), then submerge in H_2O
(10)	Bromwell (1966)	43°	.93	same as (8), then 10^{-8} torr, 350°C

FIGURE 4.11

V. DIRECT SHEAR TESTS

5.1 Scope of Tests

A preliminary series of direct shear tests were run on 30-40 mesh glass balls. The main series of tests were run on 40-60 mesh Ottawa sand.

Control tests were run in the atmosphere to determine shear strength characteristics and the Mohr-Coulomb cohesion intercept (c) and friction angle (ϕ_m). These test results are compared with tests at vacuums down to 10^{-10} torr and at temperatures to 350°C.

5.2 Test Samples

5.2.1 Materials Used

All of the direct shear tests were run on sand-size materials. This eliminated the difficult problems of trying to outgas a fine powder in a vacuum.[1]

The glass balls (ballotini) were manufactured by Potters Brothers, Inc., Carlstadt, New Jersey, of crown barium glass. The size range selected for these tests passed a No. 30 sieve (.59 mm) and were retained on a No. 40 sieve (.42 mm). The specific gravity of the balls was measured to be 2.49. Microscopic examination revealed that the spheres had a very uniform shape with a large percentage of nearly perfect spheres. The surfaces appeared smooth and nearly transparent.

---

[1] There is good evidence that the pressure in the soil was essentially the same as indicated by the gauge. The gauge was mounted behind the shear box, in a "dead zone" that was as far as possible from the pump. In one shear test where a pressure of $< 5 \times 10^{-11}$ torr was reached, the vacuum pump was shut off after running the test and the pressure rise in the chamber was noted. After two days the pressure was still below 1×10^{-10} torr, indicating good pressure equilibrium within the chamber.

The Ottawa sand used in the direct shear tests passed a No. 40 sieve (.42 mm) but was retained on a No. 60 sieve (.25 mm). This sand is essentially pure quartz (> 99%) and has a specific gravity of 2.66. The individual grains are nearly equi-dimensional, well-rounded, and have very frosted, rough-looking surfaces.

5.2.2 Cleaning Techniques

All of the test samples were pre-cleaned prior to testing. The standard cleaning technique was similar to the chemical cleaning procedure used for the friction test specimens, namely:

1. Trichloroethylene rinse
2. Acetine rinse
3. Detergent wash
4. Distilled water rinse
5. Acetone rinse
6. Dry at 70°C

A clean oven, modified to permit passing a stream of pre-purified nitrogen, was used for drying the samples. Much longer drying times were required for the direct shear specimens than for the friction specimens (several hours vs. a few seconds). Thus it is likely that more re-contamination occurred before the direct shear tests were run.

In addition to the above cleaning technique, a light acid etch was used to clean all of the Ottawa sand samples used in high vacuum tests. This etch consisted of 40% fuming nitric acid, 30% glacial acetic acid, and 30% hydroflouric acid for about 15 seconds.[1] The sample was then repeatedly washed with distilled water until the effluent showed a pH > 6. The sample was then dried in the clean oven at approximately 100°C in a nearly-closed container.

---

[1] This procedure was suggested by J.A. Ryan (1965).

Most of the atmospheric tests were run on samples that had been cleaned but not etched. However, there was no detectable difference in the atmospheric shear strength behavior between etched and non-etched samples. Also, there was no difference in atmospheric strength between cleaned and non-cleaned specimens.

5.2.3 Sample Preparation

The samples were placed in the shear box by pouring directly from the vessel used for drying.[1] The placement procedure was selected to give a reproducible, fairly loose sample. The average initial dry density for the Ottawa sand was 111.5 $\pm$ 0.5 pounds per cubic foot, giving an initial void ratio of 0.65. This is a relative density of about 50% (based on $e_{max} = 0.76$ and $e_{min} = 0.55$).

Tests were run to determine the effect of a $\pm$ 0.5 lbs./cu.ft. density variation on shear strength (at a constant $\bar{\sigma}_v$). These tests gave a value of $\Delta\tau \cong 0.01\,kg/cm^2$ for $\Delta\gamma_d = 0.5$ lbs/cu.ft. This variation is appreciably larger than any due to inaccuracies in force measurements. Thus the limiting accuracy for direct shear tests is about $\pm$ 0.01 kg/cm^2.

5.3 Force Application and Measurement

5.3.1 Normal Force

Two techniques were used for applying the normal force. For very light loads (up to $\bar{\sigma}_v = 0.07\,kg/cm^2$), stainless steel weights were placed directly on top of the shear box. For heavier loads (up to $\bar{\sigma}_v = 1.0\,kg/cm^2$), the stainless steel bellows was used. This allowed placing loads on a weight hanger outside of the vacuum.

---

[1] Either a stainless steel beaker or a porcelain evaporating dish.

When under vacuum, the normal force bellows applied a vertical stress of approximately 0.75 kg/cm^2 on the sample.[1] If the desired $\ddot{\sigma}_v$ was less than this, a counterbalancing mechanism using an overhead frame and pulleys was used to pull up on the bellows (shown in Fig. 3.1). A large stainless steel yoke was used to maintain the normal force vertical during a shear test. This yoke was cantilevered from the shaft that applied the shear force. It ensured that the normal load would translate with the top half of the shear box during a test.[2]

5.3.2 Shear Force

The connections for the shear force and the method of application are described in Section 3.4. The shear force was measured with both a proving ring and a force transducer in each test. The force transducer was connected to a sensitive millivoltmeter and read visually during a test.

5.3.3 Accuracy of Force Measurements

The normal force, which was applied by dead weights, could be easily determined within ± 50 grams. The proving ring used to measure the shear force had a sensitivity of 59 gms/division. The force transducer had a sensitivity of about 36 grams. Fifty-nine grams corresponds to $\tau \cong 0.001$ kg/cm^2. The limiting accuracy for the shear force measurements was determined by hysteresis in the stainless steel bellows used to feed through the vacuum and by friction in the ball bushings. Frequent

---

[1] This stress varied with atmospheric pressure. Therefore, it was necessary to record accurate barometer readings for each test.

[2] Due to a difference in stiffness between the yoke and the shear force mechanism, a small amount of the shear force was actually applied through the yoke (hence through the top cap of the sample). However, this force was measured by the proving ring. This somewhat undesirable feature did not affect the accuracy or the reproducibility of the results.

calibrations were run to detect changes in the bellows and bushing load-displacement curves. The actual accuracy of the shear force measurements was estimated to be within ± 150 gms., or $\Delta\tau = \pm\, 0.003\,kg/cm^2$. This is well below the limiting accuracy of $\pm\, 0.01\,kg/cm^2$ set by void ratio variations.

5.4 Test Procedure

After a test sample was prepared and placed in the shear box, the shear box was mounted in the vacuum chamber. A light normal load was applied and the two halves of the shear box were separated slightly (about .01 in.). The lateral thrust of the soil kept the upper half of the shear box separated from the bottom half to prevent metal-metal contact.

If an atmospheric test were being run, the remainder of the normal load was applied and the test was run. If a vacuum test was being run, the chamber was sealed and pumpdown began. If the test was to be run at a $\bar{\sigma}_v$ less than that due to atmospheric pressure on the bellows, then the bellows was counter-balanced during pumpdown so that $\bar{\sigma}_v$ did not ever exceed the desired value.

During a test, the shear displacement was generally applied at a rate of 0.01 in./minute. After the test was completed, the system was cooled back to room temperature (if necessary), and then returned to atmospheric pressure by bleeding in pre-purified N_2 through a liquid nitrogen-cooled trap connected to the bakeable UHV valve.

5.5 Results of Direct Shear Tests

5.5.1 Glass Balls

The results of the direct shear tests on glass balls are presented in Table 5.1 and Figure 5.1. The atmospheric tests gave $c = 0$ and $\phi_m = 27.6°$. The high vacuum tests gave $c = 0.01\,kg/cm^2$ and $\phi_m = 28.3°$.

5.5.2 Ottawa Sand

Stress vs. strain curves from the direct shear tests on Ottawa sand are shown in Figures 5.2, 5.3, and 5.4. Consolidation pressures ($\bar{\sigma}_v$) for the high vacuum tests shown in Fig. 5.3 varied slightly from the nominal 0.50 kg/cm^2. Therefore, the τ values were normalized by multiplying them by ($\frac{0.50}{\bar{\sigma}_v}$) to allow comparison of the tests. The peak points of the direct shear tests are plotted as τ vs. $\bar{\sigma}_v$ on Figure 5.5. A summary of the direct shear tests is given in Table 5.2.

The atmospheric shear tests gave c = 0.01 kg/cm^2 and $\phi_m = 36°$. The high vacuum tests gave c = .025 kg/cm^2 and $\phi_m = 41°$.

5.3.3 Discussion of Results

5.5.3.1 Effect of High Vacuum and High Temperature on Shear Strength

The effect of high vacuum, even at elevated temperatures, on the shear strength of the glass balls was very small, just within the limits of experimental accuracy. This may have been due to the moderate bake-out temperatures that were used in this test series. Or it may have been due to increased rolling between particles in the vacuum tests. This will be discussed further in a few paragraphs.

High vacuum, in conjunction with a high temperature bake-out, had significant effect on the shear strength of the Ottawa sand. The sand developed a measurable cohesion intercept.[1] The strength increases are on the order of 17% at the higher confining pressures. It is interesting to note that the same envelope was obtained regardless of whether or

[1] The cohesion intercept observed in the atmospheric tests is about the same as the possible experimental error in these tests. However, a slight cohesion intercept could be expected due to curvature of the envelope (Wissa, 1965). In the vacuum tests, visual observation of the sample during shear seemed to indicate some cohesion between the grains. For example, they did not tend to fall out of the box at high strains as they did in the atmospheric tests. None of the samples showed any cohesion after they had been returned to atmospheric pressure. However, Ryan (1965) has shown that the adhesion between silicates in vacuum is destroyed when the vacuum is released, even if the back-filling is dry N_2 as in these tests.

not the vacuum test samples were cooled back to room temperature before shearing. That is, the desorption that occurred during bake-out was irreversible, and the surfaces, once cleaned, remained clean (at least for a period of a day or so). Although no shear tests were run without a bake-out one would predict (based on the friction results in Ch. 4) that no strength increase would have occurred without a bake-out.

The stress-strain curves show that the shear strength beyond the peak decreased greatly for the vacuum tests and became approximately equal to the atmospheric shear strength. This can be explained by either 1) a decrease in μ beyond the peak (see Section 4.10.2.5) or 2) the increased dilitancy (hence higher void ratio) of the vacuum samples.

An appreciable amount of stick-slip also occurred in the high vacuum tests. This is felt to be a result of the stronger bonding forces, which caused groups of particles to fail catastrophically when their shear strength was exceeded.

5.5.3.2 Correlation of ϕ_m and ϕ_μ

The observed increases in shear strength for the Ottawa sand under high vacuum are a result of increased frictional resistance (ϕ_μ) between particles.[1] Hence, it should be possible to use theoretical curves relating ϕ_{max} and ϕ_μ to correlate the measured values of ϕ_m with values of ϕ_μ for rough quartz from Chapter IV.

The curves by Scott (1964) and Horne [Lee (1966)] that were described in Section 2.6.2 will be used to correlate ϕ_m and ϕ_μ. Figure 5.6 reproduces pertinent portions of these curves, along with the one by Caquot (1934) for comparison.

---

[1] This is true even though all of the strength increase can be accounted for by a "dilatancy correction". The tendency for larger volume changes must, ultimately, be attributed to increased friction (ϕ_μ), since the initial packing geometry, the test procedure, and the size and shape of the grains was the same in all of the tests.

Intermediate curves for any desired porosity between the close-packed and the critical void state can be approximated by using relative densities.[1] That is, at any given value of $\tan \phi_\mu$:

$$(\tan \phi_m)_e = (\tan \phi_m)_{e_{cv}} + \frac{e_{cv} - e}{e_{cv} - e_{min}} \left[(\tan \phi_m)_{e_{min}} - (\tan \phi_m)_{e_{cv}} \right] \quad (5.1)$$

where e is the void ratio at which the tests were run and e_{cv} and e_{min} refer to the critical void state and to densest packing, respectively.

Actually, this procedure turns out to be unnecessary for correlation of the Ottawa sand tests, since the small volume changes in the atmospheric tests (Table 5.2) indicates that they were run at a void ratio close to the critical voids state. Therefore, it should be possible to compare these tests directly with the Horne curve.[2]

The measured values of ϕ_m (36°) and ϕ_μ (28°) for the atmospheric tests are plotted as Δ in Figure 5.6. The point for ϕ_μ = 38° and ϕ_m = 42°, the secant angle from the high vacuum tests, is plotted as ∇ . The agreement with the Horne curve is very good, considering the many approximations involved.[3]

---

[1] This type of analysis was first suggested, to the author's knowledge, by Sjaastad (1963). However, Sjaastad used n = 48% (cubic packing) with $\phi_m = \phi_\mu$ for his lowest curve. This does not seem reasonable, since this structure should collapse to the more dense ϕ_{cv} packing (n = 42%) during shear.

[2] Even if it is argued that the tests were not exactly at the critical void ratio, this does not invalidate the analysis, since the curve that would be drawn for the actual test void ratio (using Eqn. 5.1) would be essentially parallel to the Horne curve and close to it.

[3] Ottawa sand might not be expected to show exactly the same ϕ_m vs. ϕ_μ relationship as that obtained for perfect spheres. However, the general form of the relation should be essentially the same.

This does not alter the fact that there are obviously many difficulties involved in choosing the value of ϕ_μ that controls inter-particle sliding in a shear test. There are several indications that the static coefficient of friction may not be the correct parameter. For example:

1. ϕ_m for the glass balls did not increase significantly under high vacuum. This may reflect the fact that the glass balls were more free to roll than the Ottawa sand particles. Hence the "effective" ϕ_μ did not change significantly, even though the static coefficient of friction may have increased appreciably.[1]

2. Tables 5.1 and 5.2 show that the high vacuum tests had a larger volume increase $(\frac{\Delta V}{V_o})$ at τ_{max} than the atmospheric tests. This is what would be expected if more rolling occurred in the high vacuum tests. Rolling might require an additional amount of volume increase in order to give the particles "room" to roll. It does not seem unreasonable that the energy input required to allow some rolling (with its component of volume change) might still be less than the energy required to slide all of the particles, if the static coefficient is very high.[2] Therefore, the correct or "effective" ϕ_μ would not be the static coefficient, but a somewhat lower value.

---

[1] The rolling coefficient of friction is determined primarily by the elastic properties of the material and not by bonding between the surfaces. Therefore, it would not have increased appreciably under high vacuum.

[2] Rowe (1964) and his co-workers (Horne, 1965) have argued against rolling as a significant deformation mechanism. Tests are currently being run at M.I.T. to determine whether or not rolling occurs. Tests have been run using a shear box, filled with glass balls, that is pulled across a glass plate. This test is similar to that used by Rowe to measure ϕ_μ. The glass balls, which have a colored dot on them, are observed from beneath the glass plate. Rolling of particles that appear to be carrying a normal load clearly occurs in these tests, particularly at the onset of movement. Efforts are being made to quantitize these observations.

5.6 Extrapolation of Shear Strength Results to the Lunar Surface

If there is soil on the surface of the moon, its strength parameters should be increased somewhat by the lunar vacuum and elevated temperatures. Other effects may far outweigh those of vacuum and temperature, so one cannot place much confidence in any quantitative prediction of lunar surface properties based on this investigation.

Nevertheless, the strength increases measured in these tests are larger than any previously obtained in high vacuum testing of soils, to the author's knowledge. They may aid in setting a lower limit on the possible range of lunar surface properties (e.g., $c = 0.01\ kg/cm^2$ seems a reasonable lower limit for cohesion). In addition, even small amounts of cohesion and small increases in ϕ_m may be significant for increasing the bearing capacity of a lunar dust.

5.7 Summary of Direct Shear Test Results

The following conclusions are drawn from the direct shear tests:

1. Significant shear strength increases for Ottawa sand were produced by high temperature bake-out in a high vacuum. This reflects an increased frictional resistance between particles, caused by increased cleanliness of the surfaces.
2. The shear strength remained at its high level when the samples were cooled back to room temperature before shearing. This indicates that the desorbed material was probably being effectively removed from the vacuum system.
3. Measured values of ϕ_m were compared with measured values of ϕ_μ for rough quartz surfaces using theoretical curves. The correlation of theoretical and experimental values is very good. However, it is felt that there is still appreciable uncertainty concerning the value of ϕ_μ that controls

deformation in a shear test on granular materials. Under unusual conditions, such as 1) particles that can easily roll or 2) very high values of ϕ_μ, the correlation of ϕ_μ and ϕ_m may be seriously questioned. The "recommended" value of $\phi_\mu = 26°$ to $28°$ is for "normal" conditions.

4. The measured increases in shear strength indicate that, if there is soil on the moon, its strength parameters should be increased by the lunar vacuum and elevated temperatures.

TABLE 5.1 RESULTS OF DIRECT SHEAR TESTS ON GLASS BALLS

Test No.	Pressure (torr)	Temperature (°C)		$\bar{\sigma}_v$ (kg/cm^2)	τ_{max} (kg/cm^2)	τ_{max}			Remarks
		Bake-out	Test			shear strain (%)	$\frac{\Delta V}{V_o}$ (%)	secant angle	
C-12	atmospheric	---	23°	1.0	0.53	8.7	+.0[illegible]	28°	
C-13	atmospheric	---	23°	0.25	.13	12.3	+.28	27.5°	
C-14	atmospheric	---	23°	0.043	.030	5.7		35°	
C-15	atmospheric	---	23°	0.027	.018	7.0		34°	
C-16	atmospheric	---	23°	0.070	.041	6.9		31°	
C-17	1×10^{-10}	250°	23°	1.0	.56	8.5		29°	externally heated
C-18	1×10^{-10}	200	23°	0.043	.037	3.0	+1.0	41°	externally heated
C-20	1×10^{-9}	125°	25°	1.0	.55	8.7	+.67	29°	internal heater
C-21	3×10^{-8}	250°	250°	0.027	.026	4.9		44°	internal heater

TABLE 5.2 RESULTS OF DIRECT SHEAR TESTS ON OTTAWA SAND

Test No.	Pressure (torr)	Temperature (°C)		$\bar{\sigma}_v$ (kg/cm^2)	τ_{max} (kg/cm^2)	τ_{max}			Remarks
		Bake-out	Test			shear strain (%)	$\frac{\Delta V}{V_o}$ (%)	secant angle	
E-1	atmospheric	---	23°	1.00	.73	16.5	+.13	36°	
E-3	atmospheric	---	23°	0.25	.19	13.2	+.19	37°	
E-4	atmospheric	---	23°	0.070	.061	5.9		41°	
E-5	atmospheric	---	23°	0.045	.040	8.8		42°	
E-11	atmospheric	---	23°	0.50	.39	8.1	+.37	38°	
E-12	atmospheric	---	23°	0.50	.38	5.9	+.73	37°	sample pre-etched
E-13	atmospheric	---	23°	1.00	.75	13.2	+.15	37°	
E-6	1.3×10^{-8}	358°	358°	0.070	.086	5.1		51°	all vacuum test samples were pre-etched
E-7	2×10^{-8}	350°	350°	1.00	.88	11.8	+1.18	42°	
E-8	7.6×10^{-9}	342°	342°	0.48	.43	11.3	+.94	42°	
E-9	4.8×10^{-11}	300°	23°	0.88	.77	7.3	+1.81	41°	external heaters used for bake-out
E-10	1.1×10^{-10}	300°	23°	0.51	.45	6.3	+0.90	41°	

EFFECT OF VACUUM AND TEMPERATURE ON FRICTION ANGLE
30-40 mesh glass balls

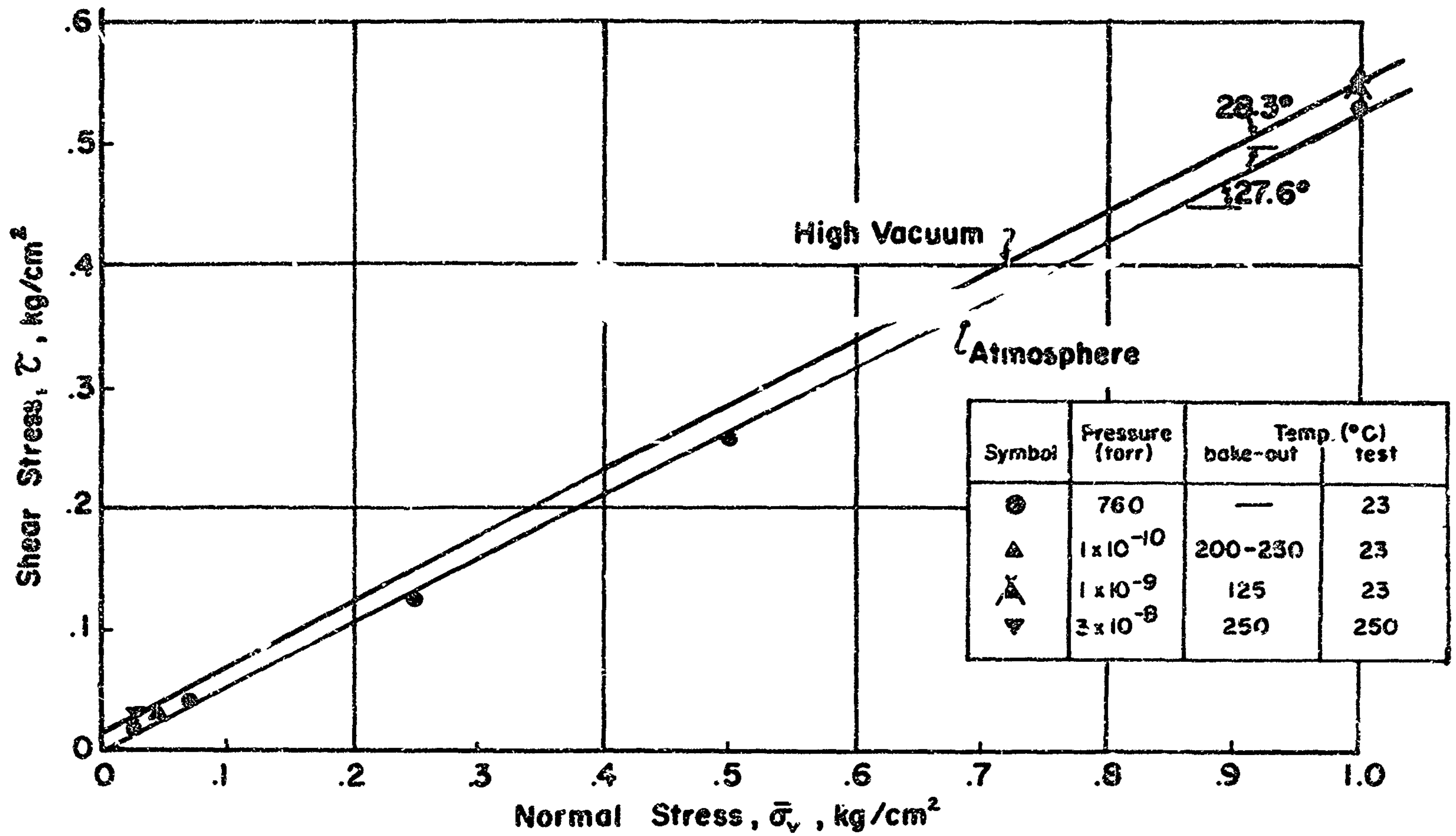

FIGURE 5.1

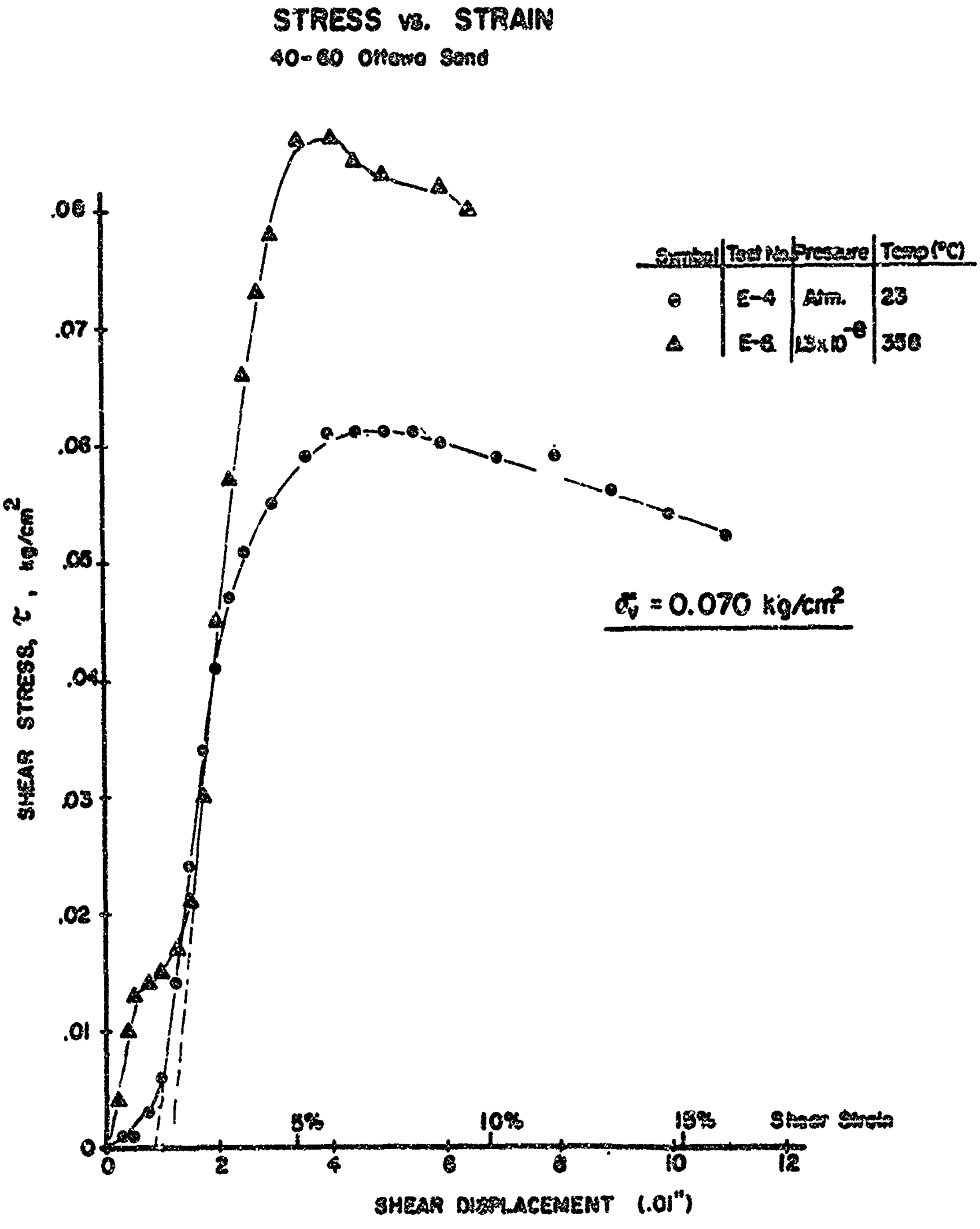

STRESS vs. STRAIN
40-60 Ottawa Sand
Symbol | Test No. | Pressure | Temp (°C)
E-4 | Atm. | 23
E-6 | 1.5x10^-8 | 356
σ_v = 0.070 kg/cm²
SHEAR STRESS, τ, kg/cm²
SHEAR DISPLACEMENT (.01")
5%
10%
15%
Shear Strain

FIGURE 5.2

STRESS vs. STRAIN
40-60 Ottawa Sand

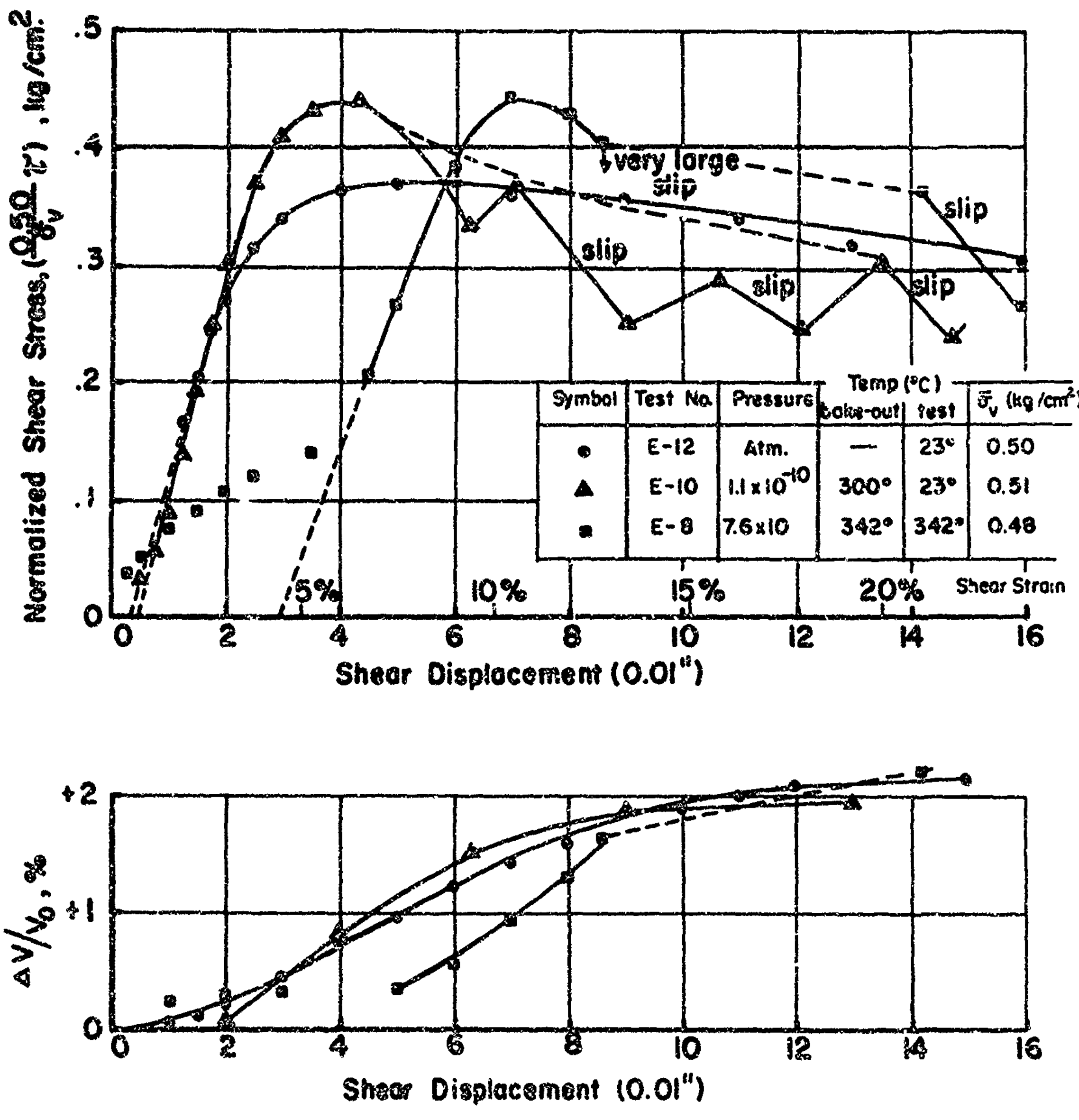

FIGURE 5.3

STRESS vs. STRAIN

40 - 60 Ottawa Sand

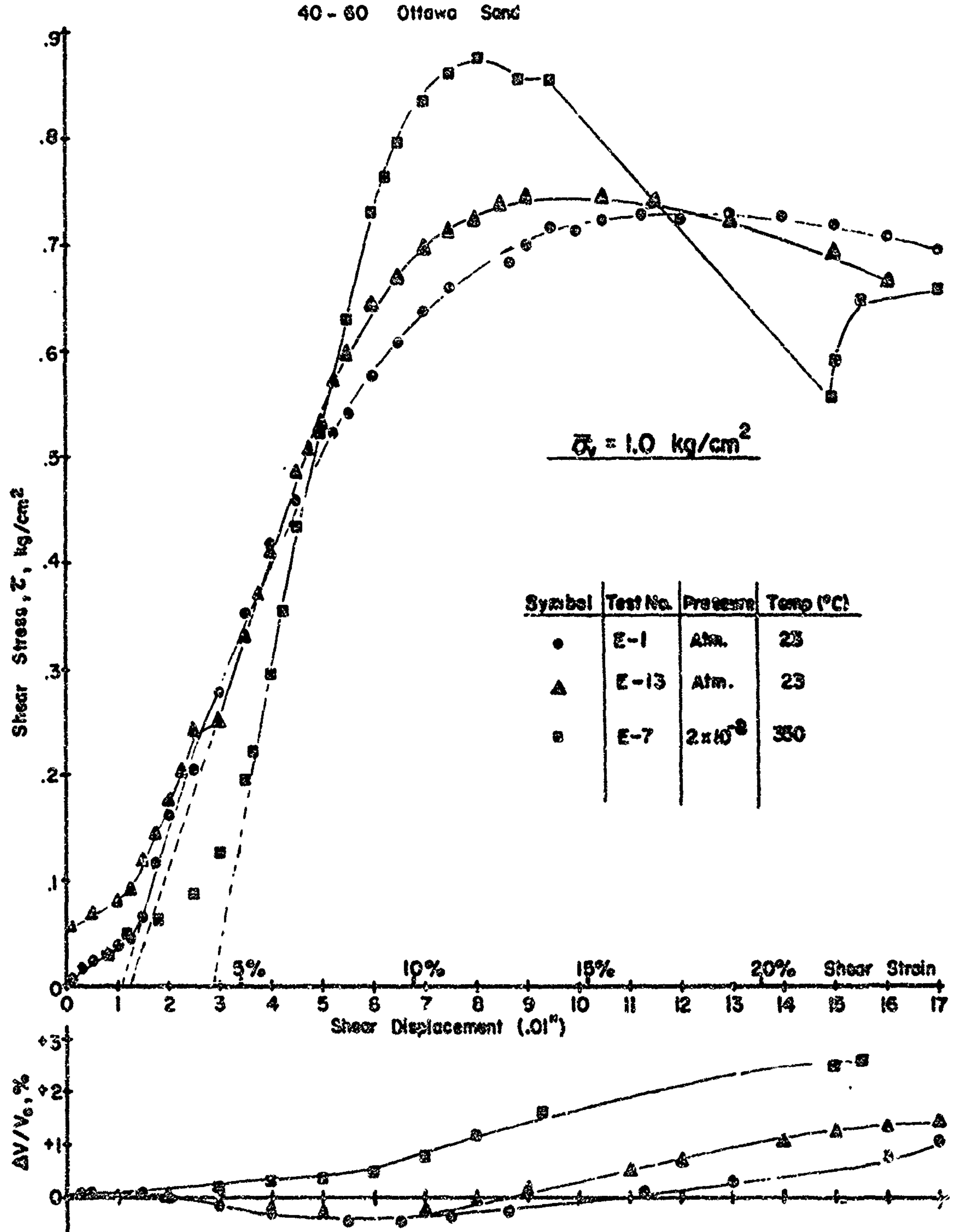

FIGURE 5.4

EFFECT OF HIGH VACUUM AND TEMPERATURE ON FRICTION ANGLE

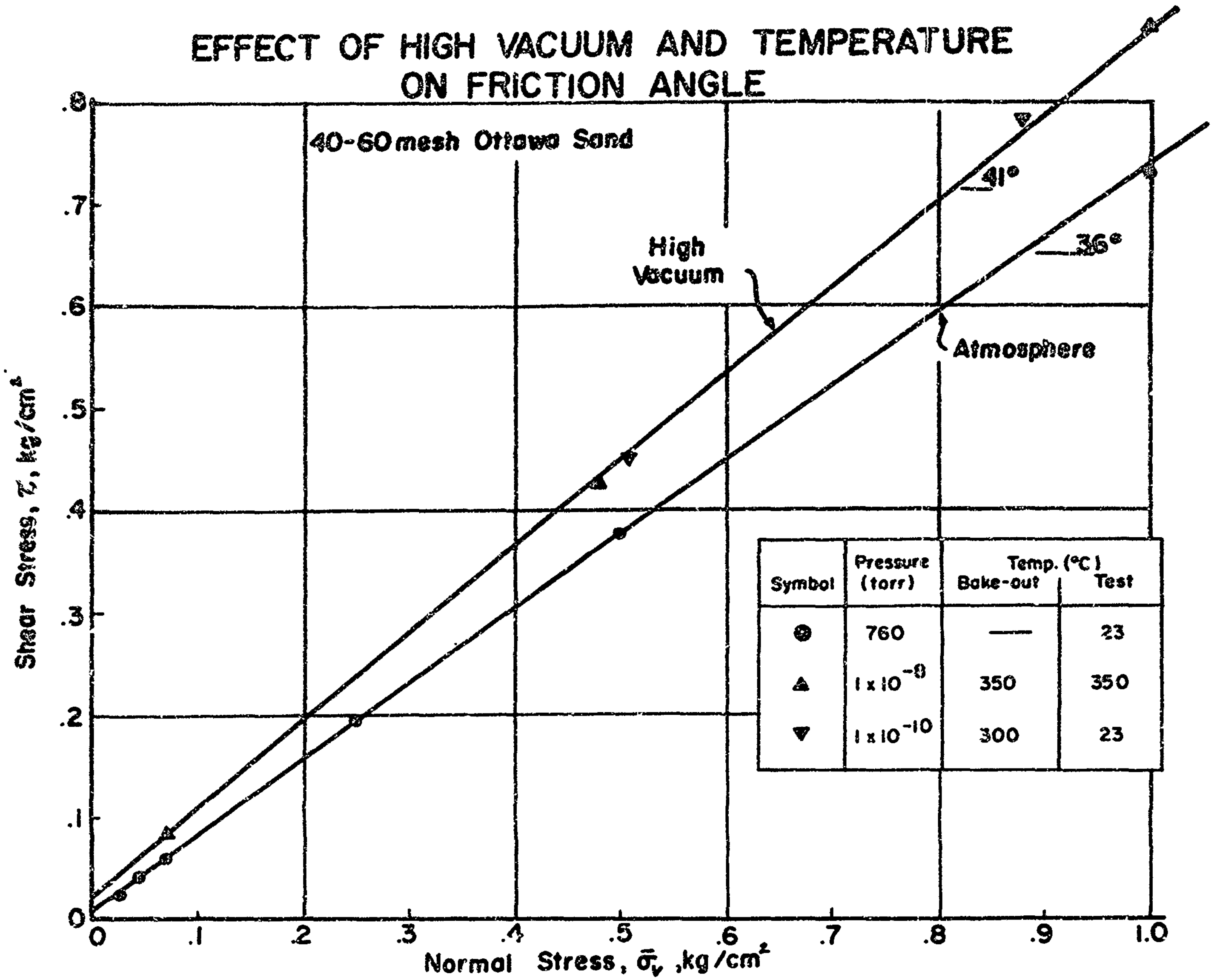

FIGURE 5.5

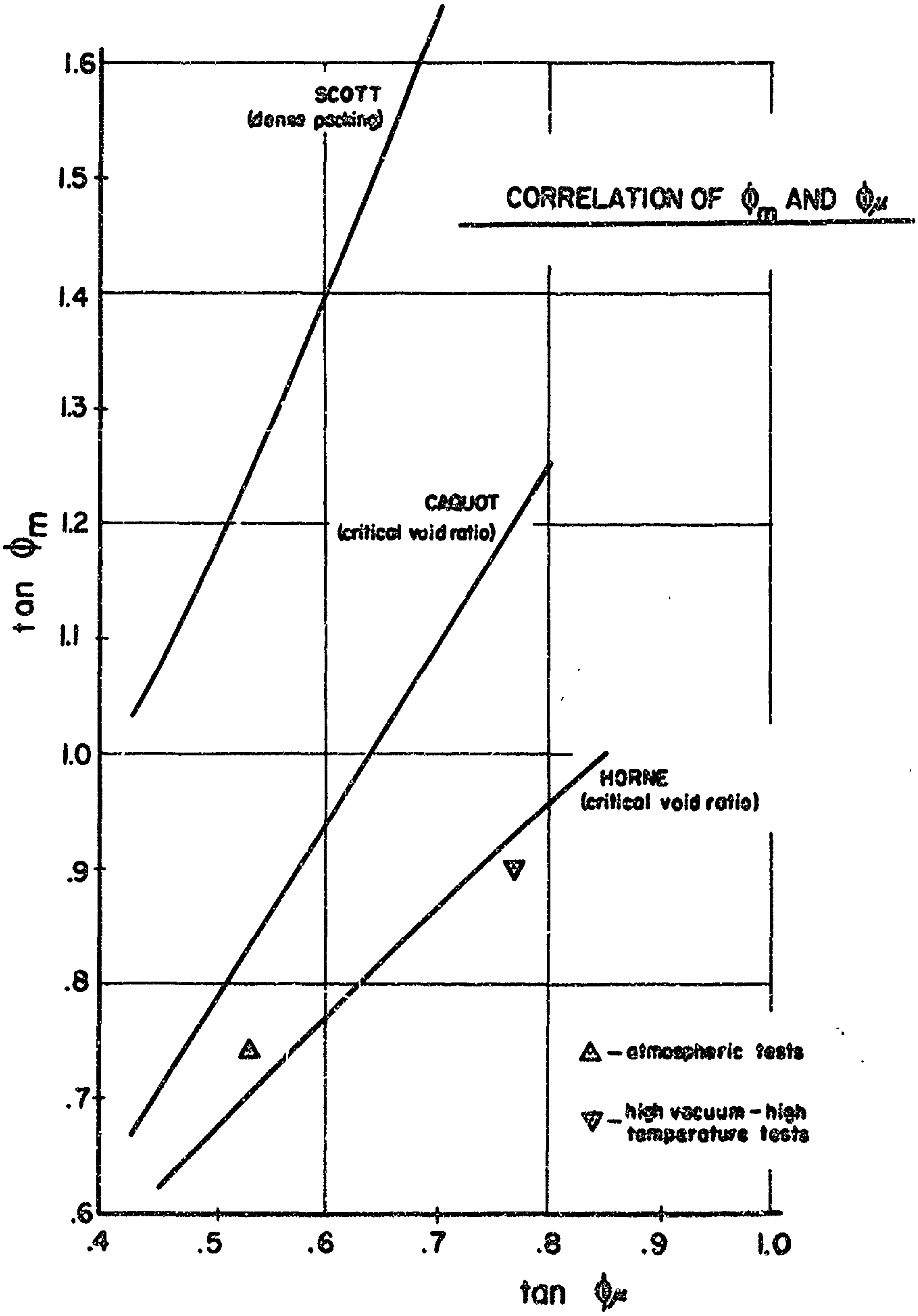
CORRELATION OF ϕ_m AND ϕ_μ
SCOTT
(dense packing)
CAQUOT
(critical void ratio)
HORNE
(critical void ratio)
△ – atmospheric tests
▽ – high vacuum – high temperature tests
tan ϕ_m
tan ϕ_μ
1.6
1.5
1.4
1.3
1.2
1.1
1.0
.9
.8
.7
.6
.4
.5
.6
.7
.8
.9
1.0

FIGURE 5.6

VI. CONCLUSIONS

The major conclusions of this investigation are as follows:

1. No single value of μ can be assigned to quartz. The experimental conditions (environment, surface treatment, cleaning procedure, surface roughness) must be carefully defined. The friction of a smooth quartz surface can vary from 0.1 to 1.0 depending on the surface cleanliness.

2. The friction of rough quartz surfaces does not show as large variations as observed for smooth surfaces. This reduces the potential error in predicting ϕ_μ values for soils (under most conditions, the use of ϕ_μ = 26° to 28° for quartz soil particles should be reasonable) whose particles always have rough surfaces.

3. The coefficient of friction of quartz increases under high vacuum (10^{-8} torr) and high temperature (350°C). μ values as high as unity can be obtained under these conditions. Vacuum alone does not produce increases in the friction.

4. The shear strength of Ottawa sand increases after a bake-out (300° to 350°C) in high vacuum (10^{-8} torr). The strength increase is still present if the surfaces are cooled back to room temperature before testing. This may be due to either 1) removal of the desorbed materials by the vacuum pump or 2) irreversible desorption.

5. There is good correlation between increases of ϕ_μ for quartz under high vacuum-high temperature and increases of ϕ_m for the Ottawa sand under the same conditions.

6. The shear strength of glass balls did not increase significantly under high vacuum and elevated temperatures. This may have been due to increased rolling in these tests, which reduced the "effective" ϕ_μ.

VII. RECOMMENDATIONS FOR FURTHER STUDY

Significant future progress in understanding the friction behavior of mineral surfaces and its relationship to the deformation properties of granular masses will depend to a large extent on sophisticated test techniques capable of determining the following:

1. A quantitative measure of the cleanliness and crystal structure of the surfaces. This will require accurate information regarding the type and amount of material adsorbed on the surfaces and its thermodynamic properties. Further developments in the fields of a) UHV technology, b) adsorption c) low energy electron diffraction (LEED), d) mass spectrometry, and e) interferometry may help to obtain these measurements.

2. A quantitative measure of the roughness of surfaces (including irregularly shaped particles) and a means of determining areas of contact between surfaces.

It is expected that improvements in the state-of-the-art of making these measurements will be swiftly followed by dramatic discoveries concerning the fundamental nature of friction.

In the meantime, much interesting and important information can be obtained regarding the fundamental factors controlling the friction of mineral surfaces:

1. The effect of much higher temperatures (to 1000°C or so) on the friction of quartz should be investigated. The use of high vacuum will aid in desorbing the contaminants and ensure that significant recontamination of the test surfaces does not occur.

2. The frictional characteristics of virgin quartz surfaces prepared in vacuum should be investigated. These surfaces could be prepared by either 1) electron bombardment or 2) cleavage

in ultra-high vacuum. Accurate measurements of adhesion and surface energy could also be made on these surfaces. In addition, the effect of controlled amounts of various contaminants could then be investigated by bleeding them into the vacuum system.

3. Variations of ϕ_μ should be measured for glass in air and vacuum and correlated with measurements of ϕ_m for glass balls. Such tests, in conjunction with carefully run "Rowe-type" ϕ_μ tests, may help delineate the effect of particle rolling in the deformation of a granular mass.

4. Attempts should be made to produce granular assemblies, possibly of quartz, whose particles have very smooth surfaces. It should be possible to produce very large changes in ϕ_μ for such particles and thereby obtain further experimental verification of the relationship between ϕ_μ and ϕ_m.

5. Further measurements for other minerals of the coefficient of friction and of shear strength should be made under carefully controlled ultra-high vacuum and high temperature conditions. In particular, minerals likely to occur on the moon, such as olivine and obsidian, should be tested.

6. Measurements should be made to determine the effect of surface cleanliness on the frictional behavior of layer silicates. These results can then be correlated with shear strength measurements in an attempt to delineate the role of inter-particle friction in the shear strength of clay soils.

VII. LITERATURE CITED

1. Archard, J.F. (1957). "Elastic Deformation and the Laws of Friction", Proceedings of the Royal Society, A243, pp. 190-205.

2. Bishop, A.W. (1954). Correspondence on "Shear Characteristics of a Saturated Silt, Measured in Triaxial Compression", Geotechnique, 4, pp. 43-45.

3. Bowden, F.P. and Tabor, D. (1942). "The Mechanism of Metallic Friction", Nature, V. 150, pp. 197-199.

4. ________________ (1950). The Friction and Lubrication of Solids, Part I, Oxford Univ. Press, London.

5. ________________ (1964). The Friction and Lubrication of Solids, Part II, Oxford Univ. Press, London.

6. Bowden, F.P., Young, J.E. and Rowe, G. (1952). "Part II. Friction of Non-Metals. Friction of Diamond, Graphite and Carbon: The Influence of Adsorbed Films", Proc Roy. Soc., A212, pp. 485-488.

7. Brace, W.F. (1963). "Behavior of Quartz During Indentation", The Journal of Geology, V. 71, No. 5, pp. 581-595.

8. Caquot, A. (1934). Equilibre des Massifs a Frottement Interne. Stabilite des Terres Pulverulents eu Coherentes. Gauthier-Villars, Paris.

9. Dantu, ₋. (1961). "Etude mechanique d'un milieu pulverulent forme de spheres egales de compacite maxima", Proc. 5th Int. Conf. on Soil Mech. and Found. Eng., 1, pp. 61-66.

10. Halajian, J. D. (1964). "The Case for a Cohesive Lunar Surface Model", Grumman Aircraft Eng. Corp., Report No. ADR-04-04-64.2.

11. Hardy, Sir. W.B. (1936). Collected Works, Cambridge Univ. Press.

12. Hardy, W.B. and Doubleday, I. (1922). "Boundary Lubrication-The Temperature Coefficient", Proc. Roy. Soc., A101, pp. 487-492.

13. Hardy, W.B. and Hardy, J.K. (1919). "Note on Static Friction and on the Lubricating Properties of Certain Chemical Substances", Phil. Mag. Suppl. 6, Vol. 38, No. 223, pp. 32-48.

14. Holland, L. (1964). The Properties of Glass Surfaces, John Wiley and Sons, Inc., N.Y.

15. Horn, H. M. (1961). An Investigation of the Frictional Characteristics of Minerals, ScD. Thesis, Univ. of Ill., Urbana, Illinois.

16. ______________ and Deere, D. U. (1962). "Frictional Characteristics of Minerals", Geotechnique, 12, pp. 319-335.

17. Horne, M. R. (1965 "The Behavior of an Assembly of Rotund, Rigid, Cohesic ss Particles, Parts I and II", Proc. Roy. Soc., A286, pp. -97.

18. King, R. F. and Tabor, D. (1954). "The Strength Properties and Frictional Behavior of Brittle Solids", Proc. Roy. Soc. A223, pp. 225-238.

19. Lee, I. K. (1966). "Stress-Dilatancy Performance of Feldspar", Proc. ASCE, Soil Mechanics and Foundations Division, V. 92, No. SM2, pp. 79-103.

20. Mitchell, J. K. (1964). "Current Lunar Soil Research", Proc. of the ASCE, Soil Mechanics and Foundations Division, V. 90, No. SM3, pp. 53-83.

21. Nadai, A. (1950). Theory of Flow and Fracture of Solids, McGraw-Hill Book Co., Inc., N. Y.

22. Newland, P. L. and Allely, B. H. (1957). "Volume Changes in Drained Triaxial Tests on Granular Materials", Geotechnique, 7, pp. 17-34.

23. Penman, A. D. M. (1953). "Shear Characteristics of a Saturated Silt, Measured in Triaxial Compression", Geotechnique, 3, pp. 312-328.

24. Rowe, P. W. (1962). "The Stress-Dilatancy Relation for Static Equilibrium of an Assembly of Particles in Contact", Proc. Roy. Soc., A269, pp. 500-527.

25. Rowe, P. W. (1964). Closure to "Stress Dilatancy, Earth Pressures, and Slopes," Proc. ASCE, Soil Mechanics and Foundations Division, V. 90, No. SM4, pp. 145-180.

26. Ryan, J. A. (1965). "Experimental Investigations of Ultra-High Vacuum Adhesion as Related to the Lunar Surface", Douglas Report SM-47914, Douglas Aircraft Co., Inc., Santa Monica, California.

27. Salisbury, J. W. and Glaser, P. E., editors (1965). "Studies of the Characteristics of Probable Lunar Surface Materials", Special Reports No. 20, Air Force Cambridge Research Laboratories, Bedford, Mass.

28. Scott, R. F. (1964). Principles of Soil Mechanics, Addison-Wesley Publishing Co., Inc., Reading, Mass.

29. Sjaastad, G. D. (1963). "The Effect of Vacuum on the Shearing Resistance of Ideal Granular Systems", Ph. D. Thesis, Princeton University.

30. Tabor, D. (1951). The Hardness of Metals, Clarendon Press, Oxford.

31. Terzaghi, K. (1925). Erdbaumechanik, Franz Deuticke, Vienna.

32. Thurston, C. W. and Deresiewicz, H. (1959). "Analysis of a Compression Test of a Model Granular Medium", J. Appl. Mech., 26, Trans. ASME 81, pp. 251-258.

33. Timoshenko, S. and Goodier, J. N. (1951). Theory of Elasticity, McGraw-Hill Book Co., Inc., N. Y.

34. Tschebotarioff, G. P. and Welch, J. D. (1948). "Lateral Earth Pressures and Friction Between Soil Minerals", Proc. 2nd Int. Conf. Soil Mech. and Fdn. Eng., V. 7, pp. 135-138.

35. Vey, E. and Nelson, J. D. (1965). "Engineering Properties of Simulated Lunar Soils", Proc. ASCE, Soil Mech. and Fdns. Division, V. 91, No. SM1, pp. 25-52.

36. Wissa, A. E. Z. (1965). "Effective Stress-Strength Behavior of Cemented Soils," Sc. D. Thesis, Mass. Inst. of Technology.

APPENDIX A

OBTAINING A CLEAN ULTRA-HIGH VACUUM

A. Obtaining an Ultra-High Vacuum

The ultimate pressure of a vacuum system, p_u, is determined by the following equation:

$$p_u = \frac{Q_t}{S} \qquad (A.1)$$

where Q_t is the total gas flow, in torr-liters/sec., and S is the speed of the pump in liters/sec. at the pressure p_u. The production of ultra-high vacuum is a matter of reducing the ratio of gas influx to pumping speed. If a clean vacuum is desired, it is more reasonable to reduce the gas flow than to increase the pumping speed.

The gas influx is due to four sources:

1. backstreaming of gases from the pump
2. desorption of gases from surfaces within the system
3. leaks in the system welds, gaskets, etc.
4. permeation of gases through the walls of the system

Item 4 is seldom a problem at pressures above 10^{-11} torr and will not be considered further. Items 1 through 3 can (and must) be reduced by careful system design. The magnitude of gas load resulting from each of these and methods for reducing them will be briefly considered.

Backstreaming of Gases From the Pump

Both ion pumps and diffusion pumps, the two major methods for obtaining a high vacuum, are sources of gas. Diffusion pumps, which utilize a vaporizable fluid, are likely to contaminate the system with this fluid. Backstreaming in diffusion pumps is reduced by placing a cold surface between the pump and the chamber which will trap and condense

the backstreaming molecules. The effectiveness of this trap (or usually a series of traps) determines the cleanliness of the vacuum.

Ion pumps are less susceptible to backstreaming, but can release appreciable amounts of low molecular weight materials, particularly H_2, H_e, and CH_4, into the system if they are not operated properly. Generally speaking, ion pumps provide a very clean vacuum without the use of elaborate and costly trapping devices.

Desorption of Gases Within the System

Any surface that has been exposed to the atmosphere is contaminated by adsorbed gases. The ease with which gas can be removed depends upon how tightly they are held, i.e., the adsorption energy. Physically adsorbed water can be removed by slight warming at pressures around 10^{-3} torr. Chemically adsorbed oxides, on the other hand, may require heating to 2000°C at 10^{-9} torr. The thermodynamics of desorption will be considered in more detail in Appendix C. However, the importance of minimizing outgassing within the system can be easily shown.

At 10^{-10} torr, there are about 3×10^6 molecules in each cubic centimeter of space within a vacuum chamber. On each square centimeter which is covered with a monolayer of gas, however, there are about 10^{15} molecules. Even if the adsorbed gas is reduced to 10^{-6} of a monolayer, there will usually be an order of magnitude more gas on the surface than in the volume of the system at 10^{-10} torr.

The rate of desorption can be decreased by cooling the walls of the vacuum chamber. Generally it is more practical to heat the chamber walls, increasing the rate of desorption and driving off most of the adsorbed gas, which is removed from the system by the pump. When the system is then cooled back to room temperature a very good vacuum is obtained. By this means, the outgassing of stainless steel can be reduced from an initial value of about 10^{-8} torr-liter/sec/cm^2 to less than 10^{-14} torr-liter/sec/cm^2.

Leaks in the System

Eliminating leaks is an essential part of high vacuum technology. Careful welding procedures, careful handling of all parts to prevent scratches or nicks, and use of knife-edge sealed metal gaskets will give a system with no detectable leaks larger than 10^{-10} std. cc./sec. A leak of 10^{-10} std. cc./sec. will only consume about 1 liter/sec. of the pumping speed at 10^{-10} torr.

Apart from actual leaks to the atmosphere, care must be taken to minimize so-called virtual leaks, which are due to small pockets of trapped air or contamination. These leaks arise from poorly welded joints which entrap air and from improperly cleaned materials. They are difficult to detect, the only evidence for their existence being the failure of the system to reach low pressures. Virtual leaks often release their gas slowly, causing a system to remain at 10^{-6} to 10^{-8} torr for days or months.

Virtual leaks can be minimized by careful welding, always welding on the vacuum side to prevent crevices or air pockets; careful cleaning of all materials exposed to the vacuum; and elimination of all high vapor pressure materials, such as rubber gaskets.

B. The Cleanliness of a Vacuum

The pressure of a vacuum system is an inadequate measure of its suitability for maintaining a clean surface. Because the time required to pump a system down and to complete a test may be several days or even weeks, the types of gases that make up the vapor phase are as important as the pressure level.

Consider, for example, an inadequately trapped diffusion pump using the lowest vapor pressure pump fluid available (DC705 with a room temperature vapor pressure of less than 1×10^{-9} torr). Although the pressure of this system will remain in the 10^{-10} torr range, in a matter of hours a monolayer of oil will have covered everything within the system, and the layer will continue to grow at a rate of about 5 Å/hour

(Holland, 1964, p. 343).

If the total pressure is 10^{-6} torr, however, and the only gas present is helium, this may be considered a very clean vacuum, because helium has a very low adsorption energy and will not contaminate a surface at this pressure.

To analyze the residual gas composition requires a mass spectrometer. In lieu of such an instrument, a simple test involving the wettability of clean surfaces was used to check for contamination.

<u>Wettability of Clean Surfaces</u>

A drop of water placed on a clean metal surface will spread rapidly and show a low contact angle, because of the strong adhesive forces of the solid surface. If, however, a minute amount of organic contamination is present, the drop of water will not wet the surface.

Several small strips of 304 stainless steel were carefully cleaned using detergent, chemical solvents, and an acid bath (40% HNO_3, 3% HF at 70°C for 20 min.). When exposed to the atmosphere, these strips would remain wettable for 10-15 minutes.

An attempt was made to find a suitable means for storing these strips that would maintain their wettability. The most successful technique was to place them in a clean glass-stoppered bottle in a 200°C oven. This would maintain their wettability for a few hours.

One of these strips was placed in the high vacuum test chamber prior to pumpdown for a direct shear test. The total time required for this test was 7 days. When the metal strip was removed from the chamber at the end of this time, it was as wettable, or slightly more so, than just after cleaning.[1] This indicates that the elaborate precautions taken to produce a clean vacuum were, at least to this extent, successful.

---

[1] High vacuum, then, can be considered as a suitable means for storing wettable strips!

APPENDIX B

VACUUM PRESSURE INSTRUMENTATION

It was anticipated that vacuum levels below the dectability of standard Bayard-Alpert ionization gauges would be obtained with the ion pump vacuum system. Bayard-Alpert gauges generally reach an x-ray limit at about 1×10^{-10} torr, below which they cannot be used.

Therefore a GE Cold Cathode Gauge was used for pressure indication. The cold cathode gauge is generally considered capable of detecting pressures as low as 10^{-13} torr.

To check the accuracy of the GE gauge, it was calibrated against a Bayard-Alpert gauge. Vacuum gauge calibration data have verified the linearity of Bayard-Alpert gauges down to 10^{-9} torr.

The gauges were mounted in the empty vacuum chamber equidistance from the pump. Good vacuum technology practice was used during the calibration run, including outgassing of the Bayard-Alpert gauge before taking readings, waiting for equilibrium pressures, etc. A Granville Phillips Variable Leak was used to bleed in gas to enable attaining desired pressures between 10^{-4} and 10^{-10} torr.

The calibration curve is shown in Figure B-1. The two gauges gave very good agreement in the 10^{-4} to 10^{-8} torr pressure range. Below 10^{-8} torr the GE gauge indicated a lower pressure than the Bayard-Alpert Gauge. When the Bayard-Alpert gauge read 2×10^{-10} torr,[1] the GE gauge read almost a decade lower.

After this calibration had been run, it was learned that Varian Associates had performed a similar calibration. Data points from their calibration are also shown on Figure B-1. The agreement between the two calibrations is excellent.

---

[1] The x-ray limit of this particular gauge is about 5×10^{-11} torr.

At the present time a great deal of controversy exists regarding the accuracy of pressure readings in the ultra-high vacuum region. Cold cathode gauge adherents maintain that their gauges read true pressures and that Bayard-Alpert gauges indicate pressures that are too high, due to adsorption on the collector wires, outgassing of the hot filament, etc. Owing to a desire to obtain the lowest possible pressures, the current trend in the vacuum industry is to believe (and to buy) the gauge that reads the lowest pressure.

No attempt has been made by the author to resolve this controversy. The pressure readings given in this report are those indicated by the GE gauge, unless otherwise noted.

GE COLD CATHODE GAUGE CALIBRATION

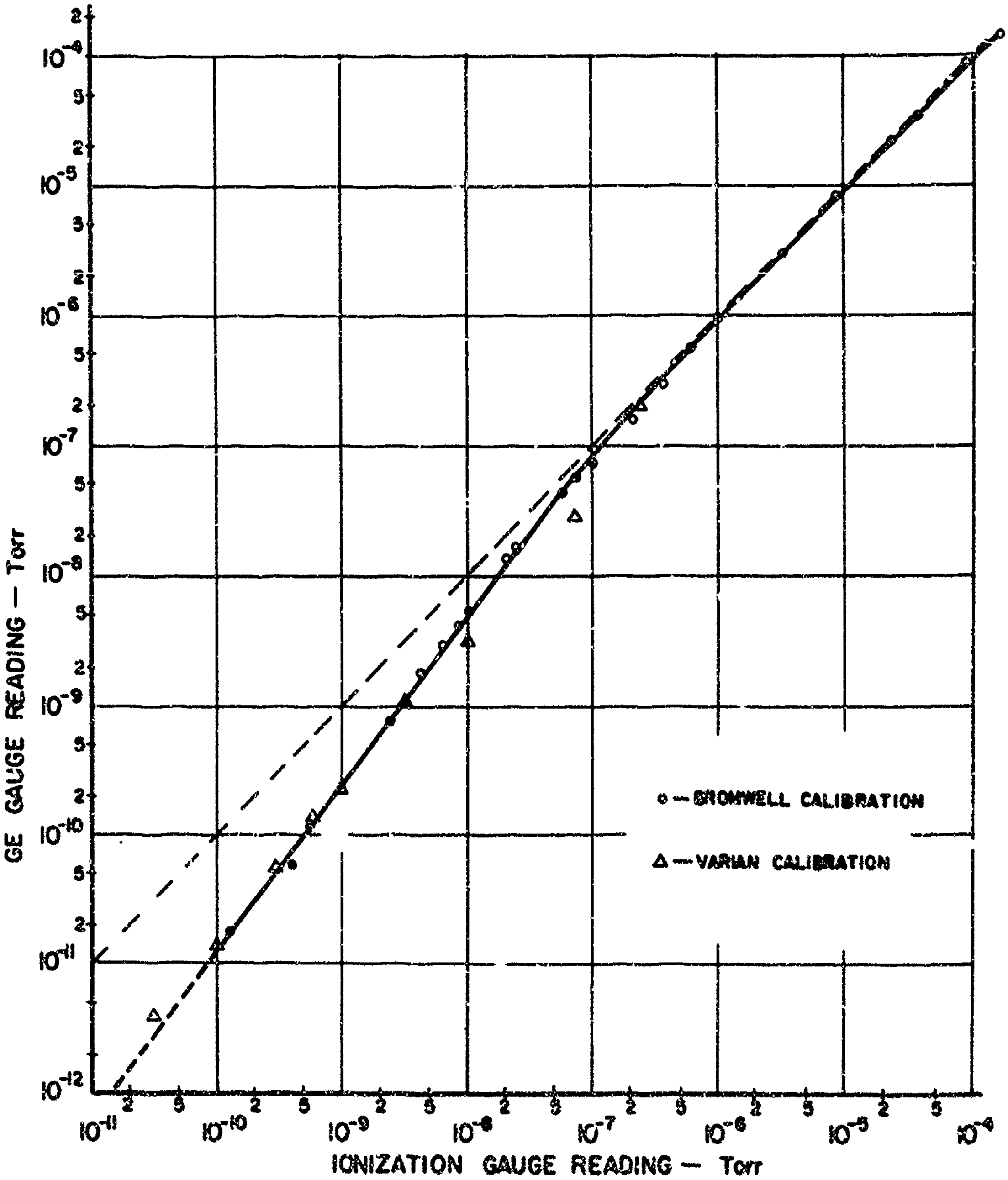

FIGURE B-1

APPENDIX C

KINETICS OF HIGH VACUUM ADSORPTION

Adsorption is a dynamic process, with gas molecules continuously arriving at and leaving the surface. Equilibrium is always achieved by equating the number of arriving molecules per unit area to the number of departing molecules per unit area. If the average time of residence, τ, is very large, the time scale will be greatly expanded and the dynamical nature becomes more a mathematical convenience than an observable phenomenon.

To prevent appreciable adsorption on a surface, the average residence time must be very small compared to the time required for a new molecule to arrive at a given surface site. If the concentration of molecules on the surface is taken as Γ molecules/cm^2, then

$$\Gamma = Z\tau \tag{C-1}$$

where Z is the rate of arrival of molecules to the surface, molecules/cm^2/sec. and τ is the average residence time in seconds. Z is given by kinetic theory (Brunauer, p. 61):

$$Z = \frac{pN}{(2\pi MRT)^{1/2}} \tag{C-2}$$

where

p = pressure of the gas
N = Avogadro's number
M = molecular weight of the gas
R = universal gas constant
T = absolute temperature, °K

for water vapor,

$$Z = 8.3 \times 10^{21} \frac{p}{\sqrt{T}} \tag{C-3}$$

where p is measured in mm. of Hg.

Γ may also be expressed in terms of the concentration of molecules per surface site. Since monomolecular coverage for water corresponds to about 1.2×10^{15} molecules/cm^2, this leads to

$$Z' = \frac{Z}{1.2 \times 10^{15}} = 6.9 \times 10^6 \frac{p}{\sqrt{T}} \tag{C-4}$$

and

$$\Gamma' = Z'\tau \quad \text{molecules/surface site/sec.} \tag{C-5}$$

τ is given by an Arrhenius type equation:

$$\tau = \tau_0 \exp(Q/RT) \tag{C-6}$$

where

$\tau_0 = 10^{-13}$ sec. = time for a specular reflection

Q = adsorption energy, Kcal/mole

For no adsorption, we would require $\Gamma' = 0$. However, this is an impossible situation which requires either zero pressure or infinite temperature. As a practical matter, we can take $\Gamma' = 0.1$, which corresponds to maintaining one-tenth of a monolayer on the surface. Thus most of the surface sites will be vacant most of the time.

Combining equations (4), (5), and (6) leads to an equation relating Q, p, and T as follows:

$$\Gamma' = Z'\tau$$

$$0.1 = (6.9 \times 10^6 \frac{p}{\sqrt{T}} [10^{-13} \exp(Q/RT)]$$

which gives, with sufficient accuracy for this analysis,

$$\frac{p}{\sqrt{T}} \exp(Q/RT) = 10^5 \tag{C-7}$$

Taking the $\log_e$ of both sides of equation (7)

$$2.3 \times 5 = \ln p - \frac{1}{2} \ln T + Q/RT$$

or

$$Q = T \ln T + 4.6\, T\, (5 - \log_{10} p) \qquad \text{(C-8)}$$

For pressures between 10^{-4} and 10^{-16} torr, and temperatures between 200°K and 2000°K, the T ln T term contributes 8% to 11% of Q. A simplified equation can be obtained by taking this term as 10% of the total Q:

$$Q = 5.1\, T\, (5 - \log_{10} p) \quad \text{cal/mole} \qquad \text{(C-9)}$$

A plot of Equation (C-9) is given in Fig. C-1. Independent confirmation of the general validity of this derivation appears to be given by Becker (1958). He measured the adsorption of various gases on a small tungsten ribbon, and by use of a fast-responding ion gauge was able to calculate the number of molecules desorbed when the ribbon was quickly heated to a temperature T. Becker gives the adsorption energy, Q, in electron volts/molecule as

$$Q = \frac{T}{350} \quad \text{e.v.}$$

where T is the absolute temperature at which desorption occurred. Becker gives no indication of how this equation was derived. However, it can be shown to correspond to Equation (9) derived earlier in this appendix. Since 1 e.v. = 23 Kcal/mole, Becker's equation may be written as

$$Q = \frac{T}{15.2} \quad \text{Kcal/mole}$$

The pressures used in Becker's experiments were around 10^{-7} torr which, when put into Equation (9) gives

$$10^3 Q = 5.1\ T[5 - (-7)] = 61.2$$

$$Q = \frac{T}{16.3}$$

which agrees very well with Becker's value.

TEMPERATURE AND PRESSURE CONDITIONS
FOR 0.1 MONOLAYER COVERAGE

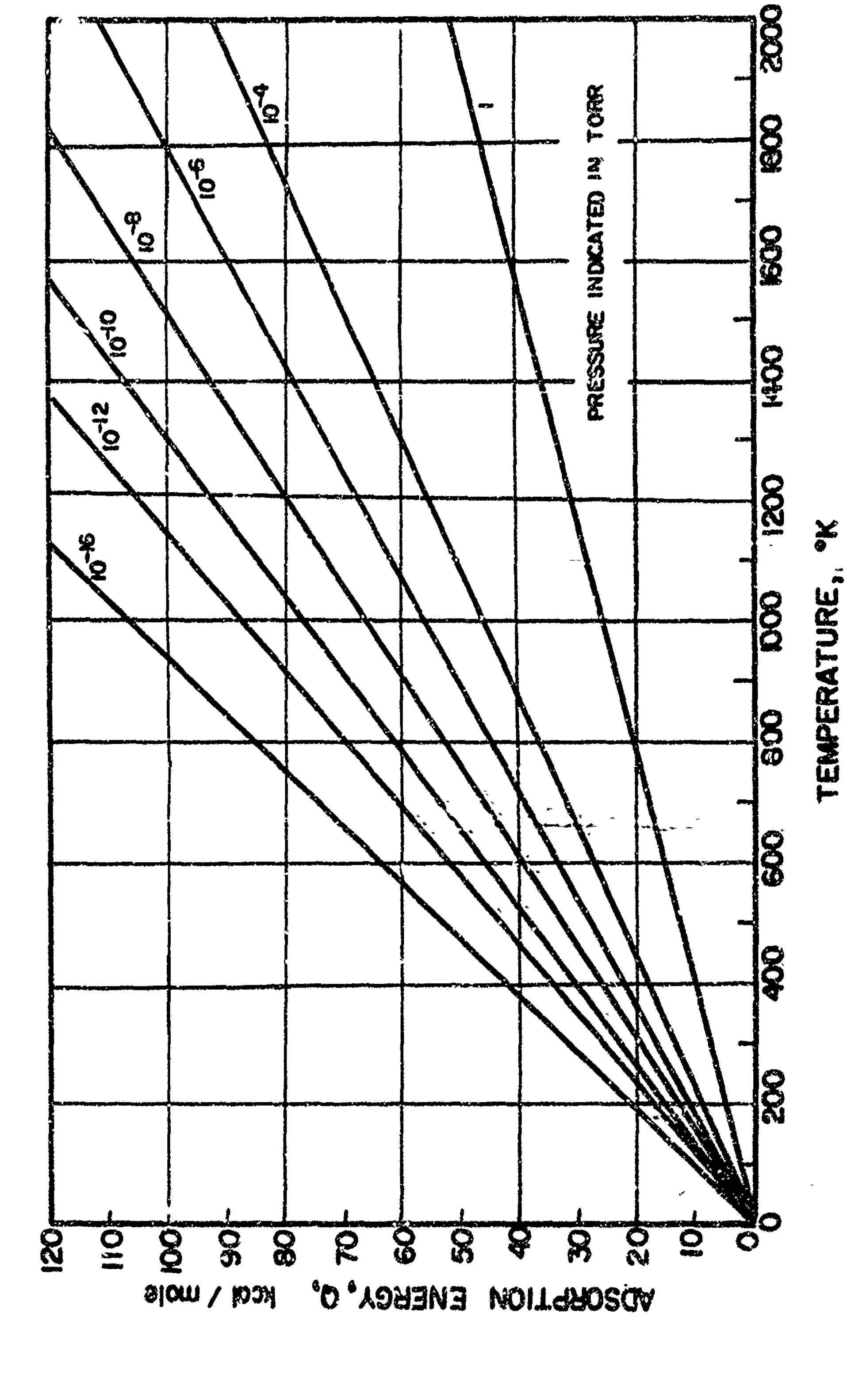

FIGURE C-1

Unclassified
Security Classification

DOCUMENT CONTROL DATA - R&D

(Security classification of title, body of abstract and indexing annotation must be entered when the overall report is classified)

1. ORIGINATING ACTIVITY (Corporate author) Massachusetts Institute of Technology Cambridge, Massachusetts	2a. REPORT SECURITY CLASSIFICATION Unclassified 2b. GROUP

3. REPORT TITLE
RESEARCH IN EARTH PHYSICS; THE FRICTION OF QUARTZ IN HIGH VACUUM

4. DESCRIPTIVE NOTES (Type of report and inclusive dates)
Contract Phase Report 7

5. AUTHOR(S) (Last name, first name, initial)
Bromwell, Leslie G.

6. REPORT DATE	7a. TOTAL NO. OF PAGES	7b. NO. OF REFS
May 1966	119	36

8a. CONTRACT OR GRANT NO. DA-22-079-eng-457 b. PROJECT NO. 1-V-0-14501-B-52A-01 c. d.	9a. ORIGINATOR'S REPORT NUMBER(S) Research Report R66-18 9b. OTHER REPORT NO(S) (Any other numbers that may be assigned this report) U. S. Army Engineer Waterways Experiment Station Contract Report 3-101

10. AVAILABILITY/LIMITATION NOTICES
This document is subject to special export controls and each transmittal to foreign governments or foreign nationals may be made only with prior approval of U. S. Army Engineer Waterways Experiment Station.

11. SUPPLEMENTARY NOTES Conducted for: U. S. Army Engineer Waterways Experiment Station, CE, Vicksburg, Miss.	12. SPONSORING MILITARY ACTIVITY U. S. Army Materiel Command Washington, D. C.

13. ABSTRACT
The purpose of this investigation was to determine the fundamental factors controlling the frictional properties of quartz surfaces, with emphasis on the effects of surface cleanliness. Ultra-high vacuums (to 10^{-10} torr) and high temperatures (to 350°C) were combined with chemical cleaning and careful handling techniques to produce the maximum surface cleanliness. The coefficient of static friction under varying environmental conditions was measured for quartz, 304 stainless steel, and granite. Direct shear tests were run on a quartz sand (40-60 mesh Ottawa sand) and on 30-40 mesh glass balls. The coefficient of friction of smooth quartz was found to vary from 0.1 to 1.0 depending on the surface cleanliness. The friction of rough surfaces showed a much smaller variation, which has important implications for granular soils. Ultra-high vacuum, combined with a high temperature bake-out, produced significant increases in both the angle of friction, ϕ_μ, of quartz (about 8°) and the peak friction angle, ϕ_m, of quartz sand (about 5°). The cohesion intercept for the quartz sand also increased by about 0.02 kg/cm². A good correlation, using theoretical curves, was obtained between changes in ϕ_m and ϕ_μ for quartz. The high vacuum-high temperature test conditions simulate aspects of the lunar environment. Therefore, the test results may yield useful information regarding the properties of postulated lunar soil models involving significant thicknesses of granular particles.

DD FORM 1 JAN 64 1473

Unclassified
Security Classification

Unclassified
Security Classification

14. KEY WORDS	LINK A ROLE	LINK A WT	LINK B ROLE	LINK B WT	LINK C ROLE	LINK C WT
Quartz						
Friction						
High vacuum effects						
Temperature effects						
Surface cleanliness						

INSTRUCTIONS

1. ORIGINATING ACTIVITY: Enter the name and address of the contractor, subcontractor, grantee, Department of Defense activity or other organization (corporate author) issuing the report.

2a. REPORT SECURITY CLASSIFICATION: Enter the overall security classification of the report. Indicate whether "Restricted Data" is included. Marking is to be in accordance with appropriate security regulations.

2b. GROUP: Automatic downgrading is specified in DoD Directive 5200.10 and Armed Forces Industrial Manual. Enter the group number. Also, when applicable, show that optional markings have been used for Group 3 and Group 4 as authorized.

3. REPORT TITLE: Enter the complete report title in all capital letters. Titles in all cases should be unclassified. If a meaningful title cannot be selected without classification, show title classification in all capitals in parenthesis immediately following the title.

4. DESCRIPTIVE NOTES: If appropriate, enter the type of report, e.g., interim, progress, summary, annual, or final. Give the inclusive dates when a specific reporting period is covered.

5. AUTHOR(S): Enter the name(s) of author(s) as shown on or in the report. Enter last name, first name, middle initial. If military, show rank and branch of service. The name of the principal author is an absolute minimum requirement.

6. REPORT DATE: Enter the date of the report as day, month, year; or month, year. If more than one date appears on the report, use date of publication.

7a. TOTAL NUMBER OF PAGES: The total page count should follow normal pagination procedures, i.e., enter the number of pages containing information.

7b. NUMBER OF REFERENCES: Enter the total number of references cited in the report.

8a. CONTRACT OR GRANT NUMBER: If appropriate, enter the applicable number of the contract or grant under which the report was written.

8b, 8c, & 8d. PROJECT NUMBER: Enter the appropriate military department identification, such as project number, subproject number, system numbers, task number, etc.

9a. ORIGINATOR'S REPORT NUMBER(S): Enter the official report number by which the document will be identified and controlled by the originating activity. This number must be unique to this report.

9b. OTHER REPORT NUMBER(S): If the report has been assigned any other report numbers (either by the originator or by the sponsor) also enter this number(s).

10. AVAILABILITY/LIMITATION NOTICES: Enter any limitations on further dissemination of the report, other than those imposed by security classification, using standard statements such as:

(1) "Qualified requesters may obtain copies of this report from DDC."

(2) "Foreign announcement and dissemination of this report by DDC is not authorized."

(3) "U. S. Government agencies may obtain copies of this report directly from DDC. Other qualified DDC users shall request through ______________."

(4) "U. S. military agencies may obtain copies of this report directly from DDC. Other qualified users shall request through ______________."

(5) "All distribution of this report is controlled. Qualified DDC users shall request through ______________."

If the report has been furnished to the Office of Technical Services, Department of Commerce, for sale to the public, indicate this fact and enter the price, if known.

11. SUPPLEMENTARY NOTES: Use for additional explanatory notes.

12. SPONSORING MILITARY ACTIVITY: Enter the name of the departmental project office or laboratory sponsoring (paying for) the research and development. Include address.

13. ABSTRACT: Enter an abstract giving a brief and factual summary of the document indicative of the report, even though it may also appear elsewhere in the body of the technical report. If additional space is required, a continuation sheet shall be attached.

It is highly desirable that the abstract of classified reports be unclassified. Each paragraph of the abstract shall end with an indication of the military security classification of the information in the paragraph, represented as (TS), (S), (C), or (U).

There is no limitation on the length of the abstract. However, the suggested length is from 150 to 225 words.

14. KEY WORDS: Key words are technically meaningful terms or short phrases that characterize a report and may be used as index entries for cataloging the report. Key words must be selected so that no security classification is required. Identifiers, such as equipment model designation, trade name, military project code name, geographic location, may be used as key words but will be followed by an indication of technical context. The assignment of links, rules, and weights is optional.

Unclassified
Security Classification